STUDY OF THE EFFECTS OF COMPOSITION AND SINTERING PARAMETERS ON DIELECTRIC PROPERTIES OF ZIRCONIA AND NIOBIUM OXIDE DOPED BARIUM TITANATE CERAMICS

BY

MD SAZZAD HOSSAIN
STUDENT NUMBER 0409112014
JUNE 8, 2011

A THESIS SUBMITTED TO THE DEPARTMENT OF MATERIALS AND METALLURGICAL ENGINEERING IN PARTIAL FULFILLMENT OF THE REQUIREMENTS FOR THE DEGREE OF MASTER OF SCIENCE IN ENGINEERING (MATERIALS AND METALLURGICAL ENGINEERING)

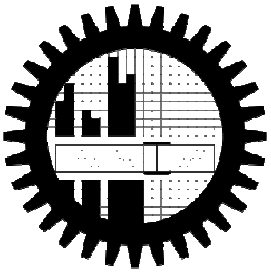

DEPARTMENT OF MATERIALS AND METALLURGICAL ENGINEERING
BANGLADESH UNIVERSITY OF ENGINEERING AND TECHNOLOGY

The thesis titled "STUDY OF THE EFFECTS OF COMPOSITION AND SINTERING PARAMETERS ON DIELECTRIC PROPERTIES OF ZIRCONIA AND NIOBIUM OXIDE DOPED BARIUM TITANATE CERAMICS" submitted by Md. Sazzad Hossain, student no 0409112014 P, session April 2009 has been accepted as satisfactory in partial fulfillment of the requirement for the degree of Master of Science in Materials and Metallurgical Engineering on June 2011.

Board of Examiners

1. _____ Chairman (Supervisor)

Dr. Md. Fakhrul Islam
Professor
Materials and Metallurgical Engineering department
BUET, Dhaka

2. _____ Member (Co-Supervisor)

Dr. A. K. M. Abdul Hakim
Chief Engineer and Head
Materials Science Division
Atomic Energy Center
BAEC, Dhaka

3. _____ Member (Ex-officio)

Dr. Md. Aminul Islam
Professor and Head
Materials and Metallurgical Engineering department
BUET, Dhaka

4. _____ Member

Dr. K. M. Sorowardi
Assistant Professor
Materials and Metallurgical Engineering department
BUET, Dhaka

5. _____ Member

Dr. Obaidul Islam
Professor
Department of Physics
University of Dhaka

CANDIDATES' DECLARATION

IT IS DECLARED HEREBY THAT THIS THESIS PAPER OR ANY PART OF IT HAS NOT BEEN SUBMITTED TO ANYWHERE ELSE FOR THE AWARD OF ANY DEGREE

.....

Md. SAZZAD HOSSAIN

Dedicated to

THE PEOPLE WHO SACRIFICED
THEIR HAPPINESS TO SEE ME HAPPY

ACKNOWLEDGEMENT

The Department of Materials and Metallurgical Engineering has given me the opportunity to work with some of the finest equipments in modern times through this thesis. Despite various limitations the department ensured me consistent access to all these facilities. This not only helped me carry out the research efficiently but also acquainted me with some of the most modern facilities and their functions. First, I pay my utmost gratitude to the Department of Materials and Metallurgical Engineering.

I am eternally grateful to my advisor, my research supervisor and my revered mentor Professor Dr. Md. Fakhrul Islam. He provided mewith the technical base needed to undertake the research, always pointed me to the right direction and corrected my mistakes. Being a very busy person he spared me his valuable time regarding my work. I thank him from the bottom of my heart for his sincere cooperation, priceless advices and consistent encouragements and motivation. Had he not been in there, the research could not be completed.

I would like to convey my heartiest regards to my respected Co-supervisor Dr. Abdul Hakim. He granted me access to all the cutting edge facilities in Atomic Energy Center, Dhaka as per my need and therefore practically made this thesis work possible. Successful or not, if there is just one gain from this thesis, then I owe that to Dr. Hakim.

I so very much want to thank Mr. Md. AlMamun, Engineer of Atomic Energy Center, Dhaka for his priceless assistance with Scanning Electron Microscopy. For the same reason I owe special thanks to Mr. Yousuf Khan for his assistance with the microscopy which was one of the most significant tasks in my thesis. With or without any schedule I bothered him for help and he provided the best of his assistance from his valuable time.

I pay my gratitude to Mr. Maksud for helping me with the operation and handling of the various equipments.

I am deeply grateful to Mr. Ahmadullah and Mr. Shahjalal for their kind assistance with the laboratory works.

I express thanks to all my revered teachers and friends for helping me either directly with my work and/or with information and motivation.

Table of contents

List of Figures

List of Tables

ABSTRACT

In this research, the effects of $ZrO_2$and Nb_2O_5addition to $BaTiO_3$ and sintering parameters on the dielectric properties were observed. When $BaTiO_3$ ceramics are doped with ZrO_2 or Nb_2O_5, the substitution of Ti^{4+} ions by Zr^{4+}or Nb^{5+}ions is expected, which isa temperature dependent process and can significantly alter the dielectric properties. However, it is also proved that a very small addition of ZrO_2 or Nb_2O_5 e.g. 0.1 to 2wt% has the potential to yield very good dielectric characteristics. In this thesis the optimum sintering temperature yielding the smallest grain size along with 95-97% of theoretical density was found to be 1290°C for both 1 and 2 wt% ZrO_2 added samples and 1275°C for 0.1 to 0.3 wt% Nb_2O_5 added samples. The experiments revealed that low soaking time e.g. 0 minute, can yield the best combination of sintering outputs. Double stage sintering was found to give better control over the grain size and thus more effective for the dielectric properties. The smallest grain size achieved was 500 nm for ZrO_2 added samples and 600 nm for Nb_2O_5 added samples. Images from SEM suggested that the inhibition to grain growth in $BaTiO_3$is a function of the amount of dopants and sintering parameters. Above 1300°C, significant grain growth was observed for ZrO_2 added samples and the grains reduced in size with increasing ZrO_2 content from 1 to 2 wt% $BaTiO_3$.Microstructures showed the grain size to be finer in 2 wt% samples than in 1 wt% samples. These observations suggested ZrO_2 diffusion inside $BaTiO_3$ lattice above 1300°C and therefore the need for higher amount of ZrO_2 to inhibit grain growth. For Nb_2O_5 modified samples 1320°C was the maximum sintering temperature and yet no significant grain growth occurred. Nb_2O_5 was found to yield the same microstructural effects brought by ZrO_2 with addition of much lower amount than that of ZrO_2. 1275°C sintering was found to yield the best dielectric characteristics for Nb_2O_5 added samples.XRD analysis showed reduction in tetragonality in both pure anddoped $BaTiO_3$samples after sintering followed by decrease in cubic to tetragonal transition temperature and suppression of curie peak to some extent. The shift of tetragonal to orthorhombic transition point to higher temperatures was also understandable from the experiments.Such shifting of cubic-tetragonal peak and tetragonal-orthorhombic peak towards each other is a plausible cause of the rise in dielectric constant at intermediate temperatures.Nb_2O_5 added samples showed similar characteristics. At low temperatures where ZrO_2 is known to linger at grain boundaries, long sintering time by means of double stage sinteringhas shown to improve permittivity on many occasions.Nb_2O_5 added samples were found to yield increasing dielectric constant with the percent increase in Nb_2O_5content even with lower percent theoretical density achievement.The permittivity (k) was found to yield consistent and flat response with temperature.ZrO_2doped samples have shown permittivity (k) values as much as 3500 and that for Nb_2O_5 samples were found to be as high as 6500.

CHAPTER 1
INTRODUCTION

1.1 Scope of Barium Titanate based electronic materials

Dielectric characteristics of materials are of one of the greatest importance in the field of electronic application of materials. Due the distinctive structural characteristics ceramic materials are known as good insulators and therefore are referred to as dielectric materials. A range of unique properties arises due to ceramic's interaction with the applied electric field. Structural and thermal stability, weight, size etc exposed dielectric ceramics to versatile applications with success. Extensive research has been carried out from the beginning with resultant attractive properties. Current research activities show promising future with more dynamic applicability of these ceramic materials.

Among the ferroelectric materials, polycrystalline Barium Titanate finds extensive application in the electronic industry mainly as ceramic capacitors. The multilayer ceramic capacitor (MLCC) is one of the remarkable inventions offering very high dielectric constants and low losses. Some other applications include piezoelectric devices, electroluminescent panels, and pyroelectric elements, polymer matrix composites for embedded capacitance in printed circuit board and heaters and sensors with positive temperature coefficient of resistivity (PCRB).

The dielectric materials available in the early 1900's all had dielectric constants less than 10. Higher dielectric constant materials came at around 1930. Like Rutile which has a constant of 80 to 100. Barium titanate was discovered at 1940 having constants around 1200 to 1500 [49]. This high dielectric characteristic made scientists doing research on structural characteristics of barium titanate. Later it was found that modification of its structure by chemical substitution yields improved dielectric properties. For examples 10 wt% calcium zirconate plus 1 wt% magnesium zirconate results in dielectric constants above 5000. If 10 wt% calcium zirconate and 10 wt% strontium zirconate are added, then the dielectric constants can be as much as 9500. In recent days constants up to 18000 has been reported.

Since modern science is directed towards the miniaturization of the electronic equipments, the ferroelectric ceramic components serves to get the smaller sized components and large value of capacitance in the field of dielectrics. In such a multi layer ceramics reduction of layer thickness and increasing the number of layers cause to give the best of capacitance. In near future, the dielectric thickness will become less than a micron and the number of layers may exceed 1000.

1.2 Need for modification of Barium Titanate structures

Despite the advantages offered by $BaTiO_3$ regarding small sized capacitors their use is limited by number of operating variables. The electric field strength and the operating temperatures are strong determinants of dielectric constants.

Dielectric properties also vary significantly up on the following factors –

- Size of individual grain and grain boundaries
- Presence and distribution of the impurity
- Stress imposed by surrounding grains
- Presence of second phase particle
- Condition of the material at the start of manufacturing
- Procedure of manufacturing and various processing variables

The dependence on temperature along with other properties such as the dielectric constants can be modified by forming solid solutions or doping the base perovskite with a range of compositions. Successful attempts are made to substitute the atoms of perovskite from different lattice positions e.g. the corner atoms or atoms positioned at the octahedral holes. For example, in $BaTiO_3$, Ba^{2+} is replaced by Pb^{2+}, Sr^{2+} ions. Similarly the Ti^{4+} is replaced by Zr^{4+}, Hf^{4+}. Such doping brings certain modification to the structure of the perovskite which lead to versatility in the dielectric properties. Therefore, a considerable effort has been given to the development of best composition along with associated forming characteristics to improve dielectric characteristics.

1.3 Recent works on $BaTiO_3$ based electronic ceramics

There is uninterrupted working streak on barium titanate based ceramics since its dielectric properties were revealed. Now researchers are focusing on the processing, structure and properties of these materials and the improvement on a continuous basis.

In 2002 Yoon et al. [40] worked on the core shell structure of the acceptor rich, coarse barium titanate grains. They found that after sintering the donor rich specimen exhibited a fine grained microstructure of but significant grain growth occurred in the acceptor rich specimen over the temperature range used. Howeverin both specimens an undoped core region, several hundred nanometers in size was detected. The core shell structure appeared to be maintained in $BaTiO_3$ under the conventional sintering temperatures.

Jung [41] in 2003 experimented on grain growth behavior during stepwise sintering of barium titanate in hydrogen and air. Effects of oxygen partial pressure were studied with the samples being sintered in air with or without prior treatment in hydrogen. It was observed that without prior treatment in Hydrogen abnormal grain growth occurs below and above eutectic temperature. Treatment with hydrogen prior to sintering increases the grain size and suppresses the abnormal grain growth

Liang [42] in 2004 studied the effects of acceptor and donor dopants on the dielectric and tunable properties of barium strontium titanate with ion of magnesium, manganese, aluminum, iron, lanthanum, and niobium. It was found that small quantity of acceptor ions (magnesium, iron, aluminum) could meliorate the dielectric properties and reduce the dielectric loss.

Valen [43] in 2004 experimented on the low sintering temperature of barium strontium titanate. It was found that the addition of 0.4 % wt of lithium oxide to base powder decreases the sintering temperature to 900°C and produces ceramic with relative densities of 97%.

Cho [44] in 2004 studied the dependence of grain growth and grain boundary structure on barium titanium ratio in barium titanate. It was revealed that both these factors depend on excess of titanium oxide at 1250 and 1300^0C. Abnormal grain growth occurs with excess titanium. Grain boundaries are mostly flat or faceted with hill and valley shapes.

In 2004 Jin [45] studied the effects of external electric field on grain growth behavior of acceptor Magnesium doped and undoped, donor niobium doped barium titanate. The acceptor doped and undoped specimen showed enhanced grain growth in positive biased region. Highly donor doped specimens show grain growth in negative biased region.

Babilo[46] at 2005 studied on enhanced sintering of Yttrium doped Barium Zirconate by addition of Zinc oxide. With the use of transition metal oxide (ZnO), $BaZr_{.85}Y_{.15}O_{3-8}$ was readily sintered to above 93% of theoretical density at 1300°C.

Chun [47] in 2004 the abnormal grain growth occurring at the surface of a sintered barium titanate specimen. It was found that when the powder compact was sintered in air the abnormal grain growth occurs at the surface of the specimen. The evaporation of Barium titanate from the surface followed by the formation of the eutectic liquid is suggested to be causing it. When the evaporation of powder was suppressed by embedding the specimen in the same powder, no exaggerated grain growth was observed.

Wang [48] studied the effect of grain boundary structure on diffusion induced grain boundary migration in barium titanate. The effect of grain boundary structure either rough or faceted, on diffusion induced grain boundary migration has been investigated in barium titanate. Strontium titanate particles are scattered on the polished surface of two kinds of barium titanate with faceted or rough boundaries. The samples with faceted boundaries are annealed in air and that with rough boundaries are annealed in Hydrogen. The samples with rough boundaries show appreciable grain boundary migration. Hardly any migration occurred in samples with faceted boundaries. The low migration was attributed to low grain boundary mobility.

1.4 Challenges and targets of this thesis

First off, the way this thesis is intended to perform is new under the present circumstances of the department. Moreover, there are only a few people who have worked with such topics. Hence there is a lack of experience and source of information on this occasion. The procedure does not follow the conventional calcination-sintering route. On this point of view the work imposes entirely a new challenge. However the work, if done correctly has the potential to yield material with unique dielectric characteristics than that achieved from a conventional calcination and sintering route. From these respects the research is definitely exciting and worthy of being followed.

Although the work involves handling of nanopowders which requires certain degree of cautiousness to ensure throughout maintenance of appropriate composition and cleanliness, however the preparation of the compacts is kept simple; the biggest challenge is to achieve fine grain structure with minimum porosity. From this view, the toughest task is to find the optimum sintering temperature which can bring the desired microstructure. Control of the geometry of samples is another challenge to take over. Since this is attributed entirely on the rate of heating and cooling during sintering, the heating/cooling rate needs to be optimized as well.

Finally the structure property relationships need to be realized. Here a particular composition is related to the microstructure that results upon firing and the associated dielectric properties are correlated with all these variables.

As mentioned of the use of powder which has a size in nanometer range;such powders possess very high surface energy and consequentially,are more reactive than coarser powders. Hence the sintering temperature needs to be modified accordingly. For example, the temperature followed for larger sized powders is generally much higher thanfor that in case of nano powders.

CHAPTER 2
LITERATURE REVIEW

2.1 Introduction

There are number of materials that possess electrical conductivity, which means various charge carriers like electrons, ions can pass through it. These are conductors. On the other hand, there are also materials through which these conductors of electricity cannot pass through. These are insulators. There are certain other groups of materials, which in general acts as insulators. However, they can be made to have dipole structures by forming a combination of a couple of conductor plates and the insulator material (nonmetallic) sandwiched in-between as shown in figure 2.1. This certain arrangement is capable of storing charges without passing any of carriers through the insulator.

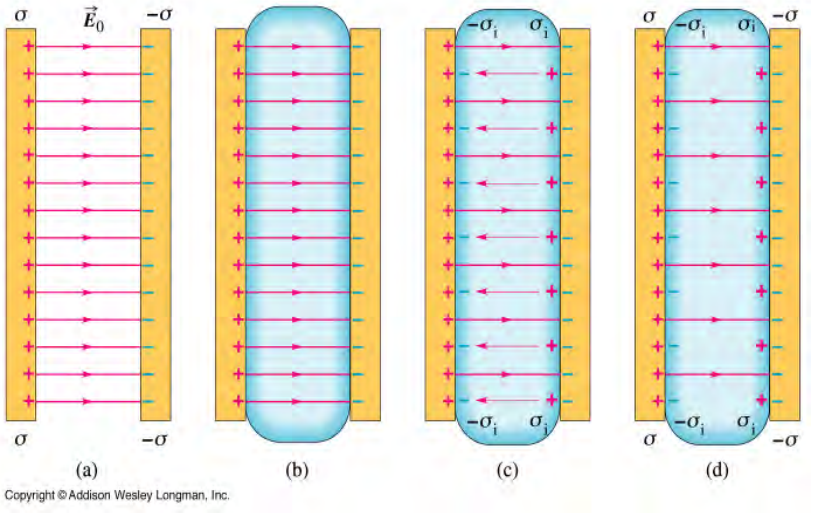

Figure 2.1: (a) Electric field of magnitude E_o between two charged plates.
(b) Dielectric being placed in between.
(c) The surface charges induced and their field (thinner lines).
(d) Resultant filed of magnitude Eo/K when a dielectric is between charged plates.

This charge storing capability of the class of insulator materials is known as DIELECTRIC PROPERTIES. The insulator material is called DIELECTRIC.

Dielectrics in capacitors serve three purposes:

1. to keep the conducting plates from coming in contact, allowing for smaller plate separations and therefore higher capacitances;
2. to increase the effective capacitance by reducing the electric field strength, which means you get the same charge at a lower voltage;

3. and to reduce the possibility of shorting out by sparking (more formally known as dielectric breakdown) during operation at high voltage.

2.2 Dielectrics– A Holistic Approach

Dielectric materials are most widely related to the capacitors in an electric circuit. Hence, concept of various dielectric properties, like dielectric constants, dielectric loss factors, dielectric strength etc requires the knowledge of capacitance (the ability of charge storage) of material.

Considering the case of a simple parallel plate capacitors with metal plates of area A and separated by a distance d, and the medium inside being simply vacuum, when a voltage V is applied across the plates, one of the plates will acquire a net charge of +q and other will get a net –q. The charge is directly proportional to the applied voltage V as in-

$q=CV$ or $C=\frac{q}{V}$---------- *(1)*

Where Cis the proportionality constant called the capacitance of the capacitor. The SI unit of capacitance is coulombs per volt (C/V) or Farad (F).

The capacitance of a capacitor is a measure of its ability to store electric charge. The more charge stored at the upper and lower plates of the capacitor, the higher is its capacitance.

For parallel plate capacitor, with a vacuum in the space between the plates, the capacitance of the capacitor is –

$C_0 = \frac{A}{d} \in_o$---------- *(2)*

Where, A = area of the plates

d = distance between the plates

$\in_0$ =permittivity of vacuum, constant having value of 8.85×10^{-12} F/m

Now, if a dielectric material fills the space between the plates, the capacitance of the capacitor is increased by a factor *k,* which is called the dielectric constant of the dielectric material. For a parallel plate capacitor with a dielectric between the capacitor plates, capacitance-

$C = \frac{A}{d} \in_0 k$or $C = \frac{A}{d} \in$---------- *(3)*

Where, $\in$= permittivity of the dielectric medium which is greater in magnitude than $\in_0$. The factor *k* is known as relative permittivity or the dielectric constants, which is equal to the ratio of the permittivity of the dielectric medium to that of vacuum. As in-

$k = \in/\in_0$ ---------- *(4)*

Dielectric constant is greater than unity and represents the increase in charge storing capacity by insertion of the dielectric medium between the plates.

It is important to note that the electric field between the capacitor plates is reduced by the presence of the dielectric. Because, the induced surface charges on the dielectric cause an electric field in the opposite direction of the original field in the charged capacitor as shown in figure 2.1. These fields tend to cancel each other resulting in a reduction of the original field.

2.3 Polarization

When the atoms or molecules of a dielectric are placed in an external electric field, the nuclei are pushed with the field resulting in an increased positive charge on one side while the electron clouds are pulled against it resulting in an increased negative charge on the other side. This process is known as polarization and a dielectric material in such a state is said to be polarized. There are two principal methods by which a dielectric can be polarized: **stretching and rotation**.

The interaction of dielectric with the field varies from free space since it contains charge carriers that can be displaced, and charge displacements within the dielectrics can neutralize a part of the applied field.

From equation 1 and 2 the surface charge in vacuum, $\sigma_{vac}$is given as in-

$$\sigma_{vac} = \left[\frac{Q}{A}\right]_{vac} = \in_0 \frac{V}{d} = \in_0 E \quad \text{----------} (5)$$

Where, E = Applied electric field across the plates of the capacitor, V/m.

Similarly, equation 1 and 3 directs to the surface charge on the metal plates in the presence of dielectrics, which is-

$$\left[\frac{Q}{A}\right]_{Die} = \in_0 k \frac{V}{d} = \sigma_{vac} + \sigma_{pol} \text{----------} (6)$$

Where, σ_{pol}= Excess charge per unit surface area present on the dielectric surface. This numerically has the same dimension as the polarization, P of the dielectric material.

Σ_{pol}= P ----------*(7)*

The total charge can be divided to *free charge* Q/k that sets up the electric field and voltage toward the outside; the other portion being the *bound charge*, is neutralized by polarization of the dielectric. Schematically it can be represented that the total electric flux density D is the sum of the electric field E and the dipole charge P:

$D=\in_0 E + P = \in' E$---------- *(8)*

Polarization P is the surface charge density of the bound charge, equal to dipole moment per unit volume of material.

$P = N \bar{\mu}$---------- *(9)*

In other words, the total charge on the capacitor D is the sum of the charge that is present in vacuum and an extra charge that results from the polarization of the dielectric material P. Thus polarization can equivalently designate either the bound charge density or the dipole moment per unit volume. From 8-

$P =\in' E - \in_0 E = \in_0 (k-1) E = \chi_{die} \in_0 E$ ---------- *(10)*

Where, χ_{die}= dielectric susceptibility of the material.

$X_{die} = k-1 = P/ \in_0 E$ ---------- *(11)*

The susceptibility is the ratio of the bound charge density to the free charge density.

Considering from microscopic point of view –

The charge carriers in dielectric materials cause to react with and affect the electromagnetic radiation. The relationship between applied field and the medium can be considered as resulting from the presence of elementary electric dipoles having an average dipole moment, $\bar{\mu}$. If the dipole moment is represented by two charges of the opposite polarity, + and –Q, separated by a distance δ, and then $\bar{\mu}$ equals Qδ.

$\bar{\mu} = Q\delta$ ---------- *(12)*

With the above considerations if the center of electron charge moves by an amount δ, then the total volume occupied by these electrons would be Aδ. If the number of molecules per unit volume by N then the total charge appearing in that volume Aδ is AδNQ.

Over the range of optical frequencies the source of this dielectric polarization is the shift of the electron cloud around the atomic nucleus. The average dipole moment is proportional to the local electric field strength (E') that acts on the particle; the proportionality constant (α) being called the polarizability.

$= \alpha E$ ---------- *(13)*

Regarding to the statement and equation 9 we can end up with –

$P = N \alpha E$ ---------- *(14)*

2.4 Mechanism of polarization

The formation of an electric dipole or polarization can happen in a number of mechanisms. Like –

1) Electronic polarization
2) Ionic or atomic polarization
3) Orientation polarization
4) Space charge polarization

2.4.1 Electronic polarization:

Electronic polarization occurs in all dielectric materials. Upon an external electric field being applied a slight relative shift of positive and negative electric charge in opposite directions occurs within an insulator, or dielectric as shown in figure 2.2. Polarization occurs when the induced electric field distorts the negative cloud of electrons around positive atomic nuclei in a direction opposite the field. This slight separation of charge makes one side of the atom somewhat positive and the opposite side somewhat negative. As soon as the electric field is removed the electrons and nuclei return to their original position and the polarization disappears. The displacement of charge is very small for this mode of polarization. Hence total amount of polarization is small compared to other modes of polarization.

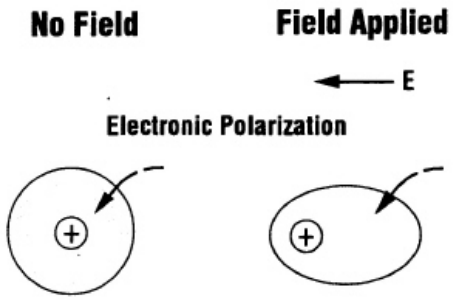

Figure 2.2: Electronic polarization

2.4.2 Atomic polarization:

It is also known as ionic polarization. It involves the displacement of positive and negative ions in relation to one another within crystal structure when an electric field is applied as in figure 2.3. The magnitude of the dipole moment for each ion pair p_i is equal to the product of the relative displacement d_i and the charge q on each ion as in-

$$p_i = q\, d_i$$

Various popular effects like piezoelectricity, pyroelectricity, ferroelectricity occurs by ionic polarization phenomena. Wide range of polarization effects are possible through this mechanism depending upon the crystal structure, solid solution and various other factors.

Ionic polarization is inversely proportional to the mass of the ions and square of the natural frequency of vibration of the ions. Covalently bonded ceramics do not show ionic polarization due to lack of charged atoms, but ionic bonded structures show ionic polarization.

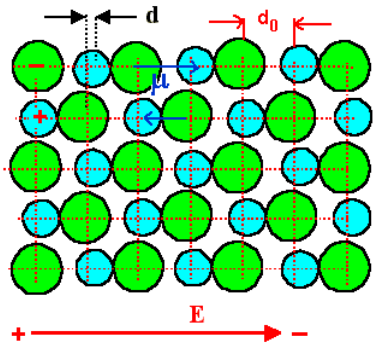

Figure 2.3: Atomicpolarization

2.4.3 Dipolar polarization:

This mode of polarization mainly attributed to the unequal charge distribution between partners in a molecule or complex ion, shown in figure 2.4. When a field is applied, these tend to line up with the electric dipoles in the direction of the field, giving rise to an orientation polarization. That is why this polarization is found only where substance possesses permanent dipole moments.

Upon electric field these permanent moments rotate into the direction of the applied field, therefore contribute to the dipolar polarization. The tendency to alignment is counterbalanced by thermal vibrations of the atoms such that the polarization decreases with the increasing temperature.

Dipolar polarization occurs at lower frequencies of the field and thus can greatly affect the capacitive and insulating properties of glasses and ceramics in low frequency applications.

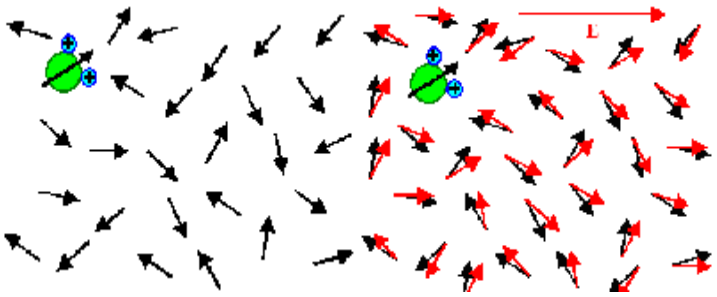

Figure 2.4: Dipolar polarization

2.4.4 Space charge polarization:

The final source of polarization is mobile charges which are present because they are impeded by interfaces, because they are not supplied at an electrode or discharged at an electrodeor they are trapped in the material during fabrication process.The condition is shown in figure 2.5. Space charges resulting from these phenomena appear as an increase in capacitance as far as the exterior circuit is concerned.

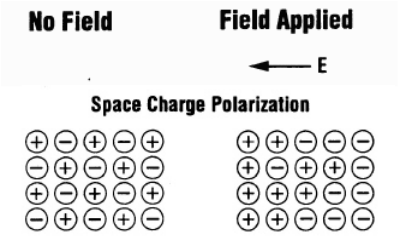

Figure 2.5: Space Charge polarization

2.5 Frequency response of polarizability

The dielectric response of solids is a complex function of frequency, temperature, and type of solid. Under dc conditions all mechanisms operate and the maximum polarization results which eventuates to the maximum of dielectric constants. An ideal dielectric is supposed to adjust itself instantaneously to any change in voltage. However in practice there is inertia to charge movement that shows up as a relaxation time for charge transport. When the frequency of the applied field increases then the mechanisms starts to fade out and the value of polarizability starts falling. Figure 2.6 shows how the applied frequency causes the polarizability to vary.

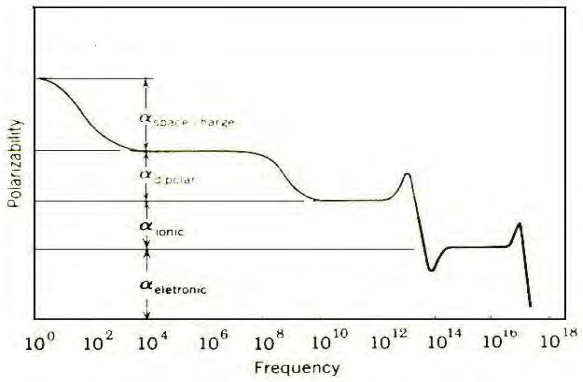

Figure 2.6: Variation of polarization with frequency

The electronic polarization is the only process that can follow the rapid change in the alternate field so to cause a variation in the polarizability. That is why this is still operative in the visible range of the spectrum and the cause factors like index of refraction which only due on to this process.

Ionic polarization processes are able to follow an applied high frequency field and contribute to the dielectric constant at frequencies up to infrared region of the spectrum. Dipolar and space charge polarization have relaxation time corresponding to the particular system and process but in general participate and contribute only at lower frequencies. As far as this thesis is concerned, this factor is very important in getting the dielectric behavior of the ceramics.

2.6 Dielectric loss

An ideal dielectric would allow no flow of electric charge but only a displacement of charge via polarization. If a thin plate of such an ideal material were placed between parallel plate electrodes to form a capacitor and if an alternating electric field were applied, the current would lead the voltage by a phase angle of$\frac{\pi}{2}$. Under these circumstances, no power will be absorbed by the dielectric and the capacitor would have zero loss.

We know voltage- $V = V_0 \sin \omega t$ hence, $Q = C\,V = CV_0 \sin \omega t$

So the current would be - $I_{chg} = \frac{dQ}{dt} = C\frac{dV}{dt} = \omega CV_0 \cos\omega t = \omega CV_0 \sin\left(\omega t + \frac{\pi}{2}\right)$

Hence we see that the applied current is leading the voltage by 90° or$\frac{\pi}{2}$ radian. At this provision, no power would be absorbed by the dielectric.

When alternating current passes through the capacitor with a dielectric in between the capacitor plates, the molecules of the dielectric fail to align instantaneously with the alternating electric field. These molecules do not keep in phase with changing field. The time required for polarization shows up as phase retardation of the charging current. As a result, instead of being 90° advanced, the angle of leading current is slightly reduced.

In this case the current I have two components. An imaginary charging component which is $I_{chg} = i\omega CV$; and a real loss component I_{loss}. The charge component is a capacitive current that is proportional to the charge stored in the capacitor. The loss current is an ac conduction current that is in phase with the voltage V and represents the energy loss or power dissipated in the dielectric material.

New lead angle is $\emptyset$. Value $90-\emptyset$ is known as loss angle and is given by symbol δ. The power factor is defined as $\cos \emptyset$ and the dissipation factor or the amount of lag as $\tan \delta$. $\tan \delta$ is also called loss tangent. For small values of δ, $\sin \delta$ (Power Factor) and $\tan \delta$ (dissipation factor) are almost equivalent.

We can define the loss factor, which is numerically the product of dissipation factor and the dielectric constant. So loss tangent –

$$\tan \delta = \frac{k''}{k'}$$

where k" is *relative loss factor* and k' is the *relative dielectric constant*.

Dielectric loss could result from several mechanisms: (1) Ion migration; (2) Ion vibration and deformation; (3) Electronic polarization. The most important mechanism to most ceramics is ion migration, which is strongly affected by temperature and frequency. The loss due to ion migration increases at low frequencies and as the temperature rises.

2.7 Dielectric strength & breakdown

An important property of dielectric materials is the ability to withstand large field strengths without electrical breakdown. Dielectric strength is a measure of the ability of the material to hold energy at high voltages. It is defined as the voltage per unit length at which failure occurs. Thus it is the maximum electric field that the dielectric can maintain without electrical breakdown.

At low field strengths there is a certain dc conductivity corresponding to the mobility of a limited number of charge carrier related to electronic or ionic imperfections. As the field strength is increased this dc conduction increases, but also when some sufficient large value of potential is reached, a field emission from the electrodes makes available sufficient electrons for a burst of currents which produces breakdown channels, jagged holes, or metal dendrites bridging the dielectric and render it unusable.

Various processes may contribute to these dielectric breakdown phenomena. However, different measurement techniques give considerable scatter in the outcomes and detail interpretations are still in some doubt.

Dielectric breakdown of insulating material under an applied field takes place two different ways. The first is electronic in origin and is referred to as intrinsic dielectric strength. The second process is caused by local overheating, arising from electrical conduction. The local conductivity increases to a point at which instability occurs and permits a rush of currents and melting and puncture is likely to occur. The tendency toward thermal breakdown increases at higher temperatures and voltages are applied for a long time.

In ***electronic breakdown***, failure occurs when a localized voltage gradient reaches some value corresponding to intrinsic electrical breakdown. Electrons within the structure are accelerated by the field to a velocity that allows them to liberate additional electrons by collision. This process continues at an accelerating rate and finally results in an electron avalanche which correspond to breakdown and sample rupture. At low temperatures (below room temperature) the intrinsic breakdown strength of crystalline materials increases with rising temperature, corresponding to increased lattice vibrations and a resulting increase in electron scattering by the lattice; a greater field strength is required to accelerate electrons to a point at which electron avalanche is initiated. On the other hand glassy material's intrinsic dielectric strength is independent of temperature at low temperatures.

Thermal breakdown behavior is associated with electrical stress of appreciable time duration for local heating to occur and it requires high enough temperatures for the electrical conductivity to increase. The loss in electrical energy causes the temperature to rise further and increase the local conductivity. This causes channeling of currents; thus local instability and breakdown occur which results in the passage of high currents along with fusion and vaporization that constitute the puncture of the insulator.

2.8 Piezoelectric ceramics

The Piezoelectric Effect is the name given to the *electromechanical interaction* of certain materials. Discovered in 1880 by Pierre and Jacques Curie [36], it is the relationship between electric polarization and mechanical stress or distortion. The word originates from the Greek word "piezein", which means, "to press". Anything, that is said to give off an electric field under mechanical stress and vice versa, is said to be piezoelectric.

The effect is explained by the displacement of ions in crystals that have a nonsymmetrical unit cell. When the crystal is compressed, the ions in each unit cell displace, causing the electric polarization of the unit cell. Because of the regularity of crystalline structure, these effects accumulate, causing the appearance of an electric potential difference between certain faces of the crystal.When an external electric field is applied to the crystal, the ions in each unit cell are displaced by electrostatic forces, resulting in the mechanical deformation of the whole crystal.

The Piezoelectric Effect has two pathways dependent on cause and effect. Two factors are involved: *Mechanical stress* and *electric polarization*. When a piezoelectric object is subjected to a physical distortion or compression, the object acquires an electric charge. This pathway, where mechanical stress leads to polarization is known as the *Direct Piezoelectric Effect*.

Object (strain) ⟶ Object (Electric Polarization)

When a piezoelectric object undergoes an electrical charge, observed mechanical distortions take place in what is known as the *Converse Piezoelectric Effect*.

Object (electrical field) ⟶ Object (stress)

An object with piezoelectric property has many applications. Quartz, a crystal with piezoelectric property, is utilized by applying an electrical field, thus leading to a deformation of the quartz. The sense of the strain depends on the direction of the field. A majority of computers contains at least one clock frequency which is generated by a quartz crystal. Aside from quartz, Rochelle salts, $BaTiO_3$,$(NH_4)H_2PO_4$, $LiTaO_3$, and $LiNbO_3$ are other noted salts and crystalline objects that display piezoelectric properties.

This electromechanical property, however, is not rare. Twenty of the thirty-two crystal classes are piezoelectric. Of the thirty-two crystal classes, twenty-one are non-centrosymmetric (not having a centre of symmetry), and of these, twenty exhibit direct piezoelectricity. Ten of these are polar (i.e.

spontaneously polarize), having a dipole in their unit cell, and exhibit pyroelectricity. If this dipole can be reversed by the application of an electric field, the material is said to be ferroelectric. Unlike the ferroelectric class of materials, piezoelectric material does not store charge after the force is removed.

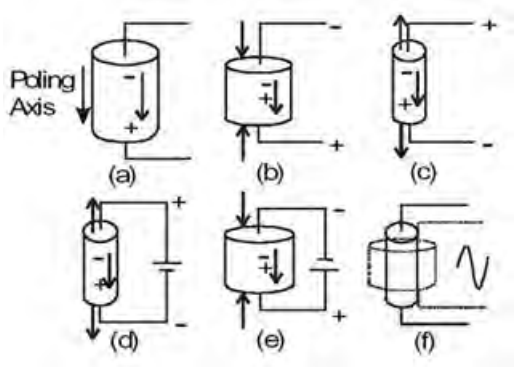

Figure 2.7: Piezoelectric effect

Figure 2.7 illustrates the piezoelectric effect. Figure (a) show the piezoelectric material without a stress or charge. If the material is compressed, then a voltage of the same polarity as the poling voltage will appear between the electrodes (b). If stretched, a voltage of opposite polarity will appear (c). Conversely, if a voltage is applied the material will deform. A voltage with the opposite polarity as the poling voltage will cause the material to expand, (d), and a voltage with the same polarity will cause the material to compress (e). If an AC signal is applied then the material will vibrate at the same frequency as the signal (f).

2.9 Pyroelectric ceramics

Pyroelectricity is the ability of certain materials to generate an electrical potential when they are heated or cooled. Because of this change in temperature, positive and negative charges move to opposite ends through migration (i.e. the material becomes polarized) and hence, an electrical potential is established.

Certain dielectric (electrically nonconducting) crystals develop an electric polarization (dipole moment per unit volume) when they are subjected to a uniform temperature change. This effect occurs only in crystals which lack a center of symmetry and also have polar directions (that is, a polar axis). These conditions are fulfilled for ten of the thirty two crystal classes. Typical examples of pyroelectric crystals are tourmaline, lithium sulfate monohydrate, cane sugar, and ferroelectric barium titanate.

Pyroelectric crystals can be regarded as having a built-in or permanent electric polarization. When the crystal is held at constant temperature, this polarization does not manifest itself because it is compensated by free charge carriers that have reached the surface of the crystal by conduction through the crystal and from the surroundings. However, when the temperature of the crystal is raised or lowered, the permanent polarization changes, and this change manifests itself as Pyroelectricity.

Crystal structures can be divided into thirty two classes, according to the number of rotational axes and reflection planes, they exhibit that leave the crystal structure unchanged. Twenty one of them classes lack a center of symmetry, and Twenty of them are piezoelectric.Of these Twenty crystal classes ten of them are pyroelectric (polar). Any material develops a dielectric polarization when an electric field is applied, but a substance which has such a natural charge separation even in the absence of a field is called a polar material. Whether or not a material is polar, is determined solely by its crystal structure. Only ten of thirty two classes are polar.

The property of Pyroelectricity is the measured change in net polarization (a vector) proportional to a change in temperature. The *total pyroelectric coefficient* measured at constant stress is the sum of the pyroelectric coefficients at constant strain (primarypyroelectric effect) and the piezoelectric contribution from thermal expansion (secondary pyroelectric effect).

The pyroelectric coefficient may be described as the change in the spontaneous polarization vector with temperature.

$$p_i = \frac{\partial \mathrm{P}s,i}{\partial T}$$

Where, p_i ($Cm^{-2}K^{-1}$) is the vector for the pyroelectric coefficient.

2.10 Ferroelectric ceramic

Ferroelectricity is a physical property of a material whereby it exhibits a spontaneous electric polarization, the direction of which can be switched between equivalent states by the application of an external electric field with a hysteresis loop being followed. If the material shows a perfect cubic lattice, no Ferroelectricity can be observed.

Ferroelectric materials are also nonlinear and demonstrate a spontaneous polarization. Typically, materials demonstrate Ferroelectricity only below a certain phase transition temperature, called the Curie temperature T_c, and are paraelectric above this temperature.

Ferroelectric behavior is dependent on the crystal structure. The crystal must be noncentric and must contain alternate atom positions to permit the reversal of the dipole and the retention of polarization after the voltage is removed. An example can be made of barium titanate, a typical ferroelectric material. Within the range of 120 to 1460 ^{0}C temperatures, the structure is cubic and therefore does not show any Ferroelectricity. Since in this temperature range, the Ti^{4+} ion lies in the centre of an octahedron of oxygen ions. The Ti^{4+} ion does shift positions and result in polarization when an electric field is applied, but it returns to its central stable position as soon as the field is removed. Hence no ferroelectric behavior is observed.

As the temperature reduces to below 120 ^{0}C, a displacive transformation occurs in which the structure shifts from cubic to tetragonal. The transition can be understood in terms of a *polarization catastrophe*, in which, if an ion is displaced from equilibrium slightly, the force from the local electric fields due to the ions in the crystal, increases faster than the elastic-restoring forces. This leads to an asymmetrical shift in the equilibrium ion positions; the ion moves to an off center position towards one of the two oxygen ions of the long axis, resulting in a spontaneous increase in positive charge in this direction and permanent dipole moment, thus exhibit Ferroelectricity.

All ferroelectrics are piezoelectric and pyroelectric; but not vice versa. For instance, tourmaline shows Pyroelectricity but is not ferroelectric. The alignment of electric dipoles is opposed by thermal vibrations and thus the property deteriorates as the temperature increases. The alignment disappears at the curie temperatures. For $T>T_c$,Curie Weiss law holds [49]:

$$\chi = \frac{P}{\varepsilon E} = \varepsilon/\varepsilon_0 - 1 = k' - 1 = \frac{3Tc}{T-Tc}$$

χ represents the electrical susceptibility, P represents polarization, E electric field, ε and ε_0 representspermittivity of material and vacuum respectively, and k' represents dielectric constants.

2.10.1Ferroelectric domains

As the material develops its charge, a 'domain' structure is developed in order to attain the minimum free energy state for the crystal.Ferroelectric domains, sometimes known as Weiss domains, are areas of local dipole alignment - with an associated net dipole moment and net polarization. 'Domain walls' separate domains from each another.Such a domain structure is shown in figure 2.8. These domain boundaries are usually described according to the angle between the domains that they separate. The most commonly found are 90° and 180° boundaries.

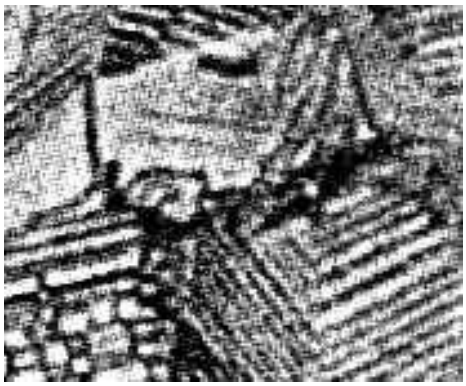

Figure 2.8: Ferroelectric Domain

The picture above shows an area of a ferroelectric material clearly displaying a domain structure. The dark lines are 90° domain walls. The domain structure and behavior of a material will critically affect its operational performance.

In the presence of an applied electric field, domains that are aligned with the direction of the field will grow at the expense of the less well-aligned domains. This may be visualized in terms of the boundary between the domains moving. The domain structure can also change over time by a process known as ageing. This causes degradation to the dielectric properties and often causes device failure due to loss of insulation resistance.

In barium titanate each titanium ion has equal probability of shifting in six directions towards one of the corners of the octahedron. As a result the tetragonal crystal contains some dipoles in one portion of the crystal in one direction, whereas others in another portion may point in a direction 90° or 180° away from the first. The regions of the crystal in which the dipoles are aligned in a common direction are the domain.

Presence of an electric field is vital for getting the maximum of domains to be aligned in one direction. The temperature also plays a vital role on that occasion. For example, maximum alignment of domains in barium titanate can be achieved by cooling the crystal through the 120° C cubic to tetragonal transition while an electric field is being applied. This is referred to as *poling*. This results in maximum polarization. It has been found upon research to characterize the domains and their activities that 180° domains are easy to remove than 90°. That is because the surface strain generated during cooling and the crystal fabrications restrict the motion of the domain. There may be many domains in a crystal separated by interfaces called domains.

2.10.2 Ferroelectric Hysteresis loop

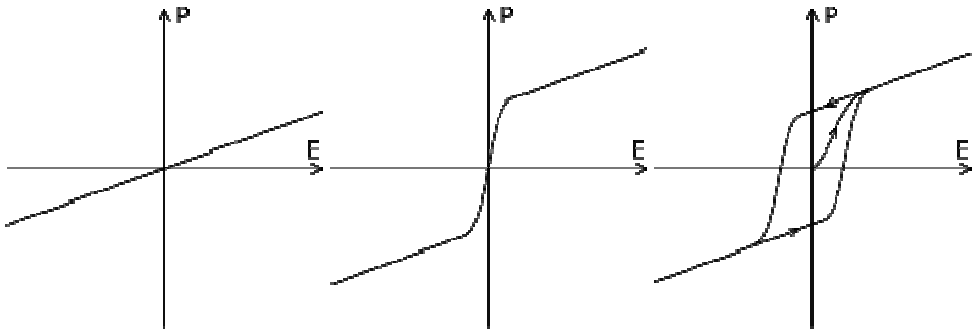

Dielectric polarization paraelectric polarization ferroelectric polarization

Figure 2.9: Response of different type of materials to electric fields

One of the prime characteristics of the ferroelectric materials is the retention of dipole without the presence of the any field and the reversibility of the direction of polarization by application of an electric field. Such reversal upon the application of the electric field results in a hysteresis loop. Figure 2.9 shows such a hysteresis loop. Where E is the applied field and P is the polarization.

Ferroelectric domains are randomly oriented prior to application of the electric field. Net polarization at zero fields is zero. At low field strengths in unpolarized material, the polarization is also reversible and nearly linear with the applied field. Here the slope of the curve gives the initial dielectric constant. At higher fields strengths the polarization increase more rapidly because of switching of ferroelectric domains that is the changing polarization direction in domains by 90 or 180; this occurs by domain boundaries moving through the crystal. At the highest field strengths the increase of polarization for a given increase in field strengths is again less, corresponding to polarization saturation, having all the domains of like orientation aligned in the direction of the applied field. This is called saturation polarization or spontaneous polarization.

When the electric field is cut off the polarization does not go to zero but remains at a finite value, called the remanent polarization, P_r. This results from the oriented domains being unable to return to their original random state without an additional energy input by an oppositely directed field. That is energy is required for change in domain orientation. The magnitude of the electric field required to return the polarization to zero is known as the coercive field E_c.

At higher temperatures, the hysteresis loop becomes fatter, and the coercive field becomes greater, corresponding to a larger energy required to reorient the domain walls. At higher temperatures, the coercive force decrease until at the Curie temperature, where no hysteresis remains, and there is only a single value for the dielectric constant.

The hysteresis here has been originated from the existence of irreversible polarization through partial polarization reversals of a single ferroelectric lattice cell. The separation of the total polarization into reversible and irreversible contributions might facilitate the ferroelectric polarization. Irreversible polarization would be important say for ferroelectric memory device, since the reversible process can't be used to store information. Similarly, a reversible ferroelectric may be a requisite of dielectric materials for application such as capacitors.

2.11 Science of Barium Titanate

With a general formula ABO_3, the A cation and the anions effectively form an FCC array with a large octahedron in the center of the cell but no available tetrahedra (because of the charge).

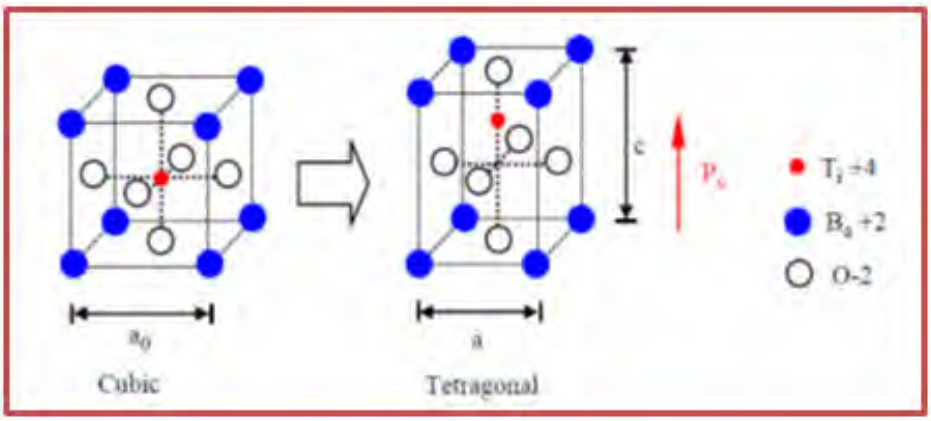

Figure 2.10: The perovskite structure ($BaTiO_3$) Showing structures below and above curie point

The ideal perovskite structure is simple cubic, and this is what we generally imply when we refer to the perovskite structure. The mineral perovskite is $CaTiO_3$ and is actually orthorhombic at room temperature, becoming cubic only at temperatures above 900°C. Other ceramics with the perovskite structure include $BaTiO_3$, $SrTiO_3$, and $KNbO_3$, each being written in the general form ABO_3. The structure is not similar to that of ilmenite ($FeTiO_3$)though, which is related to the alumina structure.

Looking at the ionic radii, a trend can be seen. The O^{2-} anion and the larger cation (A^{2+}) have similar radii, so that the structure is not just determined by O^{2-}. The larger cation and the anion

combine to form a "close-packed" arrangement with the smaller cation, B^{4+}, sitting in the oxygen octahedral interstices. The octahedra then link together by sharing corners as shown in Figure 2.10 (b).The bond strength is given as

$$Ti-O=+\frac{4}{6}=\frac{2}{3};\qquad Ca-O=+\frac{2}{12}=\frac{1}{6}$$

Each O^{2-} anion coordinates with two $Ti^{4+}$and four Ca^{2+}cations so that the total bond strength is -

$$2\times\frac{2}{3}+4\times\frac{1}{6}=+2$$

Barium titanate ($BaTiO_3$) is the prototype ferroelectric material. It has the ideal perovskite structure above 120°C. At temperatures below 120°C the small cation (Ti^{4+}) shiftsoff its ideal symmetric position at the center of each octahedral interstice. This shift creates an electric dipole; it polarizes the structure electrically, which in turn causes the material to become noncubic; this changes the cell dimensions. Spontaneous electrical polarization in the absence of an applied electric field is termed ferroelectricity. The link between electric field and mechanical deformation of the unit cell is known as the piezoelectric effect:it allows us to convert an electrical signal to a mechanical one and vice versa. This shift actually has the same origin as the flexibility of this structure: many ions can fit in the central ocahedron.Theperovskite structure is particularly important for several reasons:

- Many perovskites are ferroelectric
- Many perovskites are piezoelectric
- Many perovskites have a high dielectric constant

The perovskite structure is also of interest to mineralogists. A mineral with the perovskite structure of composition close to $MgSiO_3$ is believed to be the predominant mineral in the lower mantle (depths of about 600 km) of the earth. The perovskite structure of $MgSiO_3$ is stable only at very high pressures.

Barium titanate ($BaTiO_3$) was the first ceramic in which ferroelectric behavior was observed and is probably the most extensively investigated of all ferroelectrics. Its discovery made available κs up to two orders of magnitude greater than had been known before. This property was very soon utilized in capacitors and $BaTiO_3$ remains the basic capacitor dielectric in use today (although not in its pure form). There are several reasons why $BaTiO_3$ has been so widely studied:

Relatively simple crystal structure, durability, Ferroelectric at room temperature (θc = 120°C), easily prepared as a polycrystalline ceramic, single crystal, or thin films.

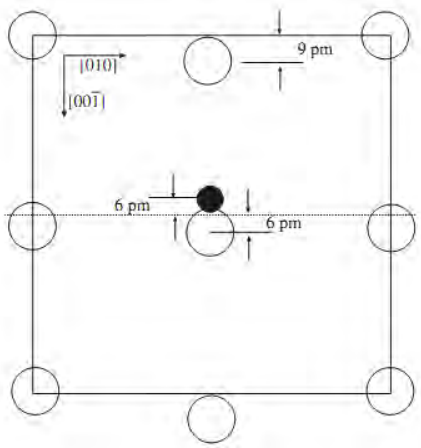

Figure 2.11: [100] projection of barium titanate showing the ion displacement below θ_c [38]

Aboveθ_c the unit cell of $BaTiO_3$ is cubic (point group m3m) with the ions arranged as shown in Figure 2.10: Each Ba^{2+} is surrounded by 12 nearestneighbor oxygen ions; each Ti^{4+} has six oxygen-ion neighbors. Together the $Ba^{2+}$and O^{2-} ions form a face-centered cubic (FCC) arrangement with Ti^{4+} fitting into the octahedral interstices. The octahedral site is actually expanded because of the large Ba^{2+}ions (r_{Ba2+} = 0.136 nm). The Ti^{4+}ion is quite small (r_{Ti4+} = 0.064 nm) giving a radius ratio with oxygen of r_{Ti4+} /r_{O2-} = 0.44. This value is close to the limiting value (≥0.414) for a coordination number of 6. The result is that the Ti^{4+}often finds itself off-centered within its coordination octahedron. This is why it is sometimes referred to as the "rattling" titanium ion (think back to Pauling's rules). The direction of off-centering may be along one of the 6 <001> directions, one of the 8 <111> directions, or one of the 12 <110>directions.

Calculation of dipole moment for $BaTiO_3$:

In the crystal of Barium titanate, both Ti4+ and O2- ions are displaced from their positions and shift towards each other. The distances by which the ions shift from the usual lattice positions (assuming the position of Ba2+ ions is fixed) need to be considered to get fixed dipole moment. The charge is the product of q and the ion charge. Therefore the dipole moments are then

$\mu(Ti^{4+})$: $(1.602 \times 10^{-19}C)(4)(0.06\times10^{-8}cm) = 3.84 \times 10^{-28}$

$\mu(O^{2-}$ top): $(1.602 \times 10^{-19}C)(2)(0.09\times10^{-8}cm) = 2.88 \times 10^{-28}$

$\mu(O^{2-}$ side): $(1.602 \times 10^{-19}C)(2)(0.06\times10^{-8}cm) = 1.92 \times 10^{-28}$

Now the number of each of the types of ions per cell is included in calculation. There is a single Ti4+/cell, there is a top-face O2- /cell and there are two side-face O2-/cell.

The total diple moment per unit cell is

$\mu = \mu(Ti^{4+}) + \mu(O^{2-}\ \text{top}) + \mu(O^{2-}\ \text{side}) = 1.056 \times 10^{-27}\text{C.cm}$

2.11.1 The effect of temperature - The phase transformations

Barium Titanate assumes two basic structures;a*perovskite* form, which is ferroelectric at certain temperatures and a *non-ferroelectric hexagonal* form. The hexagonal form is stable above 1460℃ temperatures and can stay up to room temperature metastably. At 1460℃, the hexagonal form transforms to a cubic perovskite form and it is the basic ceramic product.

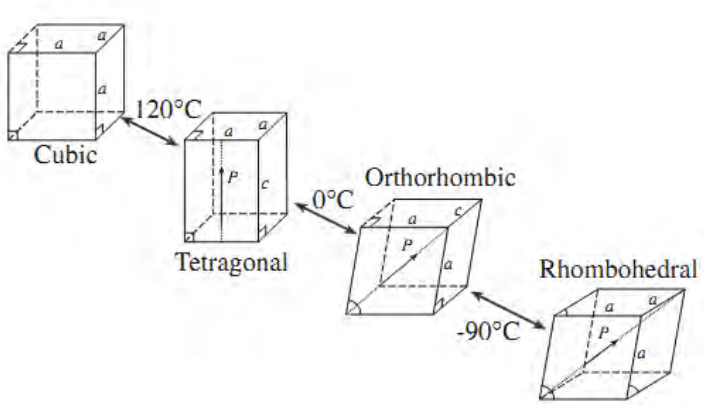

Figure 2.12: Polymorphic transitions in $BaTiO_3$

On cooling $BaTiO_3$ below θ_c (120°C) the structure spontaneously changes to the tetragonal form (point group 4 mm) with a dipole moment along the c axis. The c/a ratio becomes more than one.Such change marks the onset of extreme dielectric anomalies and the emergence of ferroelectricity. A *tetragonal* polar one replaces the centrocemetric cubic structure. The magnitude and direction of the ion displacements accompanying this transformation are given in Figure 2.12.

Upon further cooling, another polymorphic transformation occurs at 0℃, the cube here elongates along a face diagonal. The structure on this stage is pseudo monoclinic but actually is *orthorhombic*. At even lower temperatures like at -90℃, a third displacive transformation takes place and the previously turned *rhombohedral* cell elongates along a body diagonal. In each temperature range, the direction of the ferroelectric dipole parallels the elongation of the unit cell.

2.11.2 Curie point

Like any magnetic materials, all ferroelectric materials experience a temperature transition regarding its ferroelectric behavior. This temperature is called the *Curiepoint* (T_c). At temperatures higher than T_c, the material does not exhibit any ferroelectricity, whereas below this temperature, the material does show the property. It's possible that there might be more than one ferroelectric phases. In that case, the temperature at which one ferroelectric phase transforms from one phase to another is called the *transition temperature.*

The basic change through the Curie point is marked by the change in crystal structure. In the case of barium titanate for instance, a cubic lattice structure prevails above 120℃. The thermal vibration causes the titanium ions to be oriented randomly in the octahedral holes. At Curie point 120℃, the structure changes to tetragonal form on decreasing temperature. This brings a distortion in the size of the octahedral site with the titanium ion being at an off center position. This produces a permanent dipole. Hence, the phase transformation from cubic to tetragonal turns spontaneous random polarization to permanent dipole domains. This point (temperature) marks the curie point of the barium titanate crystal.

It is important to realize that the Ba-O framework suggests an interstitial site, which is much larger than the size of titanium ion. The series of reaction thus helps reducing the size of the octahedral site and allows titanium ion to be positioned more compactly. It is found that the size of the ions that make up the framework has important role in deciding the ferroelectric property. Thus, both $BaTiO_3$ and $PbTiO_3$ have ferroelectric phases since the size of both Ba^{2+} and Pb^{2+} allows Ti^{4+} ion to customize its position with the changing phase. On the other hand, $CaTiO_3$ and $SrTiO_3$ do not have any ferroelectric phase since the Ca^{2+} and Sr^{2+} ions are not large enough to offer Ti^{4+} ion enough space to move upon Curie point.

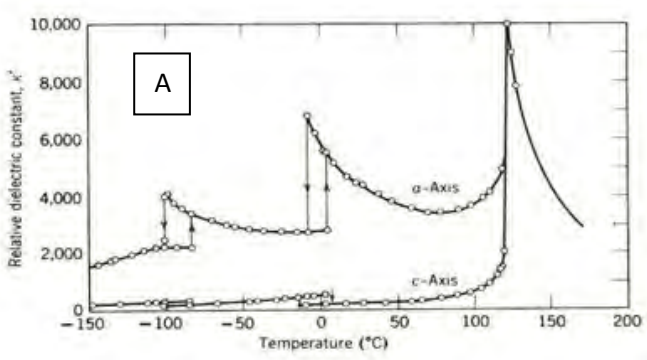

Figure 2.13 (A): Change of phases with temperature in $BaTiO_3$

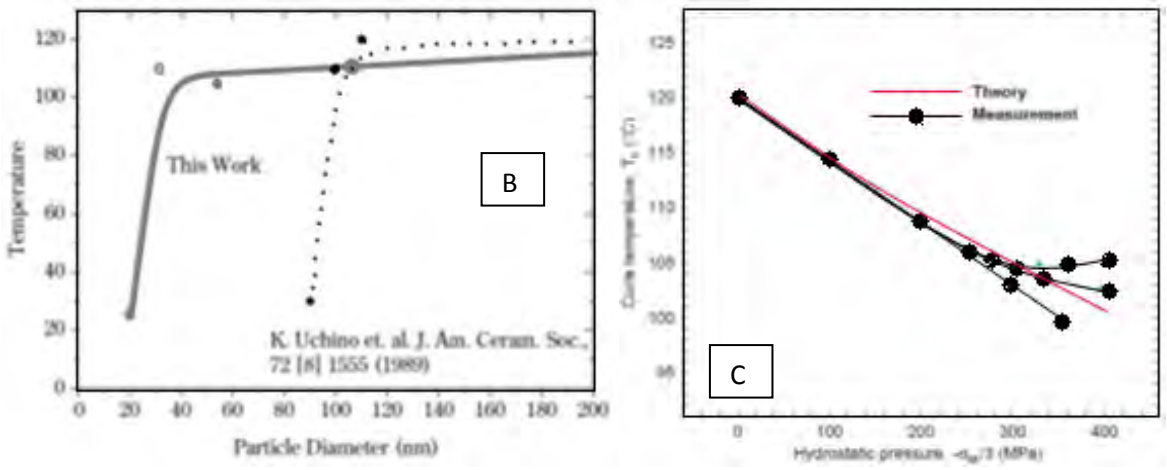

Figure 2.13(B):Change in the curie temperature as a function of particle diameter, (C)Effect of hydrostatic pressure on Curie temperature of $BaTiO_3$,respectively [2]

Figure 2.13 (A) shows the variations of relative permittivity, polarization, lattice constant with temperature for $BaTiO_3$, as the crystal is cooled from its paraelelctric cubic phase to ferroelectric tetragonal, orthorhombic, and rhombohedral phases. Near the Curie point or the transition points, various thermodynamic properties like dielectric, elastic, optical, and thermal constants show an anomalous behavior, which is attributed in the change in the crystal structure as the phase change, occurs.

2.11.3 Curie point shift in $BaTiO_3$

According to Ohna and Suzuki [7] the size effect for ferroelectric materials results in the curie temperature shift to the lower temperature. Therefore, the curie temperature shift for $BaTiO_3$nano-particles has been investigated. Figure 2.13 (B)shows the curie temperature shift as a function of the particle diameter [2]. According to them, some lattice vibration remained above the curie temperature by the secondary scattering and so on, in the case of $BaTiO_3$. They found that the

curietemperature for $BaTiO_3$nano-particles was shifted to the lower temperature at around 20-30 nm of particle diameter. This tendency was almost same as that of the result of Uchino et. al. [2, 25] measured by the change in the lattice constants as a function of the particle diameter using XRD. However, their result showed that the curie temperature shift to the lower temperature began at around 100 nm of particle diameter. This difference in the critical size for $BaTiO_3$ was ascribed to the measurement techniques of the particle diameter and the crystal symmetry.

Merz [26, 27, 28, 29, 30] has measured the pressure dependence of the transition temperature of $BaTiO_3$ over the range of pressure from0 to 400MPa. His data were reproduced by Weng [8] in Figure 2.13 (C). As the pressure increases, both the test data and the theory show a steady decrease of the transition temperature, with a slope of about -6.0×10^{-2}°C/MPa during the first 200 MPa.

2.12Composition Analysis and modification

The structure of barium titanate $BaTiO_3$ is said to be of ABO_3 type structure. An enormous effort has been exercised, since the discovery of it. From the structural aspect of the barium carbonate crystal, both A and B position can be substituted with the ions of variety of elements to bring about a wide range of modification in the properties of barium titanate. Potentially, barium titanate possesses superior dielectric properties and these substitutions rectify the various behavior of the compound on microscopic level. Some examples of substitution for both the A position (Ba^{2+}) and B position (Ti^{4+}) and there affects are discussed below in brief.

Effect of doping with Ca: Ca^{2+} ion replaces the Ba^{2+} ion in the compound upon varying extent, and the results vary with temperature. A 21 atom% Caare stable under normal firing conditions. The mixture does not affect the Curie point but significantly lowers the tetragonal orthorhombic transition temperature. This has great practical value in improving the temperature stability of the piezoelectric [49].

Single crystals of calcium-doped barium titanate have been grown by high temperature solution growth technique with 12 and 20 mol% of calcium. Dielectric constants were measured from 15 to 45 thousand and the values decreased with increasing Ca concentration. The dielectric constant also decreases with increasing frequency. The Curie temperature increased on calcium substitution in the Ba site. Hysteresis loops traced, show that the spontaneous polarization (P_s) is low for Ca doped crystals.

***Effect of doping with Ce*:**Curie temperature T_c, dielectric constants, absorption coefficients, and lattice constants of ferroelectric cerium doped $BaTiO_3$ crystals are investigated as a function of

cerium concentration. An increase of cell volume with increase doping cerium concentration deduced that the cerium ion is substituted for titanium ion. The absorption edges of crystals move toward the long wavelength with increasing Cerium content. The value of spontaneous polarization and dielectric constants of cerium doped $BaTiO_3$ are larger than those of pristine $BaTiO_3$, and this result is in accord with linear electro-optic coefficient experimental data[49].

Effect of doping with Mn:Barium titanate with a high dielectric constant is widely used in the production of ceramic capacitors. However, during sintering, large numbers of ionized oxygen vacancies and conduction electrons are created. In order to maintain an equilibrium state of electron concentration, the produced electrons are almost fully delocalized by hopping motion from one titanate site to another. These conduction electrons will lead to poor electric insulation and make the dielectric material into a semi-conductor[49].

In Mn-doped $BaTiO_3$, there exist three valence states for the manganese ions, Mn^{2+}, Mn^{3+} and Mn^{4+}. The Mn^{4+} is nearly exactly incorporated into Ti^{4+} sites and participates in the collective motion in the lattice. When some titanate sites are occupied by Mn ions at the valence 3+ or 4+, the electrons will be trapped on these sites because Mn^{3+} , Mn^{4+} are more reducible than the Ti^{4+}. Because the Mn concentration is very low, the hopping motion of the trapped electrons from one Mnsite to another is almost impossible. In other words, the electrons are effectively localized on these Mn sites. Therefore, doping with Mn into $BaTiO_3$ would reduce the conductance of $BaTiO_3$ ceramic. Two papers using EPR and dielectric spectra have been reported to support this mechanism. Here, we may verify it directly by measuring the concentration of the charge carriers in Mn-doped $BaTiO_3$[49].

Effect of doping with Dy:The substitution behavior and lattice parameter of barium titanate between solid solubility with a dopant concentration in the range of 0.25 to 1.5 mol% are studied.The influences of dysprosium-doped fraction on the grain size and dielectric properties of barium titanate ceramic, including dielectric constant and breakdown electric field strength are investigated via scanning electronic microscopy, X-ray diffraction and electric property tester. The results show that, with a dysprosium concentration of 0.75 mol%, the abnormal grain growth is inhibited. The lattice parameters of grain rise up to the maximum because of the lowest vacancy concentration.

In addition, the fine grain and high density of barium titanate ceramic result in its excellent dielectric properties. The relative dielectric constant (25 °C) reaches to 4100. The temperature coefficient of the capacitance varies from -10 to 10% within the temperature range of -15 °C -100

°C, and the breakdown electric field strength (alternating current) achieves 3.2 kV/mm. These data suggest that barium titanate could be used in the manufacturing of high voltage ceramic capacitors.

***Effect of doping withSr*:**The addition of strontium in barium titanate causes a linear decrease in Curie point. For piezoelectric ceramic, the barium-strontium titanate solid solution with little Sr^{2+} concentration offers a mean s of controlling the temperature of the Curie point, although for most practical applications any lowering is undesirable.

Interestingly, Sr doped barium titanate have higher peak values of dielectric constant than pristine [49] barium titanate. The decrease in lattice constant is neatly the same, whether it results from application of hydrostatic pressure or Sr_{2+} substitution.

Study of the reaction between barium titanate and strontium titanate shows that $SrTiO_3$ diffuses into crystallites of $BaTiO_3$. The X ray diffraction lines of $BaTiO_3$ slowly broaden and shift in spacing as reaction progresses. The $SrTiO_3$ pattern remains unchanged but gets progressively weaker.

***Effect of doping with Pb*:**substitution of Pb^{2+} for Ba^{2+} in $BaTiO_3$ raises the Curie point[49]. Complete solid solution occurs between the two end member compounds. Although lead titanate has strong ferroelectric distortion and a large polar moment, its high coercive field makes it difficult to accomplish enough poling in high $Pb2^{+}$ compositions. The substitution of lead for barium raises the Curie point monotonically toward that of lead titanate, 490°C. but it lowers the orthorhombic tetragonal and rhombohedral transition temperatures. Simultaneously the room temperature dielectric constant drops.

2.12.1 Effect of doping with Zr

Zirconia doped barium titanate has been the subject of many researches and the researches has been done in two ways. In one type, zirconia was directly added to barium titanate and in other, stoichiometric composition of zirconia doped barium titanate was tested. The two conditions presented entirely different sintering situations based on the atomic level interaction between different types of species.

For a stoichiometric sample, the crystal chemical formula is maintained across the entire ceramic material. For example, $BaTi_{0.8}Zr_{0.2}O_3$ is the stoichiometric composition of twenty percent zirconia doped barium titanate. In this material only twenty percent of the total crystals has zirconium instead of titanium in its octahedral voids. The main difference from pure barium titanate is the variation to some extent in crystallographic dimensions and electronic imbalance due to the presence of zirconium ion (86 pm) which is larger than titanium ion (74.5 pm). Otherwise the entire

material is unique in its composition across the whole material. This situation happens occasionally in a sample where zirconia is separately added to barium titanate. When zirconia is added to barium titanate and put to sintering, from the very beginning, zirconia and barium titanate stay as two separate identifiable phases. Zirconia is found to linger as fine precipitates (not precipitated though) along the grain boundariesof barium titanate grains [3,9]. During sintering the effects of zirconia presence show up in two different ways.

In first way it tries to get into barium titanate grains through diffusion where it replaces titanium ion from the crystal. However this diffusion is a limited process since zirconia itself is a very stable compound and only zirconium ion could go through the crystal. Therefore a significant amount of zirconia particles remain at grain boundaries. Since the typical sintering temperatures of barium titanate are not very high for zirconia to yield a rapid change in the crystal composition and structures, many of those particles give little response to sintering environment and cause inhibition to the movement of grain boundary of barium titanate during sintering. According to Armstrong [3] Zr^{4+} ion will not diffuse into $BaTiO_3$ lattice below 1310°C for a sintering period of 2 hours. Hence zirconia addition to barium titanate was found to yield ceramic with fine grain sizes. In case of zirconia addition to barium titanate, as it was discussed, zirconia particles stay at grain boundaries. It is also possible that the grain boundary movement and associated domain alignment is seriously affected by the strain to grain movement imposed by the zirconia precipitates which ultimately reduce the capability of grains to react to the effect of polarization and thus disrupts the yield of high dielectric constants.

Now, for those zirconia particles that get into barium titanate crystal to replace titanium ion presents some critical situations. First of all, they leave oxygen behind at the grain boundaries. A number of researchers have shown that increase in oxygen partial pressure affects the sintering process negatively. Secondly, barium zirconate is thermodynamically a more stabe compound than barium titanate. Therefore zirconium ion readily replaces the titanium ion from the octahedral position of barium titanate. For sintering above 1300°C or sintering at lower temperatures for long soaking period allows zirconium ion to move into the crystal. However, upon replacing the titanium ion, it sits stably in the octahedral hole since Zr^{4+} is much larger in size than Ti^{4+}. Therefore the crystal stays at thermodynamically more stable state which in turn stabilizes the cubic phase much more than pure $BaTiO_3$does. That is why zirconium is known to shift the curie point of barium titanate to lower temperatures; even a shift as low as to room temperature is possible according to Henning [14].

2.12.2 Effect of doping with Nb

Niobium is a donor dopant. Since niobium ion has different valences than that of the barium or titanium ion, substitution by Niobium produces a charge imbalance and charge compensation requires that electron, electron holes, or vacancies be produced.

Unit cell refinement showed that the tetragonality of $BaTiO_3$ can be changed by introducing the Niobium as dopant. The ionic radius of Nb^{5+} (=0.69Å) is almost the same as the ionic radius of Ti^{4+} (=0.68Å) but in this case it causes an increase of the unit cell volume and decrease of the tetragonality factor. The more expressed effect of niobium could be explained by the creation of a higher concentration of various defects in the crystal structure of barium titanate influencing the change of crystal lattice parameters. In addition when Niobium gets inside the $BaTiO_3$ lattice it replaces Titanium ion. In this process the crystal becomes electronically imbalanced since Niobium has a charge of +5 whereas that for Titanium is +4. Hence the crystal has +1 surplus charge when Niobium replaces Titanium. This situation can raise the mobility of charged species inside the material and therefore yield high capacitance values. At the same time Niobium ions can introduce much stronger polarization inside the material than Titanium or Zirconium ion does. This is due to niobium's higher charge than the other species which strongly shifts the Nb^{5+} ion to one side of the octahedron thus creating high polarization. Due to these reasons Nb^{5+} and other +5 charged materials are found to cause very high permittivity when used as dopant in $BaTiO_3$.

Niobium is also known to play strong role as grain growth inhibitors in barium titanate. As a result core shell structure is formed on many occasions for Niobium doped barium titanate from a low diffusivity of Nb^{+5} ions into $BaTiO_3$. The coefficient of thermal expansion of shell is higher than core. During heating of such ceramics, the core is in tension and the shell is in compression. So, there exist a large internal stress between core and shell and this stress increases with increasing Nb_2O_5 content. The shift of Curie temperature to lower temperature was attributed to internal stress resulting from the formation of core shell structure.

Nb-doping effect on the Curie temperature of $BaTiO_3$ has been reported by many researchers. Kahn [32] reported that the Curie temperature of $BaTiO_3$ was shifted to lower temperatures by Niobium addition when significant grain growth happened. Contrarily, the Curie temperature of $BaTiO_3$ moved to higher temperatures for small-grained $BaTiO_3$ ceramics when grain growth was inhibited. Cui et al. [33] reported that the Curie temperature of $BaTiO_3$ was decreased by Niobium addition.

2.13Effect of grain size on dielectric property

Grain sizes of barium titanate is very important for dielectric properties. It is now well established that reduction in grain size causes higher dielectric constants [4,5] and lower dielectric losses. Reduction of grain size depends on sintering parameters like sintering temperatures, soaking time

and the design of sintering cycle. For example, sintering with double stage heating can keep the grains from exaggerated growth [6]. Various processing techniques have been shown to be yielding fine grain structure with a very short sintering time [1]. Fine grain size achievement in conventional pressing-sintering method depends on judicious design of sintering cycles.

If the situation of grain development is analysed then it would seem that different particles with different crystal space orientation would meet up at the line of contact and then by means of grain boundary motion those regions would end up as one single grain. During the transformation from cubic phase to tetragonal phase, the crystal changes its c/a ratio to become tetragonal which is accompanied by a certain amount of volume change. The change in volume is associated with the the crystal orientation and the degree of change depends upon the surroundings of the crystal. Since it was already discussed that a single grain can hold multiple domains and since all these domains have different crystal orientation in space, there is a certain amount of resistance from surroundings to changing the volume or c/a ratio of the crystal for that matter. Its like one crystal is on the way of its surrounding crystal while the latter tries to change its dimension along one direction (c) as the first crystal is not trying to change its dimension along the same direction. This mutual resistance works accross the whole number of crystals (or domains) in a grain and therefore successful domain formation gets severely disrupted. As the grain size increases, the number of individual crystals it hold increases and therefore lesser the formation of domains in it. For a ceramic like barium titanate where its dielectric properties are heavily dependent upon these domain formation which eventually gets the material to be highly polarized, large grain sizes may have serious harmful effect on the final dielectric properties of the material.

On the other hand for fine grain sizes, the number of distinctive crystals it holds in the grain is not as much as large grains do. Therefore, as the grain size decreases, the resistance on the individual grains to changing its *c/a* ratio becomes much less across the grain. When it reaches the transition point of cubic to tetragonal phase change, it can change its dimension with much ease and thus domains can form successfully. It has been shown that the fine grain sized materials possess lower residual stress than large grain sized materials which is a representation of the same theory discussed above. Suitable design of sintering process is essential to bring such stress free microstructure. For barium titanate based materials [4, 6] double stage sintering has been proven to yield stress free grains. This thesis has been able to produce grains as small as 500 nm size by means of sintering for very short time.

In bulk $BaTiO_3$, the grain size has a string effect on the low frequency permittivity for grain sizes below approx. 10 micron. The permittivity is rising at decreasing grain sizes up to a maximum grain size of 0.5 to 0.7 micron since the internal stress caused which clamped by its surrounding

neighbors or by the increase of the number of domain walls contributing to the dielectric constants. Below this grain size the permittivity decreases sharply again due to reduction of tetragonality and of the remanent polarization.

It is suggested that the lowering of permittivity is caused by the low permittivity of interfacial layer of 0.5 to 2 nm thickness at the grain boundaries. This layer shows no difference of the composition and crystal structure in comparison to the bulk and is believed to be of photonic nature. In $BaTiO_3$ thin films significant increase in the room temperature permittivity from 500 to 900 is observed, induced by the change in morphology from granular to columnar structure.

The variation of dielectric constant with temperature for $BaTiO_3$ ceramics may vary from a fine (<1 micron) to a coarse (>50 micron) grain size. Large grained sample showed extremely high dielectric constant at the Curie point. This is due to formation of multiple domains in a single grain, the motion of whose increase the dielectric constant at the Curie point. In case of the fine grained samples a single domain forms at the grain and the movement of domain walls are restricted by the movement of grain boundaries. This leads to a low dielectric constant at the Curie point compared to the coarse-grained sample.

The room temperature dielectric constant of fine-grained samples is found to be about 3500 to 6000, which is 1500 to 2000 for the coarse-grained sample. Scientists suggested that in fine-grained sample $BaTiO_3$ must be of higher internal stress than the coarse-grained sample. This leads to a higher permittivity at room temperature. Moreover, the room temperature permittivity reaches its peak value at a grain size of about 0.7 micron.

As the $BaTiO_3$ ceramics have very high room temperature dielectric properties, they can be used in multilayer ceramic capacitor application. The control of grain size is very important on this occasion.

2.14 Motion of Domain walls with Electric field

The motion of domain walls in ferroelectrics is not simple. In an electric field a 180° wall in $BaTiO_3$ appears to move by the repeated nucleation of steps by thermal fluctuations along the parent wall. Domains misoriented by 180° tend to switch more easily than 90° domain walls since no net physical deformation is required; domains misoriented by 90° are inhibited from changing orientation by the strain that accommodates switching of c and a axes.

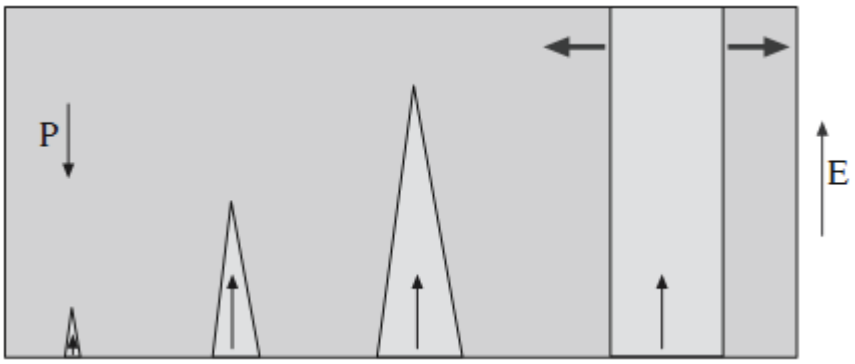

Figure 2.14: Growth of ferroelectric domain under applied field

The almost horizontal portions of the hysteresis loop represent saturated states in which the crystal is a single domain during a cycle. Defects and internal strains within the crystallites impede the movement of domain walls. Domain wall mobility has been found to decrease with time (even without an applied mechanical or electrical stress or thermal changes). This is due to internal fields

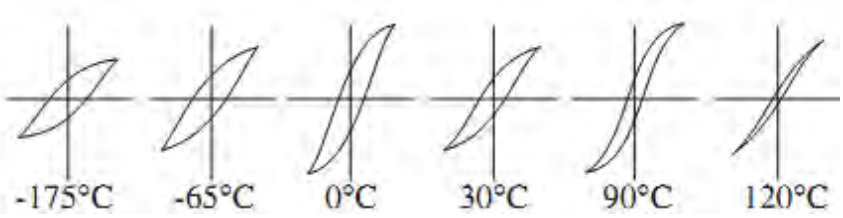

Figure 2.15: Hysteresis loop for Barium titanate as a function of temperature

associated with charged defects, redistribution of lattice strains, and accumulation of defects at domain walls. Figure 2.14 shows the way a domain moves and grows with the application of field.The size of the hysteresis loop also depends on temperature as shown in Figure 2.15. At low temperatures the loops are fatter and Ec is greater, corresponding tothe larger energy requiredfor domain reorientation. At higher temperatures Ec decreases until at $\theta_c$whereno hysteresis remains and the material becomes paraelectric.

2.15 Effect of porosity on dielectric properties

Dielectric constant depends on microstructure, especially on porosity and the number and type of phases. Sintering should provide a ceramic body that would have close to theoretical density, around 95%.

2.16Core shell structure

Core shell structure is found in many sintered materials such as doped barium titanate, silicon carbide, silicon nitride etc.In all these materials grain coarsening occur during sintering in the presence of a liquid phase. It was suggested that during the dissolution of small grains and growth on larger grains, a solid solution in equilibrium with liquid phase was observed to precipitate on the growing grains. Hence a core will have the original composition while the shell will have the composition of the newly formed solid solution.

Near-theoretical densities (~96%) were achieved when the ZrO_2-modified $BaTiO_3$ samples were sintered in the range of 1300 to 1320°C for 2 h. Microstructural observation of the as sintered surfaces revealed a near-uniform grain size as indicated for the modified $BaTiO_3$ sintered at 1320°C [9] (Figure 2.16 (A)). The average grain size of the specimen shown in Figure 2.16 (A) is 0.43 µm. The grain size decreased to 0.36 µm at 1310°C and further to 0.28 µm when the specimens were sintered at 1300°C. TEM evaluation of the microstructure showed the distribution of ZrO_2 to be nonuniform, residing primarily at the grain boundaries.

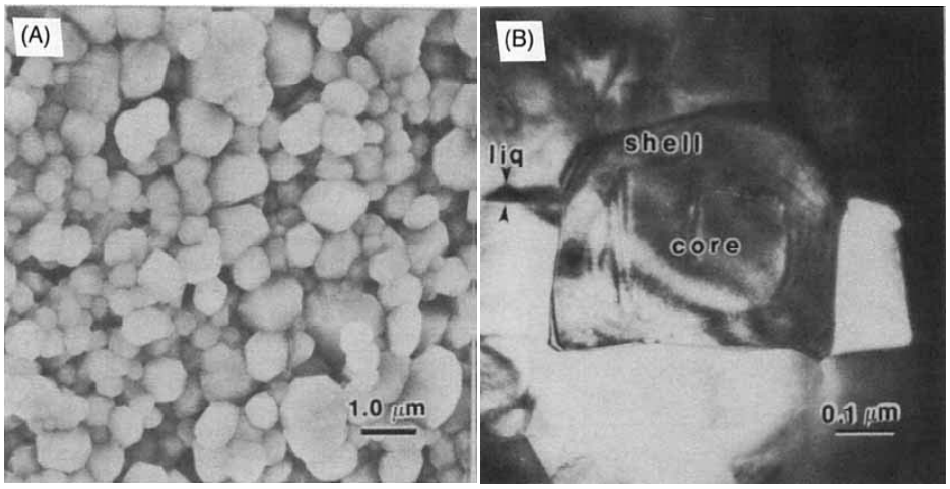

Figure 2.16: Microstructural images of BaTiO3 modified with 2.0 wt% ZrO_2 (A) SEM image of typical as-sintered surface and (B) TEM image of core-shell grain. [9]

Some ZrO_2 diffusion into the $BaTiO_3$ lattice could, however, be inferred from the slight downshift in the Curie peak. Asshown in Fig. 2.16 (B), incorporation of the ZrO_2into the $BaTi0_3$ at 1320°C coincided with the formation of core-shell grains in the microstructure and with liquid formation in the $BaTiO_3$ during sintering [9], as indicated by the arrows in Figure 2.16(B). Samples sintered at 1320°C were comprised of approximately 50 vol% core-shell grains while the ZrO_2modified

$BaTiO_3$ sintered at 1310°C had only *5* vol% of such grains and samples sintered at 1300°C had none. The X-ray intensity distribution, derived from EDS data, of Zr from a typical core-shell grain is shown in Figure 2.17. It can be seen that the relative concentration of Zr decreases as the core is approached and that no Zr is present in the core. The core-shell grains contain, therefore, a core of pure $BaTiO_3$ surrounded by a shell of Zrmodified $BaTiO_3$ [9].

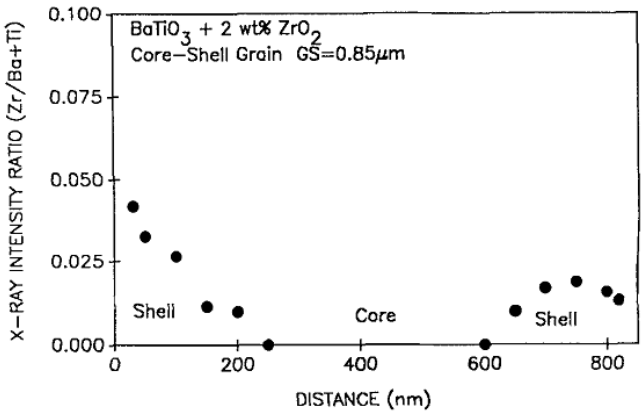

Figure 2.17: X-ray intensity ratio showing Zrdistribution across typical core-shell grain[9]

2.17Sintering of zirconia doped barium titanate compacts

The densification of ceramic compacts is called sintering. The ultimate goal is the removal of pores among the starting particles combined with the growth of grains by strong bonding with the adjacent particles. The requirements for sintering to occur are –

1. Presence of a mechanism for material transport
2. Presence of an energy source to activate and sustain this material transport.

There are a number of mechanisms suggested for sintering to happen. Primarily it happens by diffusion and viscous flow. The whole process is backed by heat energy along with the energy gradients due to particle-particle contacts and surface tension.

Barium titanate matures in the range of 1100 to 1450° C. there are a number of sintering parameters that can be controlled in order to get the desired property in the fired body. These parameters are sintering temperature, soaking time, heating and cooling rate, furnace atmosphere, thermal profile etc. Sintering process depends on the mechanism followed and consequently the texture and microstructure varies. At the initial period of the heating particle bonding occurs by surface

diffusion and else without any densification. The typical green density is found to be around 60%. As the densification proceeds the bonding completes and pores start to remove. At this stage ceramic has a chalky appearance. In this condition the dielectric properties are poor since the dielectric properties are poor for air or vacuum which are contained in the material. Pores are generally eliminated at the 95% of TD. The application of heat causes the trapped gases to escape out by diffusion and grain boundary migration.

If the temperature used for sintering is not enough then the resultant product possesses poor density and significant percentage of pores. Also too high temperature or excess holding time cause the compact to produce open structure with low density and large grain size. This in turn causes low dielectric properties. Sometimes excess temperature results in change of $BaTiO_3$ phase which poses problem in terms of microstructure and property. Hence it is customary to find the best sintering temperature by trial and error. Same argument goes for sintering time. The situation further complicates by the addition of various dopants which needs a different optimum sintering temperatures.

One important thing to consider during sintering is the particle size. Researchers showed that a proper sintering step should increase the particle size to about three to four times of its original size which would actually be the grain size of the material [11]. Therefore it is very important to start with particles as small as possible. Most of the sintering processes nowadays are done with nano powders. Beside the advantage of very fine final microstructure, the use of nano-powders serves some additional purpose. For example, finer the powder size, higher is their surface free energy which could be a great sintering aid. Since finer particles already possess quite an amount of energy, the need for energy during sintering process is reduced which is typically supplied by heat and giving the material the opportunity to become dense by holding at sintering temperatures. With finer particles both of these needs can be minimized therefore maximizing the sintering process. For example, finer particles may be sintered at lower temperatures than for the same material with coarser particles. Or the soaking period may drop to significantly low amount of time for finer particles to yield the same microstructure. The lower the sintering temperature or the soaking time, finer would be the grain size of the material. However, many processesrequire time during sintering, especially if diffusion of one phase into other is involvedfor the final property. In that case two stage sintering can be followed to yield fine microstructure and uniformity of composition across the microstructure.

2.18Applications

Barium titanate is ideal material for electronic ceramic application. Piezoelectric, pyroelectric, ferroelectric ceramics have been successfully applied in many practical applications like capacitors, microphones, transducers, thermistors, self regulated electric heating systems, spark plugs etc. Under the present circumstance of the dielectric behavior of barium titanate based ceramics, capacitor is the widespread application of these kinds of ceramics. There are two kinds of ceramics; single layer and multilayer. Single layer capacitor has pretty straight forward configuration where a dielectric is placed in between two conductor plates. Single layer capacitor has low capacitance capability because of the relative thickness of the monolithic dielectric layer.

In multilayer ceramic application higher capacitance capability is possible due to thinner dielectric layers. Multilayer ceramics are consists of alternate layers of dielectric and electrode material. Each individual dielectric layer contributes to the capacitance as the electrodes terminate in a parallel combination. The layers are kept as thin as possible since the capacitance values increase accordingly.

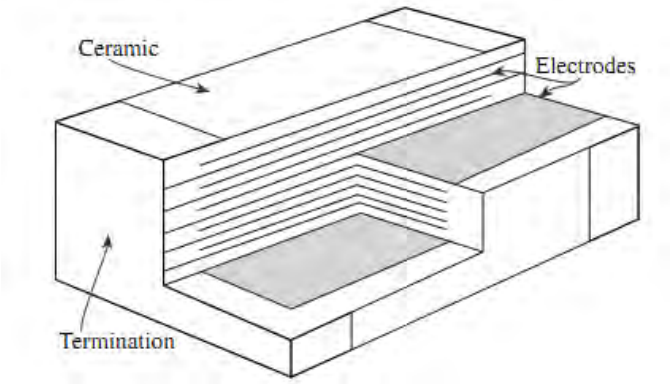

Figure 2.18: Multilayer ceramic capacitors

The advance tape casting technology has made it possible to make dielectric layers less than 20 micron thick. This combined with a high dielectric constant ceramic like barium titanate allows large capacitancevalues to be achieved in relatively small volume capacitor devices.

2.19Analysis of recent work

In 1989, the dielectric properties of barium titanate ceramics with a small addition of zirconia, ranging from zero to two percent was examined and result showed significant influence of such additions with the variation of temperature. Observations with SEM and TEM revealed

microstructural uniformity and retardation of grain growth upon sintering temperature. A new core shell structure has been revealed above 1320°C with TEM. Below 1320°C TEM showed zirconia at the grain boundaries as discrete particles [3]. X-ray diffraction analysis showed a decrease in c/a ratio with a decrease in grain size.

Zirconia has been shown by Brajer [12] and Kulscar [13] to increase the orthorhombic-tetragonal transition temperature in $BaTiO_3$, while slightly lowering the tetragonal-cubic transition.

Ceramic capacitive components typically should have high permittivity for volumetric efficiency and low temperature coefficient of capacitance for circuit performance. These capacitors are based primarily on ferroelectric compounds such as $BaTiO_3$, in which the desirable dielectric properties are obtained by isovalent or aliovalentcation substitution into the perovskite lattice. In small concentrations, substitutions of NiO, ZrO_2, Dy_2O_5 and Nb_20_5 may also act as grain growth inhibitors. These oxides modify the ferroelectric properties by controlling grain size and by suppressing or broadening the Curie peak. Curie peak characteristics, therefore, may be affected by substantial chemical substitution or by inhomogeneities which exist in the sintered material. Zirconia has been shown by Brajer and Kulscar to increase the orthorhombic-tetragonal transition temperature in $BaTiO_3$, while slightly lowering the tetragonal-cubic transition. Hennings [14]el alalso noted this phenomenon and found that the permittivity increasedto a broad maximum as the phase transition points converged. Verbitskaiaet al[15]found that $BaZrO_3$ additions to$BaTiO_3$ had an effect similar to ZrO_2 in that it decreased the axialratio *(c/a)* of the tetragonal phase, in agreement also with resultsby Kell and Hellicar. Similar reductions in the axial ratio havebeen observed with rare-earth additions to $BaTiO_3$[22, 23].In contrast,Molokhia and Issa [16] found that ZrO_2 additions to $BaTiO_3$increased the lattice parameter but had essentially no effect onthe axial *(c/a)* ratio. Additionally, at low ZrO_2 concentration thedielectric constant was observed to exhibit a nonlinear behavior, while the dielectric losses decreased with increasing ZrO_2 content. The nonlinearity of the dielectric constant was attributed to the presence of Zr^{4+} ions on interstitial positions at low zirconia concentrations and on Ti^{4+} sites at higher concentrations. Maurice [17] was able to prepare dense ceramic bodies from oxalate-derived barium titanate which showed a flattened dielectric response to ZrO_2 additions less than 2.0 wt%. This behavior was attributed to ZrO_2 particulate accumulation at the grain boundaries and to suppression of grain growth in the sintered BaTiO3. Armstrong and Buchanan further determined that the ZrO_2, resided primarily at the grain boundaries at sintering temperatures below 1320°C.

The dielectric properties of $BaTiO_3$ ceramics have been shown to be grain size dependent. Fine-grained $BaTiO_3$ exhibits permittivity of 3500 to 4000 at room temperature and values approaching

6000 has been reported. Kinoshinto and Yamaji [18] showed that as the grain size decreases, the permittivity of the material increases and a general broadening of the transition peak results. Martirena and Burfoot[22] have suggested that the room temperature permittivity of $BaTiO_3$ should markedly increase when the transition region is suppressed. However, Arlt[19] have shown that the room-temperature permittivity decreases when the transition region is suppressed. Additionally, it was determined from high-angle X-ray diffraction analysis that the degree of tetragonality decreases with grain size, giving rise to a pseudocubic structure at room temperature. In comparison, Sharma and McCartney [20] have shown that as the grain size of $BaTiO_3$ decreases, predominantly line-broadening effects, rather than distinct structural changes, are observed in the X-ray profile. Shaikh has shown also for metallo-organic-derived $BaTiO_3$, that as the grainsize decreases, the polarization also decreases, supporting earlier work by Jonker and Noorlander [21].

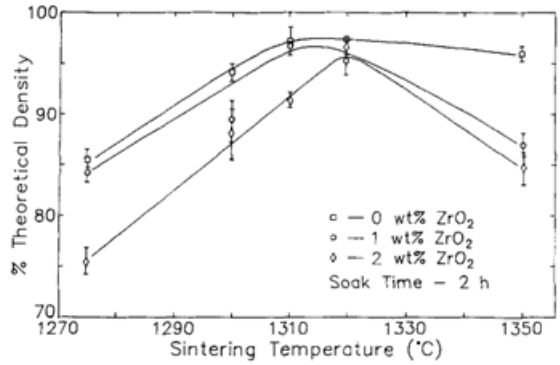

Figure 2.19: Fired density as a function of sintering temperatures for different compositions [3]

According to Armstrong et al [3], the densities of the sintered $BaTiO_3$, compacts increased with sintering temperature up to 1320°C, where maximum density was achieved for samples containing 0 and 2 wt% ZrO_2. For the samples with 1wt% added ZrO_2 maximum density was achieved at 1310°C, and at sintering temperatures above 1320°C the densities for all samples decreased (Figure 2.19).

The effects of ZrO_2 addition to $BaTiO_3$ are compared in the SEMmicrographs of as-sintered surfaces (Figure 2.20) for samples sintered at 1320°C/2 hours. With no ZrO_2 added to the $BaTiO_3$ (Figure 2.20 A), a dense microstructure consisting essentially of large grains (average grain size 32 micron) was observed. With 1 .O wt% ZrO_2 addition (Figure 2.20 B) the fraction of large grains decreased significantly, resulting in a bimodal distribution of large grains in a fine-grain matrix. In contrast, with 2.0 wt% ZrO_2 added (Figure 2.20 C), a microstructure consisting entirely of uniform small grains (average GS 0.8 micron) was obtained. Shown also in Fig. 2.20 is the effect of stoichiometry (Ba/Ti ratio) on microstructural development in the ZrO_2 modified $BaTiO_3$.

Comparison of Figure 2.20 (B) and (D) shows that as the Ba/Ti ratio increased from 0.997 to 1.002 grain size development was severely retarded, the effect being similar to increasing the overall ZrO_2 content.

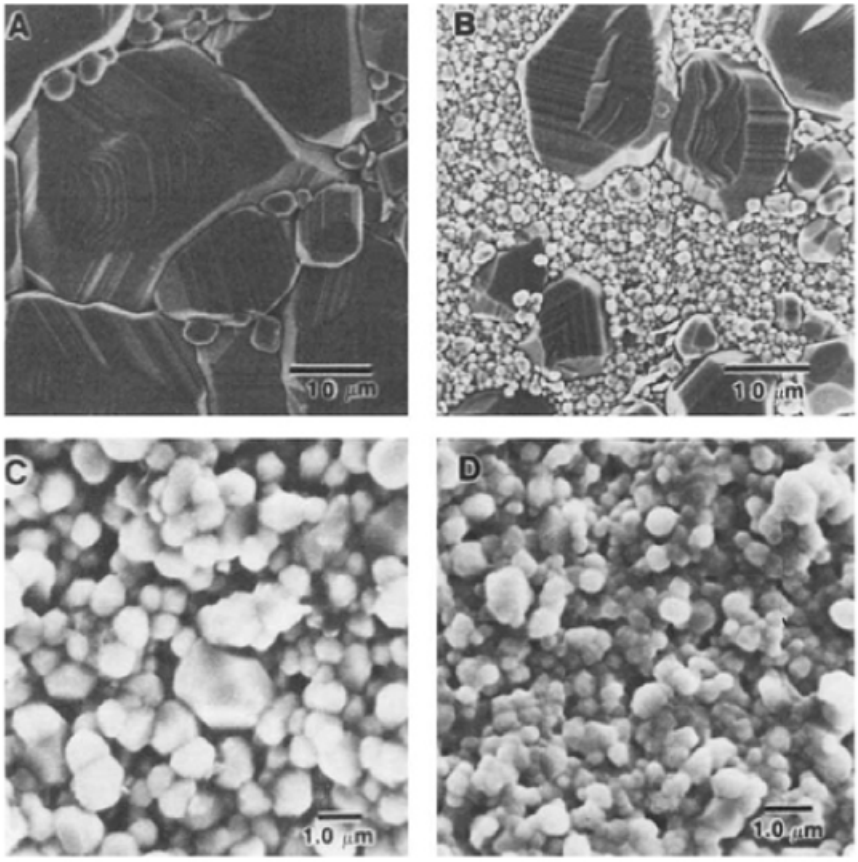

Figure 2.20: SEM image of as fired surfaces showing effect of added ZrO_2 and stoichiometry on microstructure of $BaTiO_3$ sintered at 1320° C for 2 Hours; (A) 0.0 wt%, (B) 1.0 wt%, (C) 2.0 wt % ZrO_2 (Ba/Ti=0.997) and (D) 1.0 wt% (Ba/Ti=1.002)[3]

Figure 2.21shows the progression of microstructural development (1 .O wt% ZrO_2 added to $BaTiO_3$) as a function of sintering temperature from 1310 to 1350°C for a 2 hour soak time. The SEM micrographs show uniform grain sizes for the 1310 and 1350°C samples, with the latter showing significantly larger grain sizes. In contrast, the intermediate temperature at 1320°C showed a transitional bimodal structure between the uniform large and small grain microstructure. It is clear from these data that the addition of ZrO_2 to $BaTiO_3$ suppresses grain growth but that increasing amounts of ZrO_2 (0.5 to 2.0 wt %) were needed as the sintering temperature increased, indicating progressive solubility of ZrO_2 in the $BaTiO_3$ lattice.

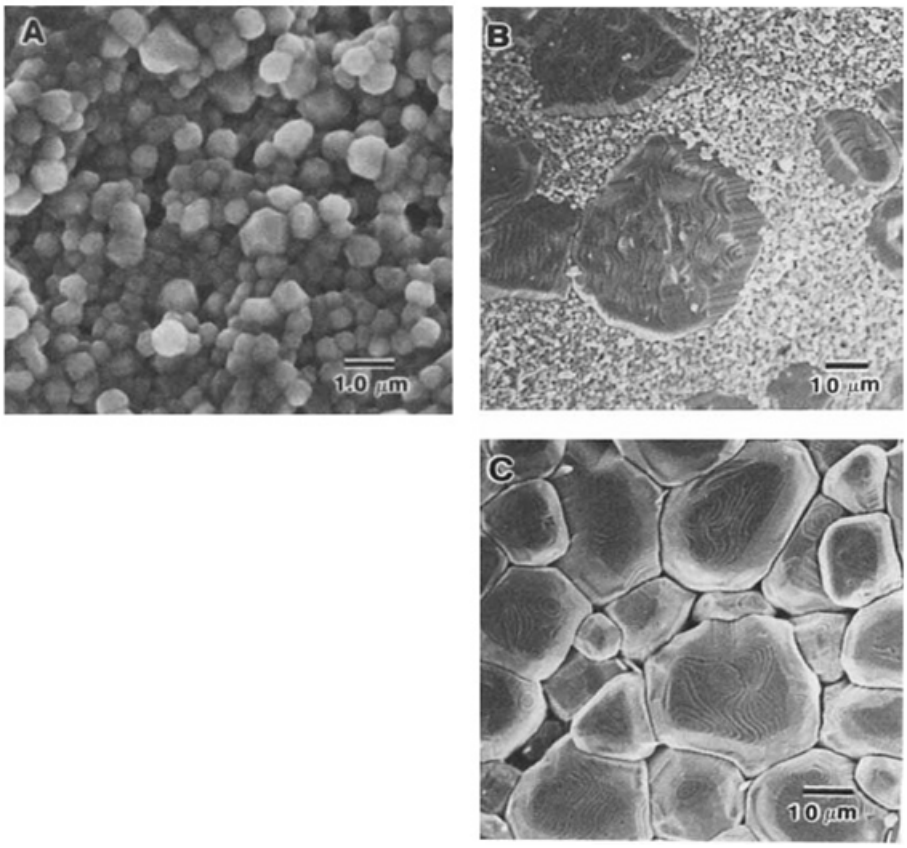

Figure 2.21: SEM images of as fired surfaces showing effect of sintering temperature on microstructure of of $BaTiO_3$;1.0 wt % ZrO_2 (Ba/Ti=0.997) (A) 1310° (B) 1320° (C)1350° for 2 hours soaking [3]

TEM micrographs of the $BaTiO_3$ with added ZrO_2 are shown in Figure 2.22. The presence of ZrO_2 particles along the grains and pore boundaries is evident for samples sintered at 1310°C/2 h (1.0 wt% ZrO_2) as shown in Figure 2.22(A). The ZrO_2 is seen as discrete particles of 0.03 micron corresponding roughly to the initial particle size of the ZrO_2 powder. However, the distribution along the grain boundaries was non-homogeneous. Energy-dispersive spectroscopy analysis of the boundary regions revealed a Zirconium bandwidth of 50 angstrom (5 nm) in samples containing 1 wt% ZrO_2 when sintered at 1300°C, the Zirconium bandwidth increasing to100 angstrom (10 nm) for samples sintered at 1310°C. In contrast, analysis of samples sintered at 1320 and 1350°C (1 .O wt% ZrO_2) showed only small, discrete regions of ZrO_2 at the grain boundaries and at triple points (Figure 2.22(B) and (C)). For the samples sintered at 1350°C, the approximate particle size of the residual ZrO_2 was found to be about 90 angstrom (9 nm).

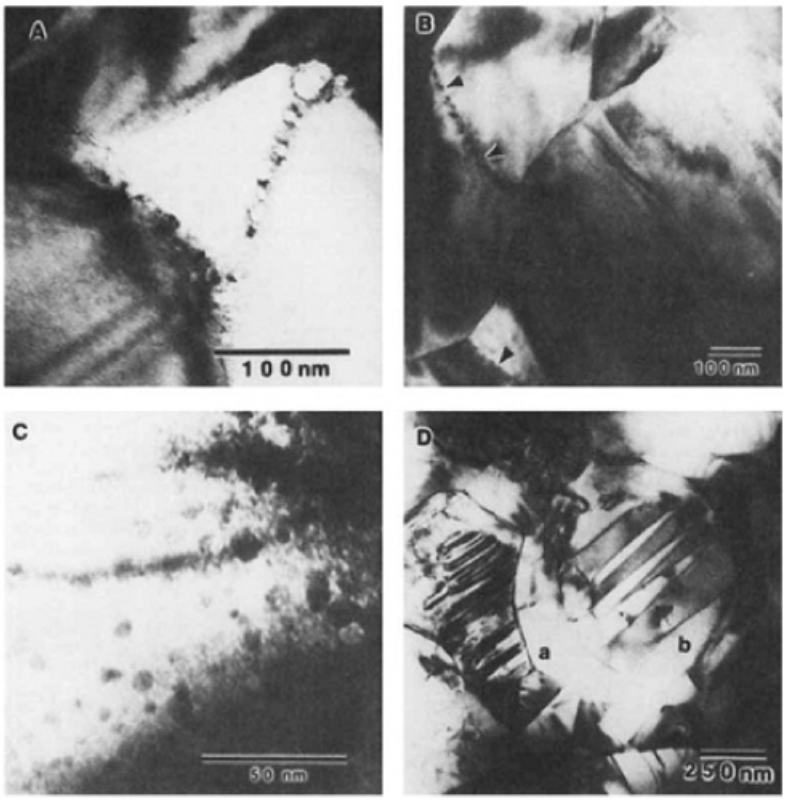

Figure 2.22: TEM images of sintered $BaTiO_3$ with 1 wt% ZrO_2; the ZrO_2 grains along the grain boundaries for samples sintered at (A) 1310°, (B) 1320°, (C) 1350°C (D) Core shell grains [3]

The above observations indicate that Zirconium had diffused into the $BaTiO_3$ lattice above 1320°C, leaving insufficient residual Zirconium along the grain boundaries to inhibit grain-boundary motion, hence the need for higher concentration of added ZrO_2 (e.g., 2 wt%) as the sintering temperature was increased. This is further indicated in Figure 2.22(D), which shows core-shell grains, characterized by a core of pure $BaTiO_3$ surrounded by a shell of Zirconium modified material.

For the grain size range below 1 micron, Figure 2.23 shows the spontaneous polarization to increase almost linearly with increasing grain size. Conversely, the corresponding coercive field decreased with increasing grain size, particularly at the smallest grain sizes, where strain and porosity effects might be expected to predominate. However, for the grain size regime > 1 micron, a logarithmic increase in polarization with increasing grain size was observed.

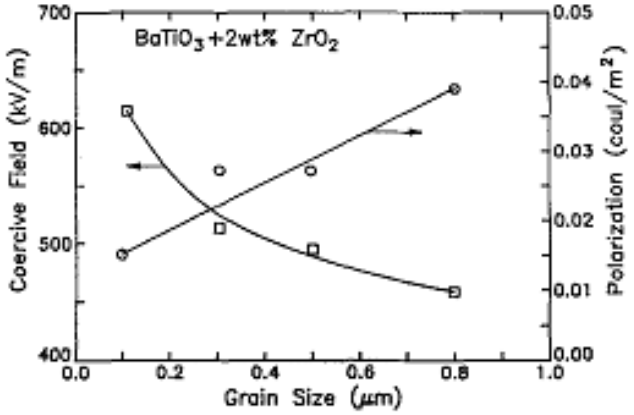

Figure 2.23: Polarization and coercive field behavior in sintered $BaTiO_3$ as a function of grain size [3]

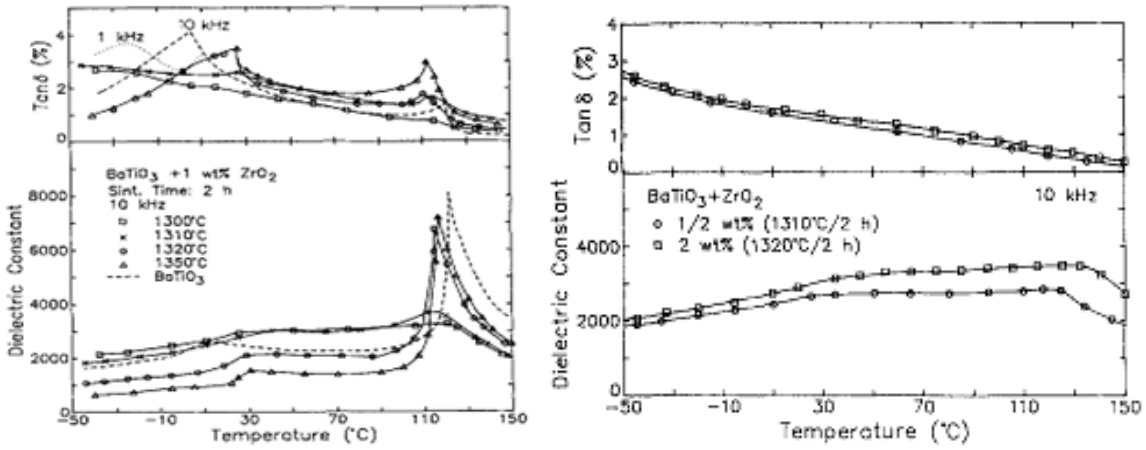

(A) (B)

Figure 2.24: Dielectric constant and loss as a function of temperature [3]

Figure 2.24 (A) shows the permittivity and loss factor, as a function of temperature, for $BaTiO_3$ samples with 1 wt% added ZrO_2 and sintered in the range 1300 to 1350°C for 2hours. The samples sintered at 1320 and 1350°C showed dielectric response and Curie peak characteristics similar to those of the unmodified $BaTiO_3$, over the temperature range 50 to 150°C. However, the Curie temperatures were 8 to 10°C below that of undoped $BaTiO_3$ reflecting some ZrO_2 solubility in the perovskite lattice. The relatively lower permittivity of the 1350°C sample can be attributed to a lower sintered density, larger average grain size, and a higher degree of tetragonality. In contrast, the samples sintered at 1300 and 1310°C showed increased permittivity and suppressed Curie peaks, the 1300°C sample displaying an essentially flat permittivity response between 30 and 125°C. Tan δdata for the 1300°C samples showed a nearly linear decrease with temperature and similarly for the 1310°C sample, except that the phase transition loss peaks were more distinct.

Losses for the 1320 and 1350°C samples were slightly higher, but similar to the unmodified $BaTiO_3$ sample, except for the inward shift of the loss peaks, resulting from the Zirconium diffusion in the $BaTiO_3$ lattice. Comparison of the 1 and 10 kHz tan δ data in Figure 2.24 (A)shows substantial frequency dependence of the loss at low temperature, for these three samples. This phenomenon was absent in the fine-grained (1300, 1310°C) samples, which would indicate that the low temperature loss is more sensitive to domain wall motion

The data in Figure 2.24 (B) summarize the optimal dielectric properties that were achieved from the work of Armstrong for the ZrO_2 modified $BaTiO_3$ system. The samples show full Curie peak suppression, linear tan δ, and an essentially flat or linear permittivity profile over a wide temperature range. Changes in capacitance with applied dc field for the 1.0-wt%- ZrO_2 modified samples sintered at 1300 to 1350°C for 2 h are illustrated in Figure 2.25. Asexpected, samples with the most uniform, fine-grained microstructures (1300°C) showed the smallest capacitance change with applied field, indicative of a lower dissipation factor and higher insulation resistance. The samples with a larger average grain size (and Zirconium resident in the lattice) show a higher capacitance deviation with applied field.

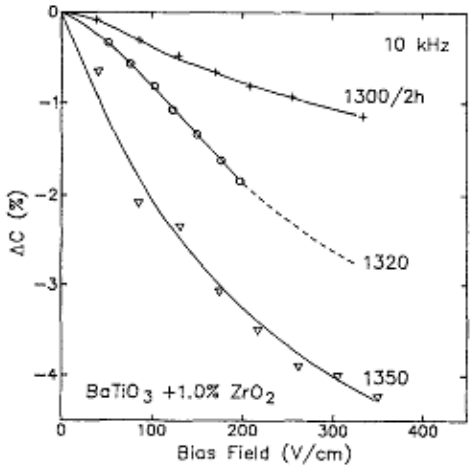

Figure 2.25: Percent capacitance change with dc bias field for 1 wt% zirconia modified barium titanate as a function of sintering temperatures[3]

These specimens all show a flattened dielectric response above the orthorhombic-tetragonal transition and a low tan δ which decreased linearly with temperature. The samples with atomic ratios < 1.000 showed higher permittivity values, this effect being due to the higher density and smaller grain size. No difference was observed in the dielectric response of samples with atomic ratios > 1.000, within the stoichiometric range examined. Tan δ for all three samples was observed to decrease linearly with temperature and showed little significant variation with stoichiometry.

2.20 Performance categories of ceramic capacitors

Z5U: Less than +22% and -56% deviation from the room temperature capacitance over the range +10 to +85°C.

Y5U: Ditto, except over the temperature range of -30 to +85°C

X7R: Less than 15% change (either increase or decrease) in the range of -55 to+125°C

Table 2.1: Coding by Electronic Industries Association for Class 2 ceramic capacitors

Code	Temperature range (°C)	Code	Capacitance change (%)
X7	−55 to +125	D	±3.3
X5	−55 to +85	E	±4.7
Y5	−30 to +85	F	±7.5
Z5	+10 to +85	P	±10
		R	±15
		S	±22
		T	+22 to −33
		U	+22 to −56
		V	+22 to −82

Table 2.2: Composition and properties of Z5U dielectrics

	Composition (wt%)			
Component	1	2	3	Role
$BaTiO_3$	84–90	65–80	72–76	Base material
$CaZrO_3$	8–13	—	—	Shifter
$MgZrO_3$	0–3	—	—	Depressor
$SrTiO_3$	—	7–11	5–8	Shifter
$CaTiO_3$	—	7–11	4–6	Depressor
$BaZrO_3$	—	7–11	7–10	Shifter
$CaSnO_3$	—	—	2–4	Shifter
Other oxides (e.g., Nb_2O_5)	1–3	8–13	0–3	Acceptors
κ (25°C, 1 kHz)	5700–7000	5500–6500	11,500–13,000	
Tan δ	≤0.03	≤0.03	≤0.03	

Table 2.3: Composition and properties of X7Rdielectrics

Component	Composition (wt%) 1	2	3	Role
$BaTiO_3$	90–97	85–92	86–94	Base material
$CaZrO_3$	2–5	4–8	—	Shifter
$BaCO_3$	0–5	—	—	Stoichiometry adjuster
$SrTiO_3$	—	3–6	—	Shifter
Bi_2O_3			5–10	Depressor, flux
Other	2–5	1–4	2–6	
κ (25°C, 1 kHz)	1600–2000	1800	1400–1500	
Tan δ	<0.025	<0.025	<0.015	

2.21Processingofbariumtitanate based ceramics

Incaseofceramicbodies,propertiesofthefinalpartslargelydependontheprocessing route.In the present days bariumtitanate powders are being processed through many routes. Of them, most modern sol-gel precipitation route, chemical precipitation, hydrothermal and combustion reaction are prominent to obtainultrapurepowders.Choicesofroutedependontheapplications.Buttillnowthe conventionalrouteisthemostpopularmethod from the industrialpointofview.Inthe conventionalroutebariumtitanateisprocessedthroughcalciningthebariumcarbonate and titanium oxide togetherata highertemperature. Thismethod is alsoknownassolid-state processingmethod. Simple $BaTiO_3$ powder can also be used. In that case no calcination is required.

Thismethodtypicallyproducesrelativelycoarseandagglomeratedparticlesnotsuitablefortheprocessingo fdielectriclayers in MLCC.Intensivemilling of $BaTiO_3$ in watertoreduceparticlesizeleadstoleachingof Ba^{+2} andastrongpHincrease,whichis detrimental for further processing. Several chemical routes have been proposed to prepare fine andweaklyagglomerated powders. However, most of thesemethodsare more expensivethanthesolid-statereactionandsomeofthemhavesignificantdrawbacks.In particular, powders produced by hydrothermalsynthesis or solution precipitation methods often contain lattice hydroxyl groups that lead to the formation of undesired porosity duringthesinteringofMLCCs.Therefore,itisoflargescientificandpracticalinterestto study the possibility to produce fine $BaTiO_3$ powders with narrow size distribution by solid-state reaction.

2.21.1 Ball milling

The raw materials like $BaTiO_3$, ZrO_2, $Nb_2O_5$are weighed and thoroughly mixed in a ball mill or in an attrition mill. Milling iscarried out to mixtherawmaterialshomogeneously.Bothfinerparticle and homogeneity of raw powders eases the diffusion controlled solid state reactions.TheschematicofaballmillisillustratedinFigure 2.26.

Figure 2.26: Ball milling

The balls should be of the same material as powders so that wear of balls does not contaminate the powder mix. For example, in the past days hardened steel balls were used in a porcelain pot. But iron has a very detrimental effect on the dielectric properties of the barium titanate based materials. At present high density polyethelene (HDPE) pots are used as the container and the Y_2O_3 stabilized ZrO_2 balls are used to mill the powders.

In the wet milling process, milling medium is another important consideration for two reasons. It must not react with the ball, the container, or the powder. Secondly, it must avoid decrease of colloidal stability. For instance, milling of $BaTiO_3$ in water medium causes tribochemical reaction. The reaction forms strongly alkaline $Ba(OH)_2$ which upset the balance, decreasing the colloidal stability of the suspension. Either non-polar liquid such as acetone, alcohol is used for polyelectrolyte stabilizers are used with water. Usually the same setup is used for milling the calcined powder. After milling the suspension is dried to evaporate the milling medium.

2.21.2 Shaping and drying

The milled powder ready for further processing is commonly referred as 'green' body. Thegreen bodies should have a certain minimum density before they can be sintered. Common practice is to achieve 60% of the theoretical density during shaping and pre-sintered state.

The desired shape and a minimum green density can be provided by various techniques including powder compaction, slip-casting, extrusion, doctor blading, dipping, etc. We should go for hot pressing although it is expensive method. But the process is becoming popular for better quality ceramic material used in high end application. The choice of the method depends on the type of powder used, particle size distribution, state of agglomeration, desired shape, and thickness of the part. Hydraulic or mechanical presses are used to press powder into desired shape at the pressure of~100 to 300 MPa. Owing to the nature of this process, only simple and symmetric shape can be prepared. No sintering aid or liquid is added to the powder for solid phase sintering route. Hence, strength of the green powder compact is achieved through addition of a suitable binder such as PVA, glycol phthalate, etc.

After shaping, the green bodies are heated very slowly to between 400-600 ^{O}C in order to remove any binder present. Initial heating rate is slow to allow the gases to come out slowly without forming cracks and blisters in the ceramic part. After the binder burnout is over, the samples are taken to a higher temperature for sintering.

2.21.3 Sintering

The densification of a particulate ceramic compact is technically referred to as sintering. Sintering is essentially the removal of the pores between the starting particles (accompanied by shrinkage of the component), combined with growth together and strong bonding between adjacent particles. The following criteria must bemet before sintering can occur:

1. A mechanism for material transport must be present.

2. A source of energy to activate and sustain this material transport must be present.

The primary mechanisms for transport are diffusion and viscous flow. Heat is the primary source of energy, in conjunction with energy gradients due to particle-particle contact and surface tension.

All properties of ceramic depends on the sintered body which is the direct result of the sintering parameter such as sintering temperature, hold time, atmosphere, thermal profile, etc. There aremany

Sintering methods used but this discussion would be limited to solid phase method. Heat causes the powder particles to develop intergranular bonds by surface diffusion and other physical driving force. The typical green density of ceramic body at the start is about 60% of TD. Strength starts to develop gradually as more and more particles bond.

At about ~80% to 90% density the pores are still open and the ceramic has a typical "chalky" appearance. The dielectric constant is usually low and the T_C is not pronounced strongly. The pores of a ceramic are generally closed at ~95% of TD. Additional heat work causes greater densification as trapped gasses diffuse out along grain boundaries. At densities below 95% of TD the presence of open pores would cause the dielectric loss and undoubtedly inferior dielectric properties.

Setting of sintering temperature is not that straight forward. Low temperature sintering results in ceramic of poor density and formation of Ba_2TiO_4. On the other hand, too high temperature and long hold time may cause open structure with low density. Also, at high temperatures grain growth is accelerated resulting in low dielectric properties. Another harmful hexagonal phase of $BaTiO_3$ may form at the temperature higher than 1460^oC. The sintering temperature and time should be optimum for proper densification to occur without abnormal grain growth. This is usually done by trial and error method depending on various process parameters.

CHAPTER 3
EXPERIMENTAL

3.1 Raw materials and their characterization

Key materials:

Powders of Barium titanate ($BaTiO_3$) nano powder – 100 nm

Manufacturer: INFRAMAT (USA)

Purity: 99.99%

Zirconium oxide (ZrO_2) nano powder – 30/60 nm

Manufacturer: INFRAMAT (USA)

Purity: 99.99%

Niobium Oxide (Nb_2O_5) nano powder – 100 nm

Manufacturer: INFRAMAT (USA)

Purity: 99.99%

Binder: Poly vinyl alcohol

Degree of polarization = 1700 to 1800

Hydrolysis = 98-99

Volatiles = max 5%

Ash = 0.7%

$_P$H of water = 5-7

Table 3.1: Element specification

Components	Atomic number	Atomic weight	Molecular weight	Density (gm/cc)
Barium (Ba)	56	137.33	-	3.51
Zirconium (Zr)	40	91.224	-	6.52
Niobium (Nb)	41	92.90	-	8.57
Titanium (Ti)	22	47.67	-	4.506
Barium titanate($BaTiO_3$)	-	-	233	6.02
Zirconia (ZrO_2)	-	-	123.224	5.89
Niobium oxide (Nb_2O_5)	-	-	265.81	4.60

3.2Sample preparation

In the initial experiments direct mixing of barium titanate and zirconia was carried out. Hence no intermediate calcinations stage was introduced. First, the powders of barium titanate and zirconia are taken at proper amount. Usually a batch of 30 grams of powder was made. Depending upon the percentage of the doped element the amount of raw materials for mixing varies.

Table 3.2: Raw powder requirements for formulation of samples

Doping level	**Powder**	**Wight of powder in batch**	**Notification**
1%	$BaTiO_3$	29.70gm	1% ZBT
	ZrO_2	0.30gm	
2%	$BaTiO_3$	29.40gm	2% ZBT
	ZrO_2	0.60gm	

The powders are taken to a laboratory type pot mill which contains Yttria (Y_2O_3) stabilized zirconia balls. The balls are of two types based on their size. One size is 3 mm and other is 5 mm. The balls and pots must be cleaned ultrasonically to remove slightest of dust which may show up as impurity in the final structure with resultant harmful properties. The balls stay at the bottom and powders stay on balls. Then acetone is added to sufficient quantity which acts as the milling media. After that, the mouth of pot is closed tightly and then shaken to mix the ingredients. Then powders are milled for 16 to20 hours so that all the zirconia can be mixed with barium titanate. After milling the powders containing acetone are separated from the balls very carefully. Then the powders are dried; for quick drying powders are kept at 100°C for 2 to 3 hours. It's very important to dry the powders completely otherwise they cannot be pressed.

3.2.1 Preparation of binder

Binder, poly vinyl alcohol is available in the form of powders. Usually 10 grams of powders are taken in to a bicker to which about 110 ml of distilled water is added. Then the mixture is put onto burner which heats the bicker up to 100°C temperatures. The mixture upon heating will yield significant amount of bubbles and the powders of PVA dissolve into water. At stage no powders will be seen in the water. But there will be considerable quantity of bubbles stuck into the viscous liquid. Keeping them for a while will cool the binder and remove the bubble. At this stage it is prepared to be used for binding the powders.

After drying, the powders are mixed with binders. Preparation of binders is stated below. Usually poly vinyl alcohol is used as binder. For 25 gram sample of powders the required quantity of binder is about 2.5 grams. Upon addition of binders the powders stick together to give a large mass. Hence the binder is added in small quantity at a time rather than adding the whole binder at once. To make sure that the binder is distributed within the powders uniformly, continuous stirring or biting is necessary. It also keeps the powders from agglomeration. Even then the powders tend to agglomerate and hence from time to time the powder is heated for 10 to 15 minutes at 100°C to disrupt agglomeration of powders. The powders may not be pressed at agglomerated condition. It should be made as fine as possible.

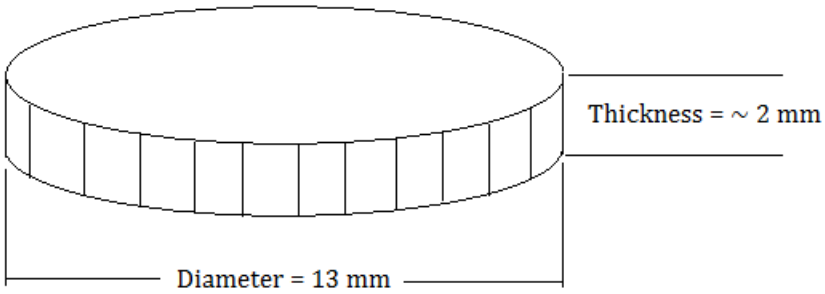

Figure 3.1: The powder compacts after pressing

Before final pressing the powders should be kept at 100°Cfor 30 to 60 minutes to make sure that all the acetone and moisture are completely removed. Afterwards, the powders are taken for pressing. The pressing die has a diameter of 13 mm, so the powders shall have the same diameter. At each pressing 1.5 grams of powder is pressed which gives a disc of about 2 mm thickness. The applied pressure on this occasion is about 150MPa corresponding to approximately 1.80 tons of load.

3.3 Drying and binder removal

After pressing the discs are kept at 110°C for about 3 hours. This will remove any moisture present within the discs.

After drying the sample discs are put into sintering furnace with a suitable sintering cycle. It should be kept in mind that the binder is removed at this stage. At about 450 to 500°C the binder is removed upon soaking for 1 hour.

Control of heating rate is crucial at this stage to avoid warping of sample at high temperatures. Sintering is marked with temperature and soaking time. Proper combination of these two is required to achieve optimum densification and close to percent theoretical density.

3.4 Sintering

A number of cycles are applied to compacts of various compositions which vary principally on the sintering temperature and soaking time. The temperature and the soaking time are modified progressively as the experiment proceeds on trial and error basis.

The dwell time at the primary stages are for the removal of binder. Usually binders' boiling point is 300^0C. Hence holding at 500°C is well enough to get the binder off of the disc. Up to this point it is important to keep the heating rate low otherwise during binder burning sample will crack down. Depending upon the composition and the samples' tendency to warp during sinter the heating rate may be changed at each stage.

Two basic types of sintering cycles were used in the experiments. First one is single-stage-heating and the other is double-stage-heating. In single stage heating the pellets were subjected to heating at one single temperature i.e. 1200 to 1400^0C to achieve densification. In double stage heating the same process is performed at two different temperatures in same cycle. The property of the final material may vary significantly due to these two types of cycle design. The selectivity of the cycles mainly depends upon the type of material and temperature optimization along with holding time is done on a trial and error basis.

Figure 3.2 shows the two types of cycles and two different ways of heating the material in double stage version.

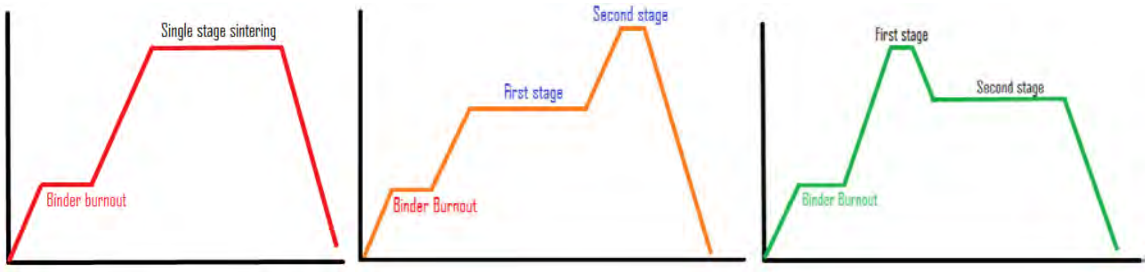

(a) (b) (c)

Figure 3.2: Single stage (a) and double stage heating (b), (c)

In the two versions of double stage sintering it is a possibility that the distribution of doping materials and other defects usual to the material upon sintering will have two different arrangements across the whole ceramic. For the cycle shown in figure 3.2(b) the material apparently will have a better chance to get distributed in the material before final densification. The cycle in figure 3.2(c) presents opportunity to smear out the atomic level defects evolved after sintering.

3.5 Property measurement

3.5.1 Percent theoretical density

After sintering ends sample's dimensions are measured e.g. thickness and diameter using a micrometer. Then the sample is weighed using electrostatic balance. From these data densities are calculated. These resultant densities are then compared to the theoretical densities and are expressed in terms of *percent theoretical density* achieved. Theoretical densities are listed below for the tested compositions.

Table 3.3: theoretical densities of different composition

Material	Theoretical density
$BaTiO_3$ doped with 1% zirconia	6.016
$BaTiO_3$ doped with 2% zirconia	6.013

3.5.2 Microstructure analysis

Although imaging under SEM does not require the surface to be polished, however since the work of this type are done on a trial and error basis, sometimes its customary to apply an etching treatment to visualize the grain boundaries to facilitate decision making for the next step. In that case sample needs to be polished. Usually three types of grit papers are used on this occasion. 500, 800 and 1200/1500 grit papers. These are made by silicon carbide. After progressive polishing on these papers discs are brought for fine polishing on a wheel where alumina powder is used as polishing media. After polishing the samples are ultrasonically cleaned in acetone and then thoroughly dried. Since ceramic sample is not conductive the samples need to be made conductive by applying a gold coating by sputtering technique. The thin gold coating causes the electron to interact with the samples' inner atomic shells so material corresponds and the image can be seen.

3.5.3 Dielectric property measurement

Dielectric properties of samples were measured using an in impedance analyzer [WAYNE KERR 6500B series]. All the measurements were subjected to AC current only. Both room temperature and high temperature frequency dependency were measured. Dielectric constant was measured from the capacitance value obtained from the analyzer according to equation as below –

$$K' = C_p d / \varepsilon_o A$$

Where k' is the dielectric constant, $C_p$is the capacitance value measured by the impedance analyzer, d is the thickness of the sample, $\varepsilon_o$is the permittivity of vacuum, A is the area of the sample in contact with the conducting layer.

A tube furnace type oven and custom sample holder was used at the department of MME. This set up was used to heat the sample during high temperature property measurement.

3.5.4 X ray Diffraction (XRD)

Extent of reaction of dopants with $BaTiO_3$formation was examined by XRD in powder form. The scanning parameters are given below in Table 3.4.

Table 3.4: Operating parameters of X-ray diffractometer

X ray source	CuKα
Tube voltage	40 KV
Current	30 mA
Degree range	20-60^o

CHAPTER 4
RESULTS AND DISCUSSION

4.1 Overview of experiments

The experiments were done in a range of temperatures. Initially experiments were conducted in the range of 1250 to 1300°C for 1-2 hours. Above 1310-1320°C zirconia particles diffuse into the lattice of barium titanate and below that temperature zirconia stay at the grain boundaries and act as inhibitors to grain growth [3]. The resultsfrom the initial experiments were unsatisfactory both from the prospect of microstructure development and dielectric property evaluation. The initial efforts were given to develop only the microstructure of the materials. The grains resulted from sintering below 1280°C were elongated and large accompanied by poor density which was a probable proof of resistance to motion of grains imposed by zirconia particles residing at the grain boundaries. Consequently, the dielectric constants of the samples found to be less than 1200. Due to high amount of porosity in the structure it was concluded that the sintering might have not been completed due to incoherent combination of sintering temperatures and soaking time.

Since the grain sizes were large and elongated in shape, attempts were made to increase the temperature keeping the soaking time unchanged in order to bring the grains to a uniform regular shape. After a number of attempts, the grain size became spherical and uniform in shape in the temperature range of 1300 to 1320°C; the grains were getting large as proposed in the work of Armstrong et al [3] since zirconia particles prefer moving into the lattice of barium titanate rather than staying at the grain boundaries at this temperatures. However, the percent densification remained below 85% of theoretical density and grain size remained in the range of 10 to 20 micron which was considered quite high and unsatisfactory. Therefore attention was focused on improving the density and microstructure of the sintered samples. Without the concern for grain size, experiments were done to improve the density of the samples by increasing the holding time. The best result in this series was achieved at 1290°C for 5 hour sintering; which yielded 89% of theoretical density. Surprisingly the grain size for 1% zirconia added samples showed significant improvement with a bimodal distribution of grains ranging from 1 micron to 25 micron.

At this point, double stage sintering was introduced in order to improve the microstructure through controlled movement of particles at the initial stage of sintering. It was assumed that at higher temperatures, if shorter soaking time was provided, the samples would just have enough time to rapidly move closer to each other and then start forming necks. Then the samples would be held at lower temperatures to promote appropriate sintering without allowing grain growth. However it still was important to recognize the behavior of the samples at first stage, the higher temperatures, in the sintering cycle. In light of this theory the samples were sintered starting from 1340°C for 45 minutes soaking time (which was 1-2 hours in the earlier experiments). It was found that the density

resulted was in the range of 86-88% of theoretical values with 5-20 micron sized grains. This study showed that the majority of the densification happens at the first stage and that may be used appropriately to get a very highly dense structure. Keeping the temperature fixed at 1340°C, the soaking time was gradually decreased to zero minute sintering and it was found that both density and microstructure were improving for the 1% and 2% zirconia added samples. Sintering at 1340°C for zero minute yielded percent theoretical density in the range of 92 to 94% and the grain sizes were reduced to 2-10 micron in size. In later attempts to reduce the grain size, the temperatures were reduced gradually from 1340°C to 1290°C at which the best possible combination of density and microstructure was achieved. The density was found to be 95-96% of theoretical density and the grains were found to be as small as 0.5 micron. However, some microstructure showed bimodal distribution of grains and they varied from as small as 500 nm to 5 microns. Further reduction in temperature showed decrease in percent theoretical density and deteriorating microstructure in terms of grain sizes. At this point, the attempt to double stage sintering yielded the best sintering condition at its first stage of sintering.

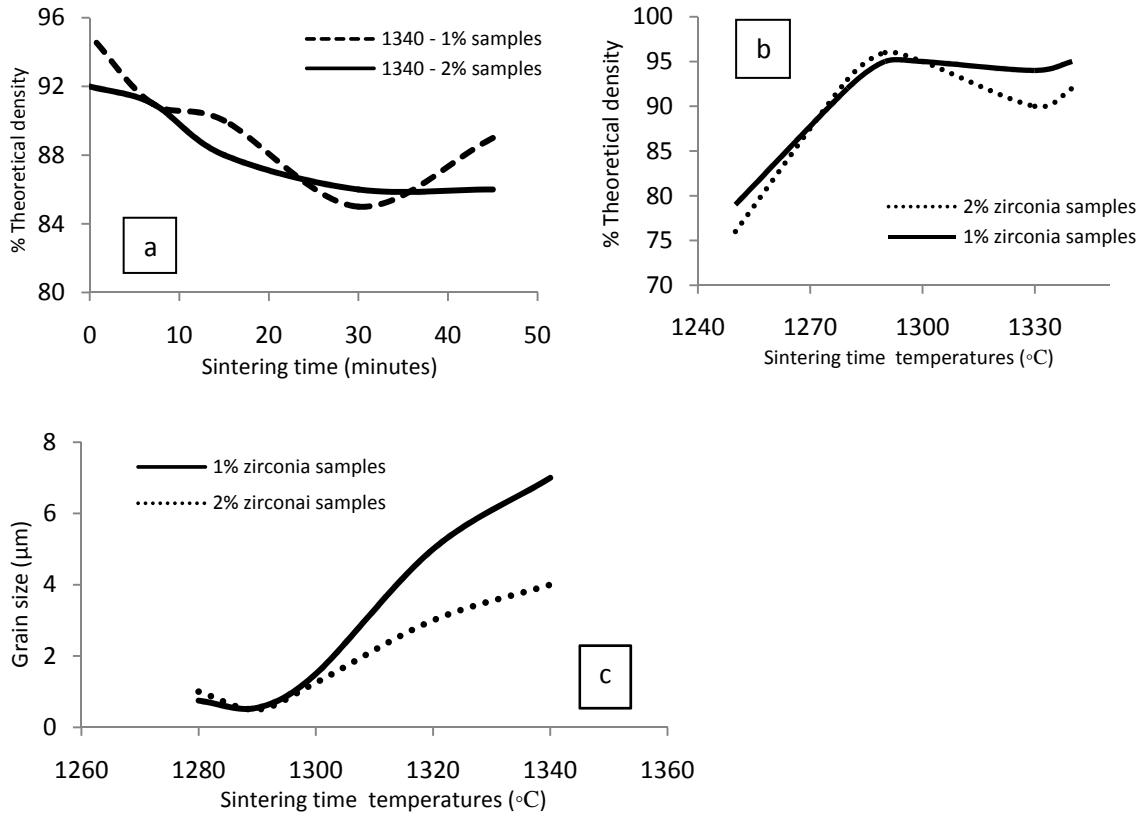

Figure 4.1: Variation of % theoretical density with sintering time at 1340°C (a); Variation of % theoretical density with sintering temperature for 0 minute sintering (b); Variation of grain size with sintering temperature (c)

This study gave the assumption that the improved grain size would contribute to dielectric properties. However, when measured, the dielectric properties were found to belower than expected values. K values were even less than that of pure barium titanate. From the analysis of earlier works of Armstrong [3] it was already established that the dielectric constant of zirconia doped barium titanate would largely depend on the way of zirconia reaction during sintering. Zirconium ion may either get into the octahedral void of barium titanate where it replaces titanium from that void or it can stay at the grain boundaries to resist grain growth which is accompanied by large strain in the barium titanate lattice and a reduction in tetragonality [3]. Since the samples regarding this problem were given no soaking time at sintering temperature, hence it was concluded that at that sintering cycles zirconia had not have the opportunity to diffuse successfully into barium titanate and therefore a pseudocubic strained lattice might have formed.

In the later studies, sintering cycle was designed to facilitate zirconia diffusion into barium titanate. For example, the samples were subject to double stage sintering where they were kept within the temperature range of 1290℃ at first stage of and then down to 1150 to 1250℃ for 1 to 15 hours and zero minute holding at second stage of sintering. From the viewpoint of microstructures the samples heated at 1200℃ or more showed the tendency to excess grain growth. Some samples showed a high amount of porosity in the structure. Below 1200℃ there were no significant variations of the microstructure from that of the samples sintered directly at 1290℃ with zero minute holding. The K values for samples sintered up to 5 hours were found to be in the range of 1000 to 1500. However, second stage sintering at 1150℃ for 15 hours yielded K values as high as 3200.

In light of the previous experiments, the study with samples of stoichiometric composition became necessary. The tests were performed with only one composition, $BaTi_{0.80}Zr_{0.20}O_3$. The samples were sintered in the range of 1250 to 1320℃ and since there was no need for diffusion the samples were subjected to zero minute holding at sintering temperatures to resist grain growth.Grain size resulted were in the range of 1to 5 microns. However, the dielectric constants were found to be as higher than that for zirconia added samples with complete suppression of curie peak and a decreasing trend of permittivity with increasing temperatures. For example the dielectric constants at temperatures ranging from 20 to 60℃ were found to be in the range of 6,000 to 3,000 at frequencies ranging from 100 Hz to 10KHz. The best dielectric constants were found from sintering at 1290℃. Below this temperature, porosity in the structure tends to increase and hence caused lower dielectric constant.

X-ray diffraction of the samples was carried out for both zirconia added and zirconia doped samples as well as pure barium titanate samples. There had not beenmuch variation in XRD plots for the pure barium titanate samples and zirconia added samples since the amount of zirconia present were really low and hence could not affect the reflection pattern by much. However, one important observation was that the twin peaks marking the tetragonality in barium titanate were disappeared from the plot of pure barium titanate to that of 1 and 2% zirconia added and 20% zirconia doped samples. The XRD data also showed marked reduction in lattice spacing and c/a ratio of the material due to sintering and hence indicated reduced tetragonality.

In later parts of this research, niobium oxide was also added by molar concentrations to barium titanate. In those experiments, samples were directly treated at the sintering conditions that were applicable to zirconia addition. For these samples 0.2 to 0.4% molar concentrations of niobium oxides added to barium titanium were used. The samples were tested with both single and double stage sintering within the temperature range of 1250 to 1300°C for zero minute to 2 hour holding. The samples sintered for zero minute yielded the best percent theoretical density achievement. The 0.4 mole% samples were most difficult to dense. However the best density was achieved for 0.3mole% samples.

Microstructural observations revealed that the amount of pores is much higher for the 0.4% samples than the other two compositions as seen from the density of these samples. The grain size of the samples remained quite fine for almost all the compositions. The grain size varied from 500 nm to 1.5 micrometers. Throughout the structure the grain were found uniform in size and one of the possible reasons behind good dielectric properties of the material.

Dielectric properties were measured within the range of 100 Hz to 10 KHz. Zero minute sintered samples yielded the best dielectric properties in majority of the cases for any of the sintering temperatures. Samples sintered at 1275°C gave the highest dielectric constant values. For various compositions the values varied from 3,000 to 7,000. From the composition point of view, 0.4 mol% niobium oxide doped samples gave the highest dielectric constants.

4.2 Summary of key experiments and results:

	First stage heating (°C)	Rate (°C/min)	Soaking time (minutes)	Second stage heating (°C)	Rate (°C/min)	Soaking time (minutes)	% TD	Grain size (µm)
1%	1250	2	600	--------	--------	--------	82.3	--------
2%							75.8	--------
1%	1280	2	300	--------	--------	--------	89	5
2%							78	12
1%	1300	2	300	--------	--------	--------	78	16
2%							75	12
1%	1320	5	300	--------	--------	--------	84	14
2%							84	7
1%	1320	5	150	--------	--------	--------	88	12
2%							87	8
1%	1320	5	120	--------	--------	--------	80	9
2%							84	5
1%	1290	5	300	--------	--------	--------	85	13
2%							82	8
1%	1290	5	180	--------	--------	--------	85	7
2%							81	10
1%	1340	5	45	--------	--------	--------	89	25
2%							86	8
1%	1340	10	30	--------	--------	--------	85	13
2%							86	9
1%	1340	10	15	--------	--------	--------	90	9
2%							88	6
1%	1340	10	7	--------	--------	--------	91	7
2%							91	5
1%	1340	10	0	--------	--------	--------	95	7
2%							92	4
1%	1330	10	0	--------	--------	--------	94	5
2%							90	3
1%	1330	20	0	--------	--------	--------	91	--------
2%							82	--------
1%	1300	10	0	--------	--------	--------	95	1.5
2%							95	1.25
1%	1290	10	0	--------	--------	--------	95	0.55
2%							96	0.5
1%	1280	10	0	--------	--------	--------	92	0.75
2%							93	1
1%	1250	10	0	--------	--------	--------	79	--------
2%							76	--------
1%	1290	10	120	--------	--------	--------	90	4
2%							90	3
1%	1290	10	0	1180	3	120	90	1.1
2%							90	1.4

	First stage heating (°C)	Rate (°C/min)	Soaking time (minutes)	Second stage heating (°C)	Rate (°C/min)	Soaking time (minutes)	% TD	Grain size (µm)
1%	1290	10	0	1150	10	120	90	0.7
2%							93	0.6
1%	1290	10	0	1150	10	300	89	--------
2%							90	--------
1%	1290	10	0	1150	10	900	91	0.5
2%							95	0.5
1%	1000	10	0	1290	5	0	96	0.5 to 0.7
2%							95	
1%	1150	5	0	1290	5	0	93	
2%							90	
1%	1150	10	120	1290	10	0	92	
2%							91	
1%	1150	10	240	1290	10	0	96	
2%							96	
1%	1180	10	240	1290	10	0	97	
2%							96	
1%	1180	10	360	1290	10	0	93	
2%							94	
1%	1200	10	30	1290	10	0	95	
2%							94	
1%	1200	10	60	1290	10	0	94	
2%							90	

4.3 Development of microstructure

According to Armstrong et al [3] zirconia added barium titanate can be sintered to around 96% of theoretical density by heating at around 1300 to 1350°C. However the best possible combination of density and microstructures were achieved at 1320°C in their experiment. The sintering temperature in this thesis started from 1250°C for 2 hours. The resulting geometry was elongated grains with a lot of visible porosity in the microstructure. Accordingly the percent theoretical density achievement was just over 70%.

Keeping all other parameters fixed, the temperatures were raised up to 1280°C, which did not bring any discernible difference to microstructure or the densification.

Based on the fact that the grain shapes were elongated along with a lot of porosity in the structure, it was assumed that higher temperature might have been required to complete the sintering. Hence temperature was increased from 1280 through up to 1340°C in various experiments.

The experiment with 1300°C for 2 hours did not yield a satisfactory outcome, so the soaking time was increased. This design was done on the assumption that increasing the temperature too much would cause grain growth. Initially as high as 5 hours of soaking time with 2°C/min of heating rate were chosen at this temperature.

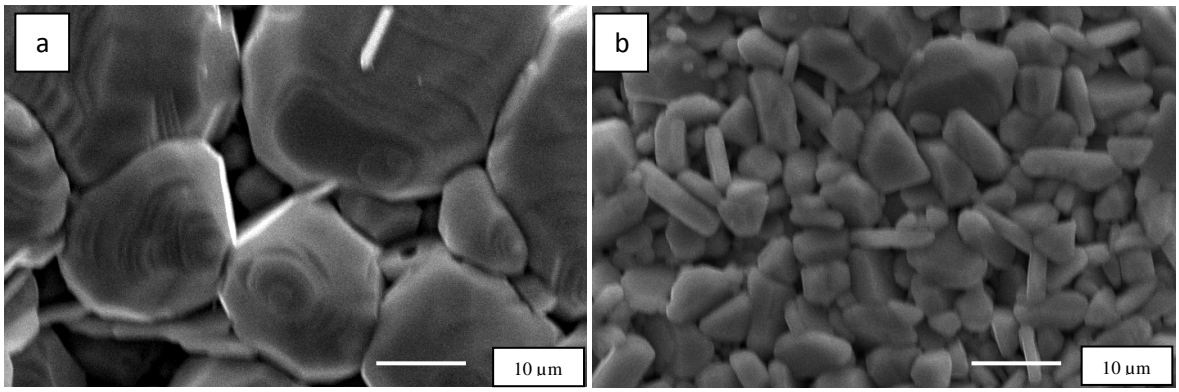

Figure 4.2: Samples sintered at 1300°C for 5 hours at 2°C/min; 1% (a) and 2% (b) Zirconia added Barium Titanate

As it can be seen from the micrograph (figure 4.2), the grains for 1% **zirconia added barium titanate (ZBT)** suffered significant grain growth and the 2% ZBT sample had still a lot of elongated grains. The percent theoretical density for these samples was 81% and 77% respectively. The temperature seemed to have affected differently to 1 and 2 % ZBT samples. It was as if the temperature was too high for 1% ZBT samples but not enough for 2% ZBT samples. Therefore the temperature was raised a little bit to 1320°C for 5 hour soaking with a higher heating rate of 5°C/min. The resulting microstructures are shown in figure 4.3.

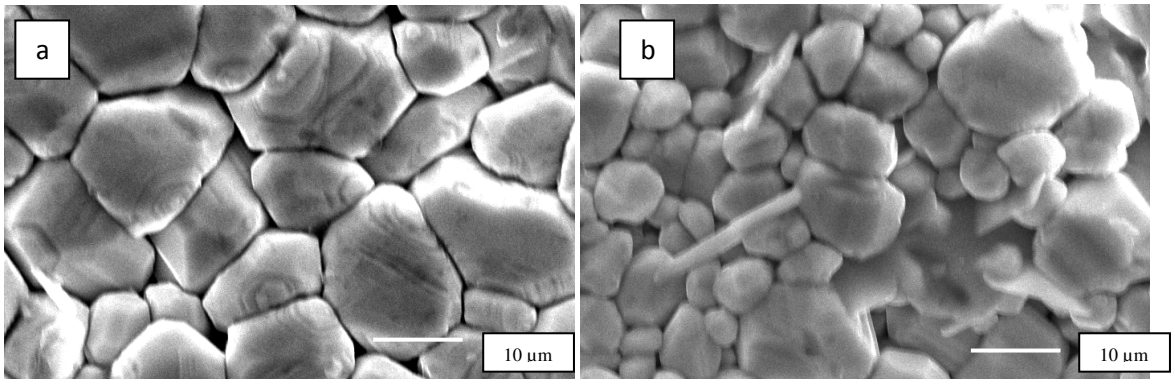

Figure 4.3: Samples sintered at 1320°C for 5 hours at 5°C/min; 1% (a) and 2% (b) Zirconia added Barium Titanate

The micrograph shown a significant improvement in both the samples. For 1% sample, The grains are little finer now and the elongated grains in 2% samples are gone. The achievement of percent theroretical density also improved to 84% for both the samples.

At this level the temperature 1320°C was kept fixed with the soaking time being reduced to 2 hours and a heating rate of 5°C/min. The accompanied microstructures are shown in figure 4.4.

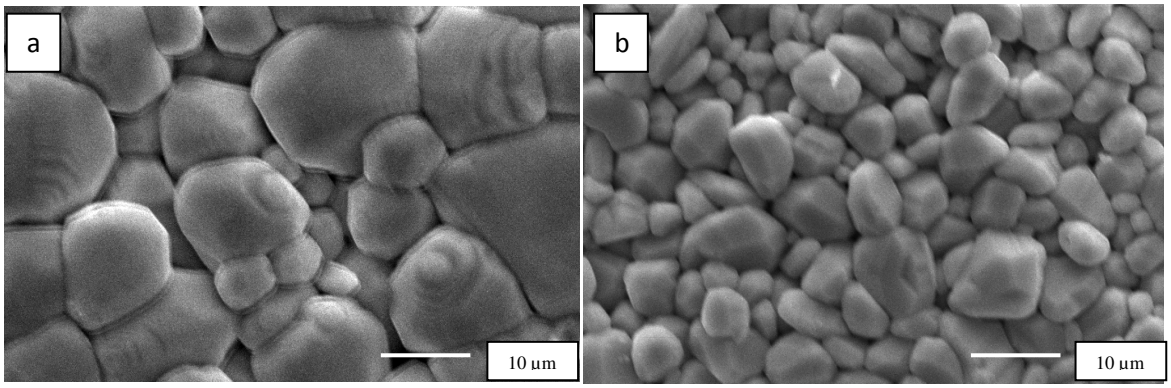

Figure 4.4: Samples sintered at 1320°C at 2 hours at 5°C/min; 1% (a) and 2% (b) Zirconia added Barium Titanate

For 1% sample, the grain size varies in a more wide range as a result of lower soaking time. This sintering caused further improvement in the percent theoretical density as well, as the values go up to 88 and 87% for 1 and 2% ZBT samples respectively. Further reduction in soaking time at this temperature (1320°C) did not bring any significant variation in microstructures; however the percent theoretical densities dropped to lower than 85%, therefore no further investigation followed that way.

At this level, temperature was reduced to lower values. Attempt was made at 1310, 1300, 1290°C. Among these results, sintering of 1% ZBT sample at 1290°C for 5 hours at 5°C/min revealed the bimodal distribution of grains (figure 4.5) which are typical in many ZBT samples. However that trend was not strongly found in 2% ZBT samples. The smaller grain size in 2% sample indicates that the amount of zirconia is more effective to act as grain growth inhibitors. The percent theoretical densities were 85% and 82% for 1 and 2% samples respectively.

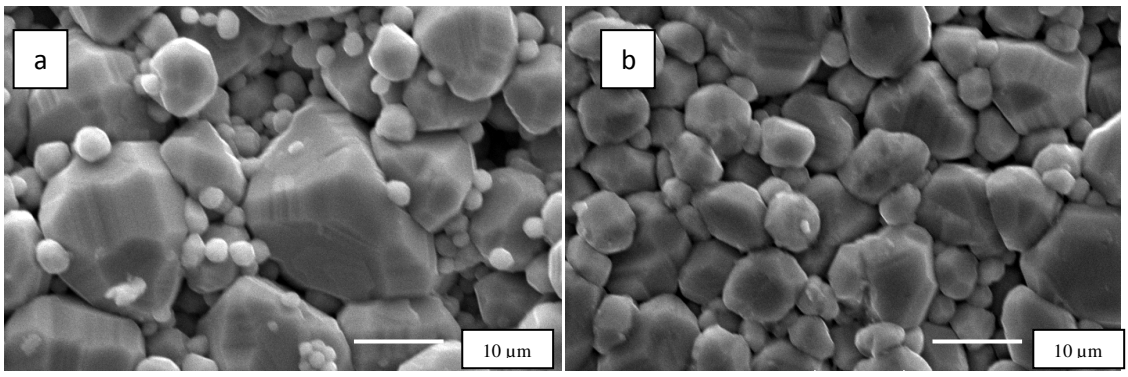

Figure 4.5: Samples sintered at 1290°C for 5 hours at 5°C/min; 1% (a) and 2% (b) Zirconia added Barium Titanate

When sintering was followed at the same temperature for 3 hours at 5°C/min, it was found (figure 4.6) that the grains in 1% ZBT sample gets finer. No significant variation was found for 2% ZBT sample. Densities were the same as that for 5 hours sintered samples.

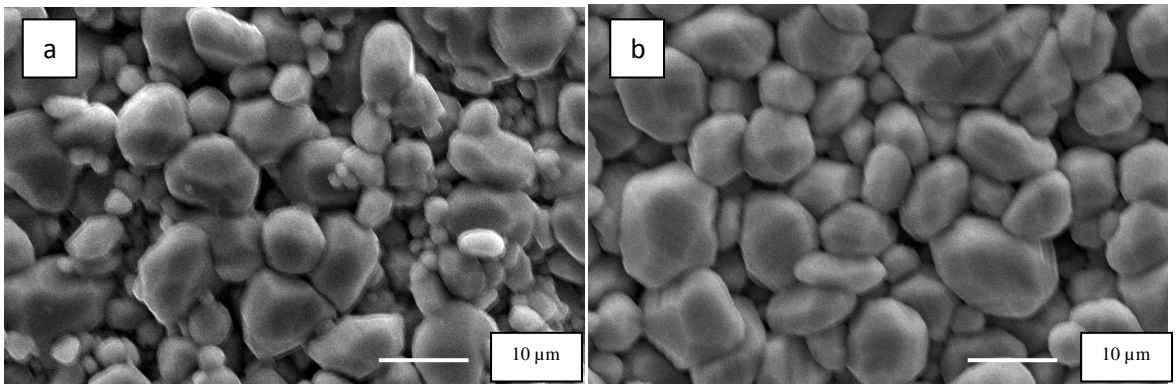

Figure 4.6: Samples sintered at 1290°C for 3 hours at 5°C/min; 1% (a) and 2% (b) Zirconia added Barium Titanate

Further reduction in soaking time did not bring any notable difference in microstructures.

At this point some alternate sintering way was aspired to yield a better composition of percent theoretical density and microstructure. In this regard, two step sintering process was adopted. The aim was to allow the particles to close the gap as much as possible at first stage of sintering which is usually a higher temperature than that at second stage. In second stage of sintering, particles undergo densification at a lower temperature without much risk of grain growth. But since that requires the full knowledge of material condition after the first stage, hence the first stage behavior was investigated in a number of attempts.

Firstly, a high sintering temperature was chosen as the first stage temperature, sintering was done for a specific period and then cooled down to room temperature. Initially sintering was done at 1340°C for 45 minutes at 5°C/min. The resulting grains (figure 4.7) were too large to set 1340°C as the first stage temperature. The structures were as follows –

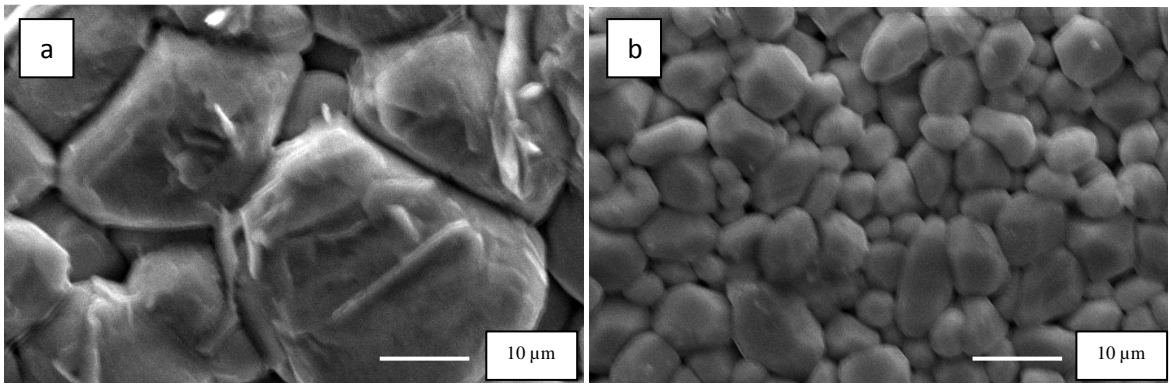

Figure 4.7: Samples sintered at 1340°C for 45minutesat 5°C/min; 1% (a) and 2% (b) Zirconia added Barium Titanate

The densities for 1 and 2% samples were 89 and 86% of theoretical density, respectively. As it can be seen from the figuer 4.7, for 1% samples both the temperature and 45 minutes of sintering time is too high and it looks like as if the surface were melted.That did not occur for the 2% ZBT sample since it contains higher amount of zirconia. Usually barium titanate has a phase $Ba_6Ti_{17}O_{40}$ that melts at around 1310°C and lower amount of zirconia have not been able to resist that.

At the later stages, two subsequent modifications were brought about in the sintering parameters. Keeping the sintering temperature same, sintering time was reduced to 30 minutes and the heating rate was raised to 10°C/min so the effective sintering time would be mcuh less than that in the earlier stages. The resulting microstructures (figure 4.8) shown improvement in samples for 1% ZBT samples and not in 2% sample. The values of percent theoretical densities were almost same as in the earlier cycles.

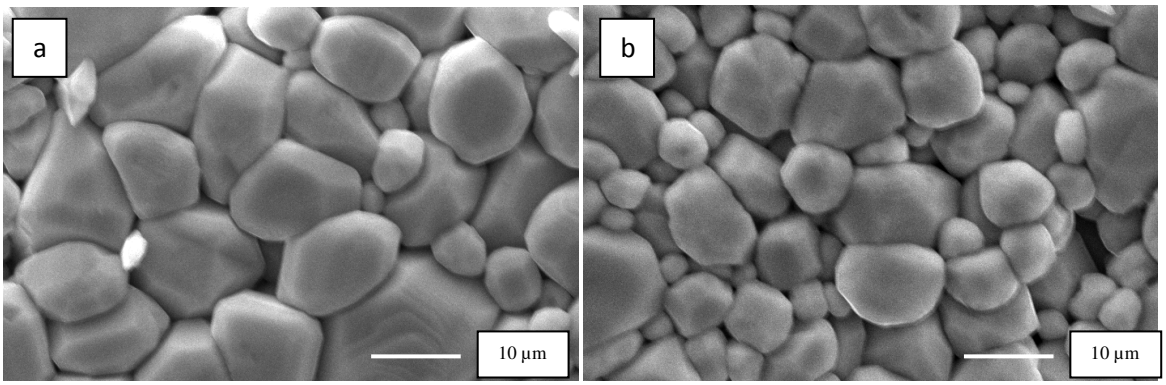

Figure 4.8: Samples sintered at 1340°C for 30 minutes at 10°C/min; 1% (a) and 2% (b) Zirconia added Barium Titanate

Later, sintering was done at the same parameters for 15 minutes (figure 4.9), 7 minutes and then for 0 minute (figure 4.10). After sintering the grain size for 1% ZBT sample had improved significantly with a consequent increase in percent theoretical density to 90%. The 2% sample also showed improvement in its densification and grain sizes.

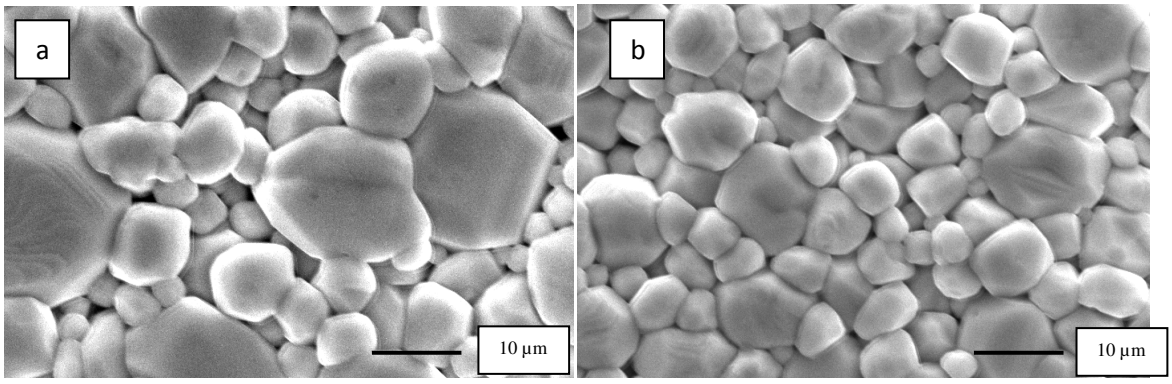

Figure 4.9: Samples sintered at 1340°C for 15 minutes at 10°C/min; 1% (a) and 2% (b) Zirconia added Barium Titanate

The percent theoretical densityfor 1 and 2% samples sintered at 1340℃ for 0 min is 95 and 92% respectively.

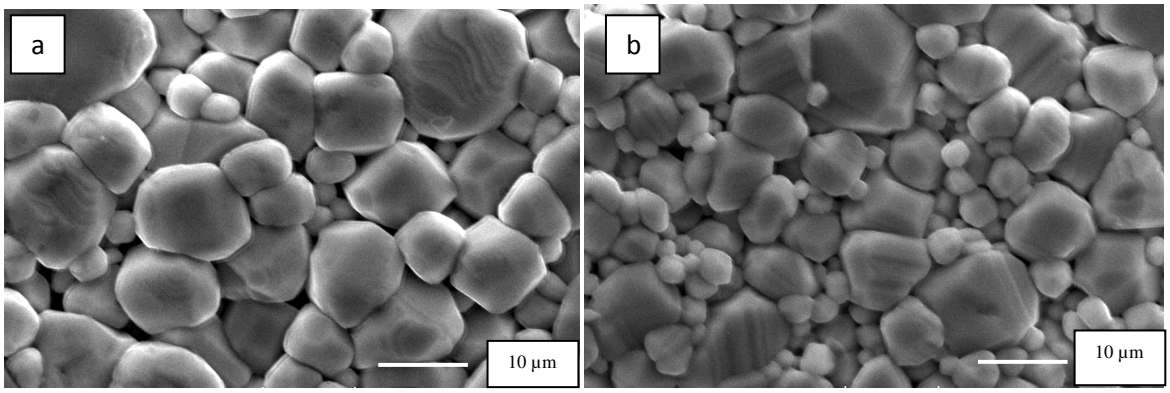

Figure 4.10: Samples sintered at 1340°C for 0 minute at 10°C/min; 1% (a) and 2% (b) Zirconia added Barium Titanate

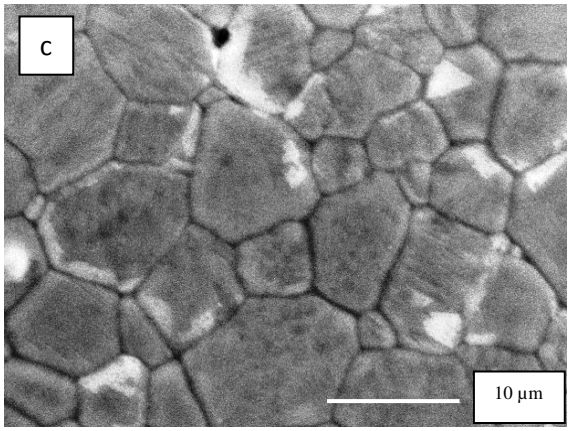

Figure 4.10: Pure $BaTiO_3$ Samples sintered at 1340°C for 0 minute at 10°C/min (c)

As it can be seen (Figure 4.10(a)) that the grain size for 2% ZBT sample for 0 minute sintering has improved to average grain size of 7 micron. For 1% sample which is still quite high, around 10 micron. The effect of zirconia addition can be seen from figure 4.10(b) which shows pure barium titanate being subject to same sintering parameters. 2% zirconia addition has much stronger effect on reducing the grain size than 1% zirconia added samples. There is a good chance that zirconia might have diffused into the structure of barium titanate at this temperature.

At this level since the sintering time variable has been maximized, therefore no alternate is left but to reduce the temperature of the first stage sintering process. It was fair to remember that these experiments were done so as to set the first stage of the double stage singering process to increase the density as much as possible with the finest grain size of the microstructure. Until now the percent theoretical density has been brought to a good magnitude but the grain size is yet to be optimized.

When sintering was done at 1330°C for 0 minute at 10°C/min, the resulting microstructures were (Figure 4.11) –

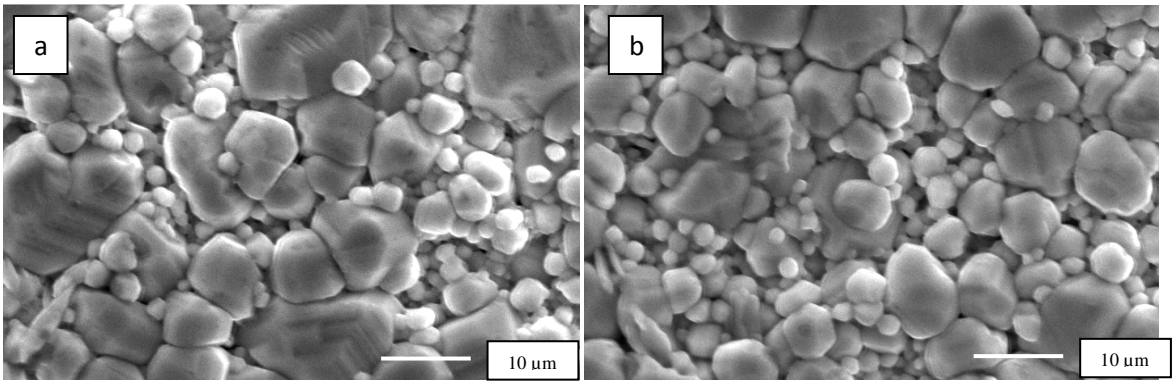

Figure 4.11: Samples sintered at 1330°C for 0 minute at 10°C/min; 1% (a) and 2% (b) Zirconia added Barium Titanate

The percent theoretical densities of the structures were 94% and 90% respectively for 1 and 2% samples. In both the structures, the amount of smaller grains is increasing significantly from the previous structures. The average grain sizes in the two structures are 6 and 5 micron respectively.

After this the heating rate was raised to 20°C/min from 10°C/min. The structures (Figure 4.12) showed no significant improvement, however higher heating rate caused warping to the structure.

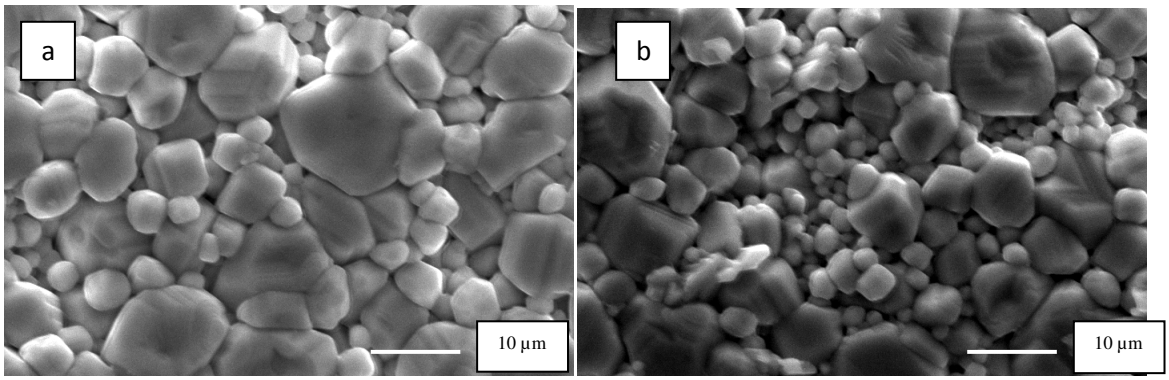

Figure 4.12: Samples sintered for 1330°C for 0 minute at 20°C/min; 1% (a) and 2% (b) Zirconia added Barium Titanate

Sintering was then done at 1300°C for 0 minute at 10°C/min. The densities of the resulting microstructure (figure 4.13) were 95% for both 1 an 2% ZBT samples. The microstructures shown a very rapid change in microstructure to a very fine grain size for a difference of 30°C. the average grain sizes for the two samples here are 2 micron.

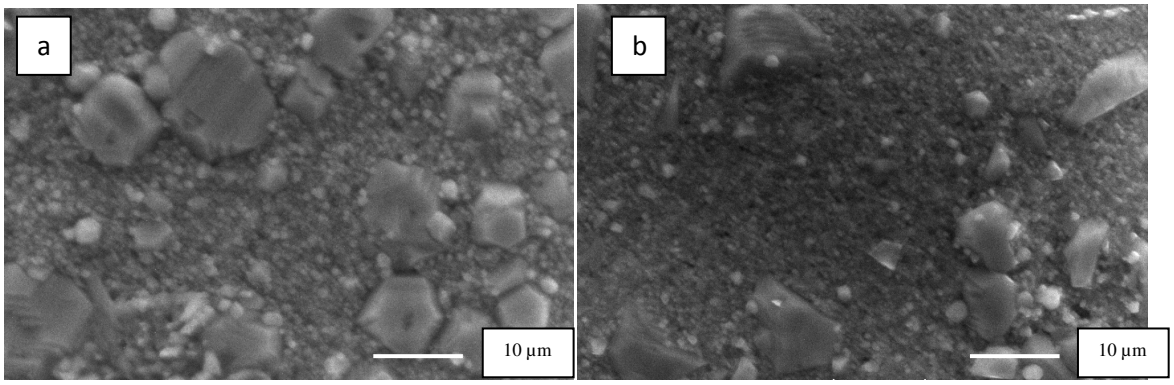

Figure 4.13: Samples sintered for 1300°C for 0 minute at 10°C/min; 1% (a) and 2% (b) Zirconia added Barium Titanate

The temperature was then further reduced to 1290°C and all other sintering parameters were kept same. The structure shown even more improvement from 1300°C sintering and the percent theoretical densities for 1 and 2% ZBT samples were increased to 96 and 95%. The grain size was reduced to less than 1 micron for both 1 and 2% samples. The microstructuresare shown in figure 4.14.

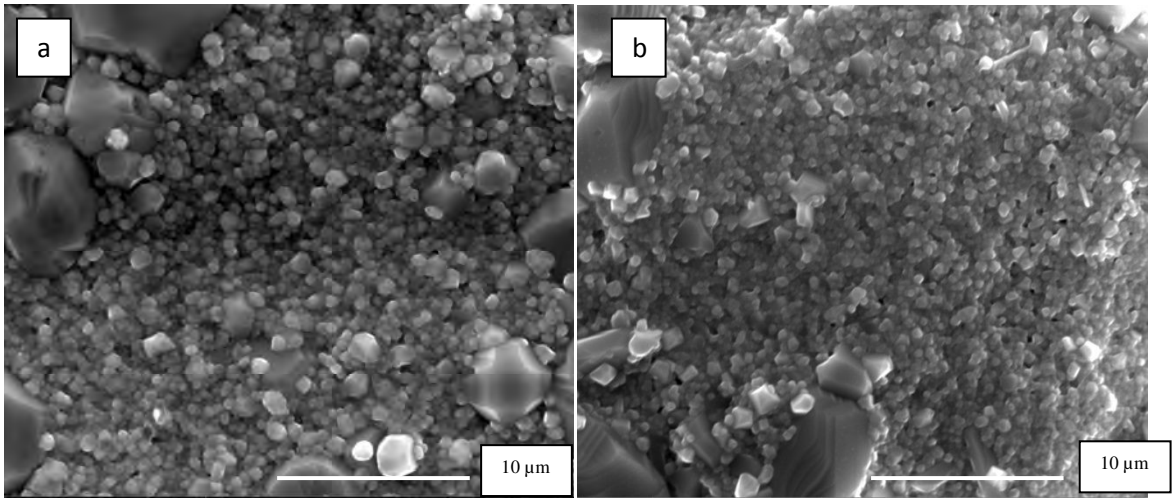

Figure 4.14: Samples sintered at 1290°C for 0 minute at 10°C/min; 1% (a) and 2% (b) Zirconia added Barium Titanate

At the same time stoichiometric samples of $BaTi_{0.80}Zr_{0.20}O_3$ was sintered at this temperature. The structure showed in figure 4.15, attained 90% of theoretical density and 4 micron of average grain size. The microstructure was shown below in figure 4.15. The key problem with the sintering of this material was that the sample got cracked after sintering on many occasions and the subsequent characterizations could not be done.

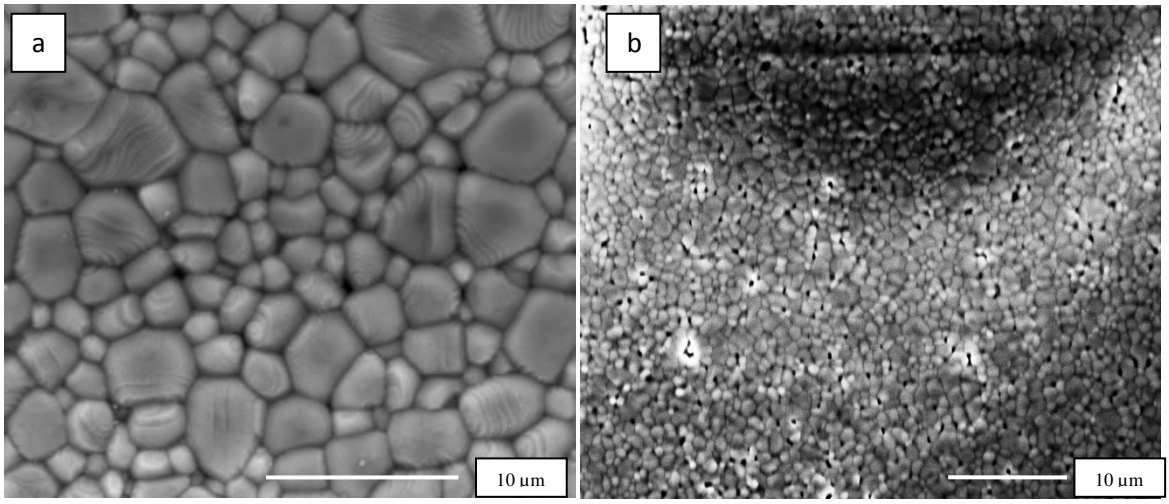

Figure 4.15: Samples sintered at 1290°C (a) and 1250°C (b) for 0 minute at 10°C/min; 20% Zirconia doped Barium Titanate

However, proper modification of heating rate on a trial and error basis makes the sample possible to sintering appropriately. Temperature was further reduced to 1280°C without any improvement in microstructure and the percent theoretical density suffered a reduction from the values achieved at 1290°C sintering.

The problem with this 0 minute type sintering is that although it yields good microstructural characteristics, but it must be kept in mind that the samples contain zirconia and the achievement of expected dielectric characteristics depend very much on degree of diffusion of zirconia in to lattice of barium titanate. Hence the current cycles are not suitablefor achieving the final aim of this research. Therefore its necessary to make proper alteration and addition to the current cycle designs to give zirconia the opportunity to more diffusion. Since keeping the grains fine is a principal requirement, the zero minute sintering is kept in the design. In addition to this low temperature sintering is added to the system either before or after the zero minute sintering to prohibit grain growth and facilitate zirconia diffusion at the same time.

Before turning to double stage sintering the result associated to single stage sintering was investigate for a one different cycle. Samples were sintered at 1290°C for 2 hours at a heating rate of 10°C/min. This study was assumed to give a comparison to samples sintered at 1290°Cfor 0 minute. The 2 hours cycles undoubtedly going to give better opportunity of zirconia diffusion, however the risk of grain growth is inevitable and there was a good chance that the two effects could nullify each other. Sintered samples (figure 4.16) yielded relatively poor percent theoretical densities of only 90 % for both the samples. There were large grains all over the structure although still bimodal distribution was observed.

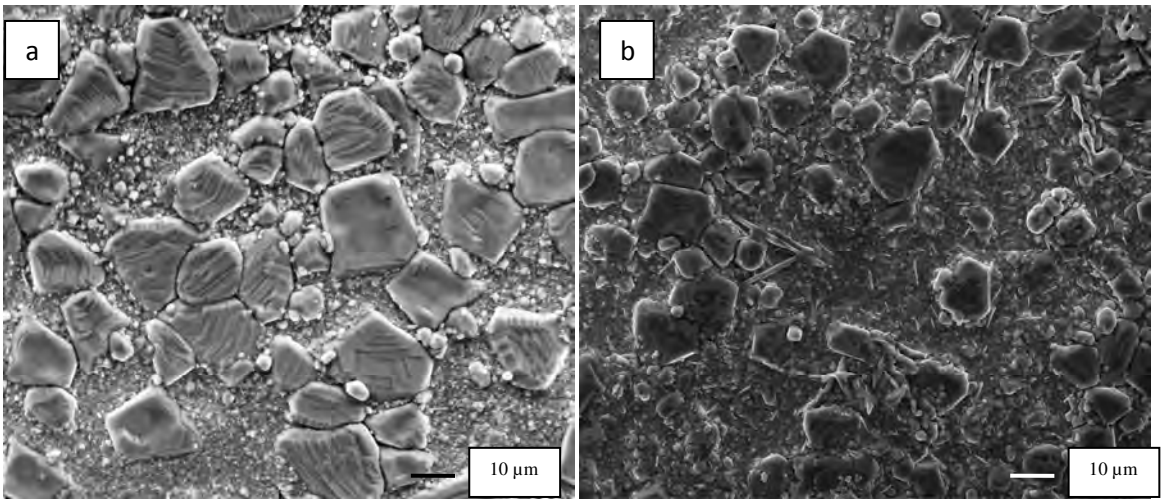

Figure 4.16: Samples sintered at 1290°C for 2 hours at 10°C/min; 1% (a) and 2% (b) Zirconia added Barium Titanate

One of first two stage cycles was first stage 1290℃-0 minute and then 1180℃-120 minutes. Unfortunately, the percent theoretical density is reduced to 90 percent for both 1 and 2% zirconia doped samples. The associated microstructures are shown in figure 4.17.

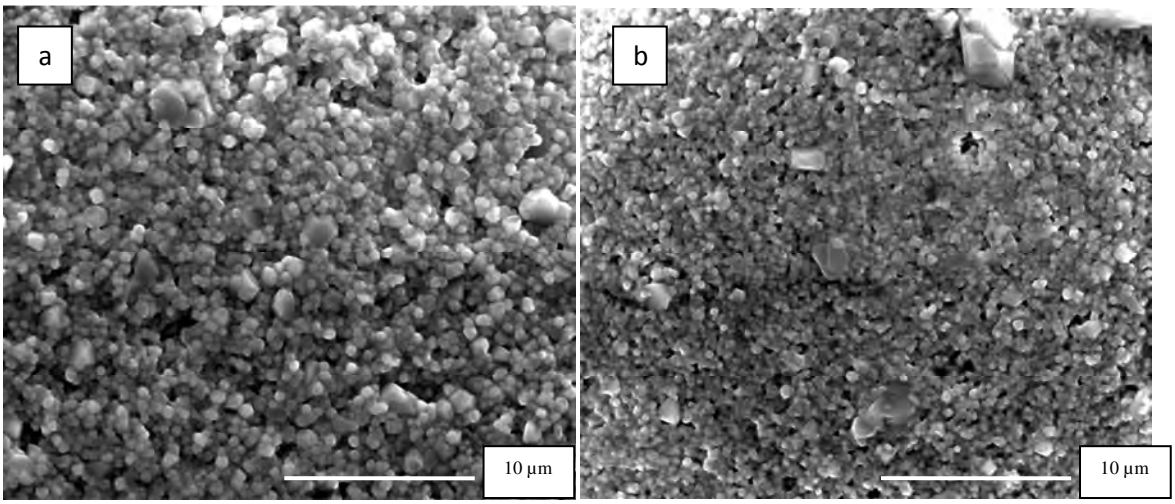

Figure 4.17: Samples sintered at 1290°C at 0 minute and then at 1180°C for 2hours at 10°C/min; 1% (a) and 2% (b) Zirconia added Barium Titanate

As can be seen from the figure 4.17, the samples contain porosity in the structure. This was a serious problem since even if zirconia had a chance to diffuse, the porosity in the structure is going the balance out that effect. The important thing to watch in the two experiments above is how the different parameters resulted the same density to both the samples. Sintering for 2 hours at high temperatures (1290°C) and the associated grain growth caused a significant reduction in density. But for the two stage the same density was achieved without any notable grain growth. It clearly shows that two stage sintering is the way to follow for getting fine grain size.

However, the first two stage was not a success from the microstructure viewpoint, hence in later efforts sintering was done by soaking the samples first at a lower temperature followe by heating at 1290°C for 0 minute. For example, the first stage sintering was done at 1150°C for two hours and then at 1290°C for 0 minute. The resulted microstructures are shown below in figure 4.18. The percent theoretical density for 1 and 2 % samples were 92 and 91% respectively. As the figures suggest, there is small variation in the two structures where 1% ZBT sample has a uniform grain size with porosity across the structure, but 2% sample tends toward bimodal distribution .

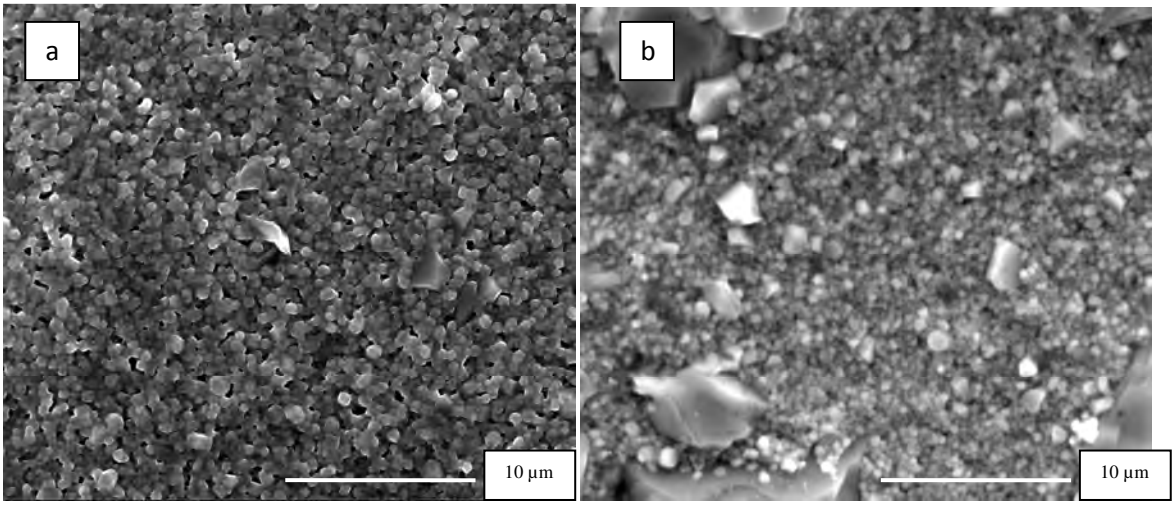

Figure 4.18: Samples sintered at 1150°C for 2 hours and then at 1290°C for 0 minute at 10°C/min; 1% (left) and 2% (right) Zirconia added Barium Titanate

Afterwards a similar cycle was carried out where first the samples were taken to 1290°C, held for zero minute and then reduced to 1150°C for 2 hours. At this point the density resulted is lower than the values received in the earlier experment. The percent theoretical density was just over 90% for both the samples. The microstructuresare shown in figure 4.19.

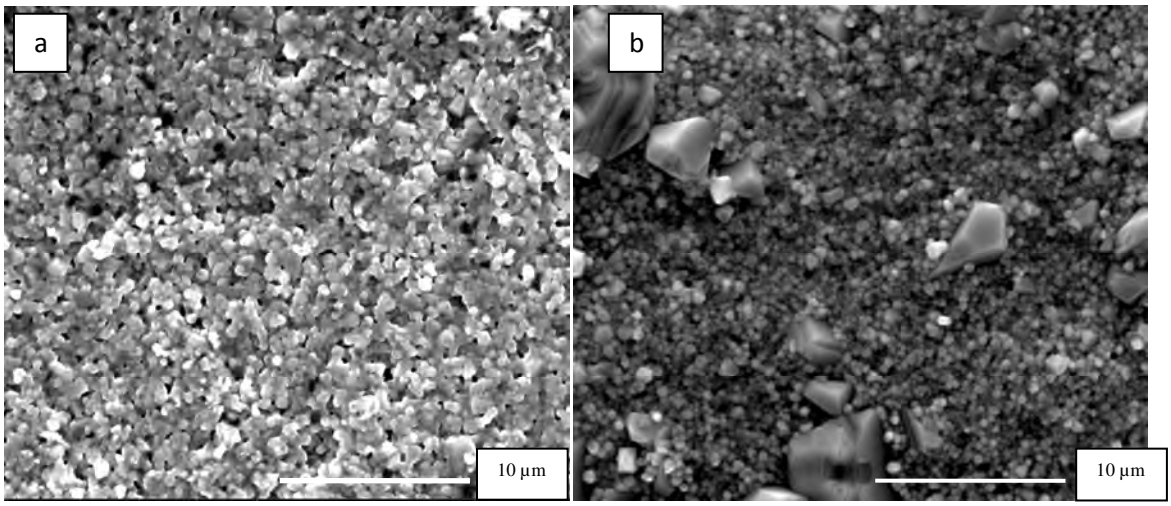

Figure 4.19: Samples sintered at 1290°C for 0 minute and then at 1150°C for 2 hours at 10°C/min; 1% (left) and 2% (right) Zirconia added Barium Titanate

Here, the 1% ZBT sample contain a lot of porosity and the 2% sample has large grains in a bimodal distribution in its structures. After these experiments, the samples were tested in these ways for higher or lower temperatures keeping 1290°C-0 minute fixed in all those cycles for various amount of time upto 8 hours. However, there has not been any significant microstructural improvement. On many occasions the density suffered a serious fall after sintering for longer period of time. However, whether the purpose (diffusion of zirconia) of doing all these has been served or not could not be ensured from the microstructural observations. That is discussed in detail in the X-ray diffraction analysis of the samples.

The next microstructures are for Nb_2O_5 doped $BaTiO_3$. The samples were sintered in three different temperatures i.e. 1250, 1275, 1300°C. The best microstructures were achieved from 1275°C sinteirng. Higher sintering time and temperature increased the grain size. Percent theoretical density was always minimum for 0.4 wt% doped samples.

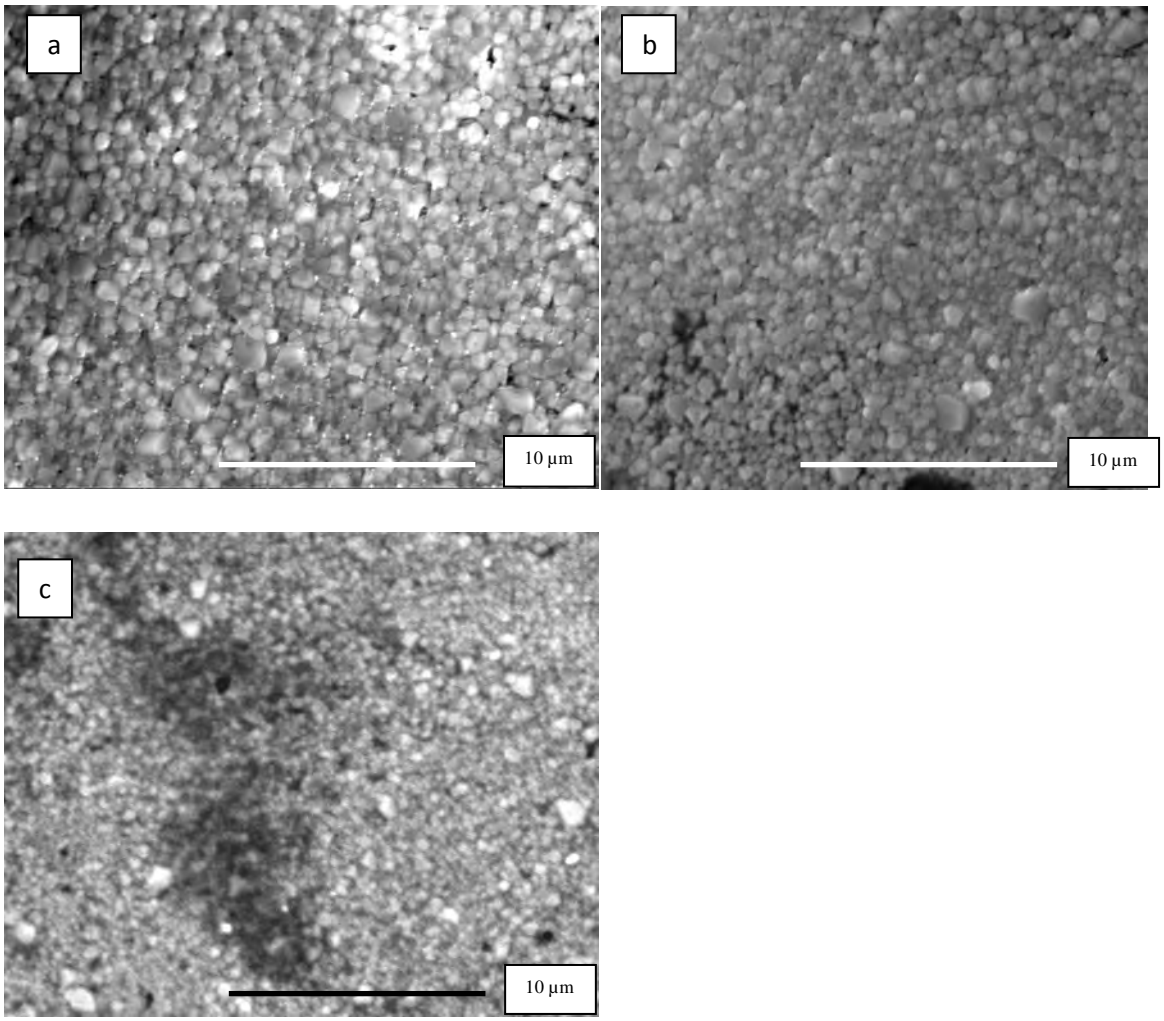

Figure 4.20: Nb_2O_5 doped $BaTiO_3$ samples after sintering at 1275°C for 0 minute; 0.2 wt% (a), 0.3 wt% (b), 0.4 wt% (c)

Figure 4.20 shows microstructure of the samples sintered at 1275°C for 0 minute on three different compositions. The density achieved in these samples are in the range of 91 to 94%. The amount of porosity is maximum in 0.4 wt% sample. The associated grain sizes of these samples are within 500 nm to 1.2 µm.

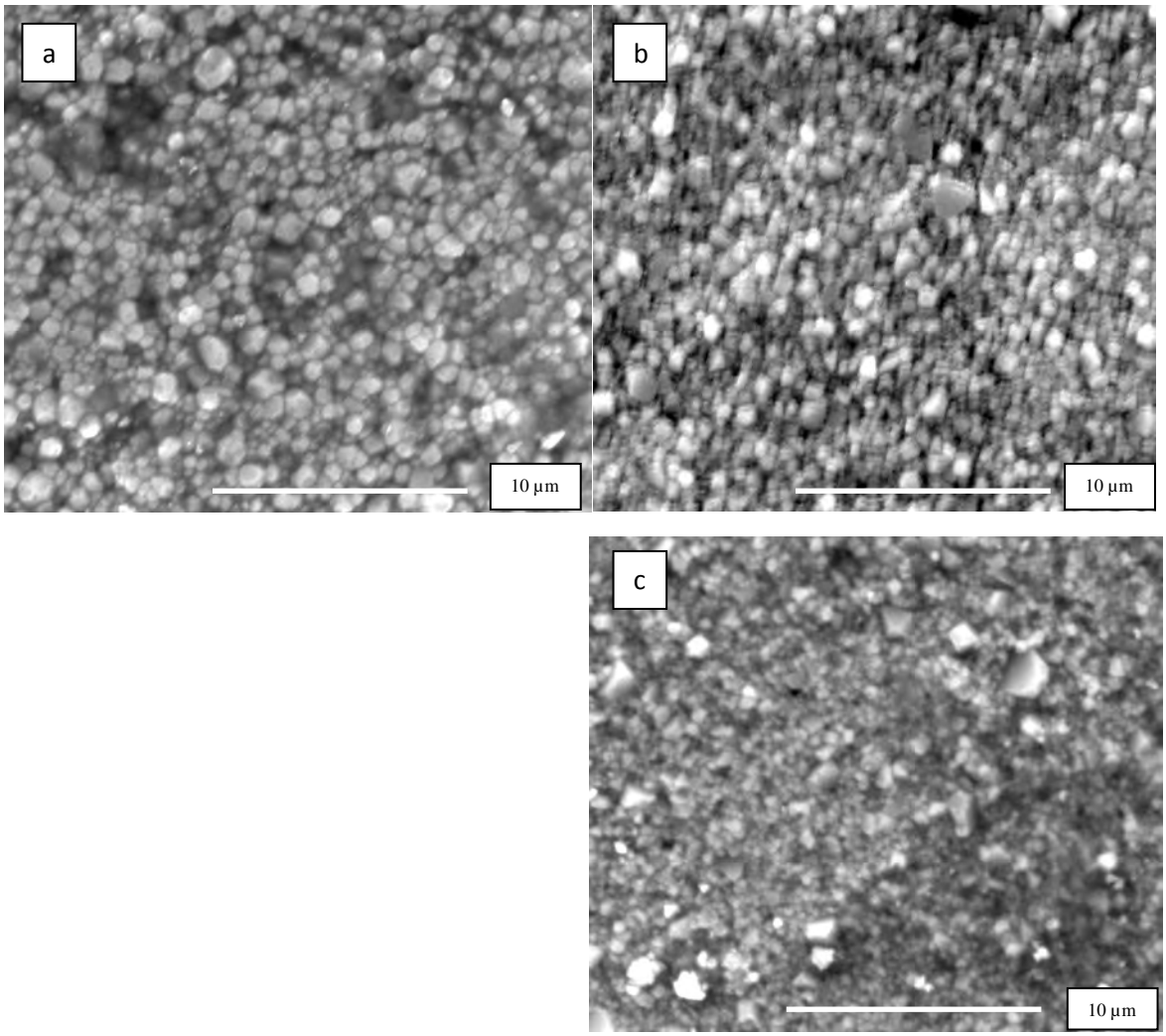

Figure 4.21: Nb_2O_5 doped $BaTiO_3$ samples after sintering at 1275°C for 1 hour; 0.2 wt% (a), 0.3 wt% (b),0.4 wt% (c)

In figure 4.21 the microstructures for three different samples sintered at 1275°C for 60 minutes is shown. The outputs of sintering is almost similar to 0 minute sintering shown in figure 4.19. The percent theoretical density achieved stayed in the range of 90 to 92% and the grain size have increased for all samples due to higher soaking time. The higher timing means Nb_2O_5 gets better chance to get into the structure of barium titanate. However no exact temperature of Nb_2O_5 diffusion was found in literatures. Diffusion ofNb_2O_5should be easier than that for ZrO_2 since niobium ion is much smaller in size than zirconium ion and thererfore can easily replace the titanium ion.

4.4 XRD analysis

Figure 4.22 (A) and (B) show the plot for pure barium titanate powder and for sample sintered at 1100°C for 10 hours. The initial powder size was 100 nm and the final grains were found to be 1 micron. The pressure used for making the pellets were 150 MPa and pressure was applied uniaxially. The XRD plot shows that the twin peaks along (200) planes and (201) planes in barium

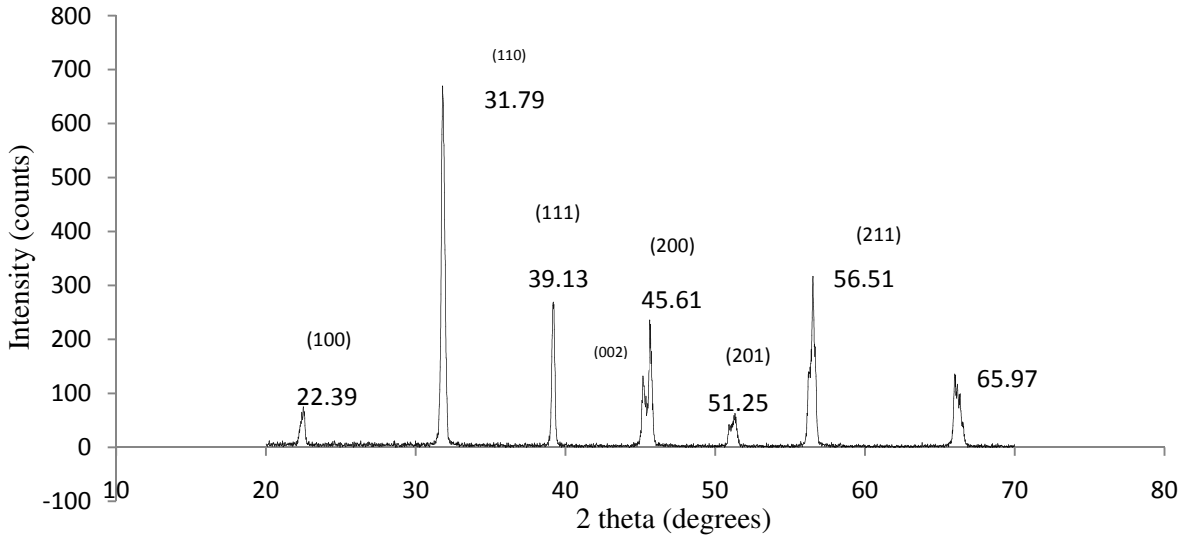

Figure 4.22 (A): XRD plot for barium titanate powder

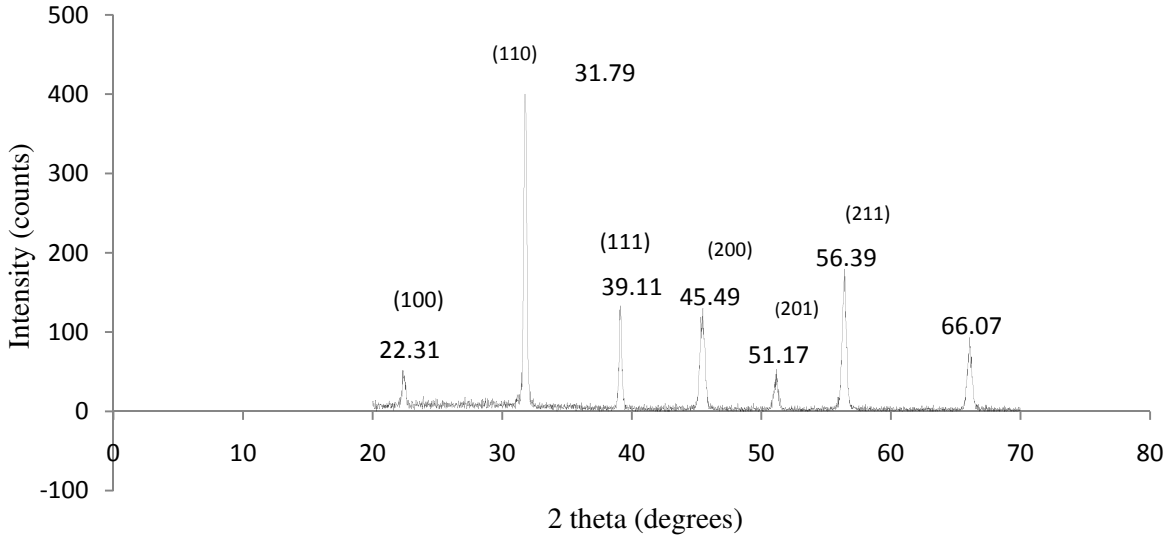

Figure 4.22(B): XRD plot for barium titanatesintered at 1100°C for 10 hours

titante powder do not appear in the barium titanate sample sintered at 1100°C for 10 hours. This is an indication of reduced tetragonality in barium titanate and it suggests that the structure may retain the cubic phase to a greater degree than it usually does. The tetragonality in powder form was found

to be 1.0196 which after sintering was reduced to 1.0066. The dielectric property measurement of this sample is also well in accordance with the XRD data where the curie temperature marking the cubic to tetragonal phase transformation was found at 110°C which is 120-130°C in general. This findings closely support the data from the work of Ohna and Weng [7, 8] who related the curie point in barium titanate with initial particle size and pressure used during sample making. The detail analysis has been included in literature review part of the thesis.

XRD data for 1% zirconia doped barium titanate samples are presented in figure 4.23. The plots are also compared with that of pure barium titanate powder from which they are made of. The figures show no significant difference in the positions of the planes from that for pure barium titanate. The notable difference is the disappearance of twin peaks as the temperature is increased and consistency in shifting of the peak to lower angles, meaning increase in lattice parameter and planar spacings. The samples sintered at lower temperatures show trace of twin peaks along (200) and (201) planes. As the temperature is increased, the effect almost diminishes slowly. Twin peaks are least recognizable for samples sintered at 1340°C. The fact to notice here is that 1% zirconia doping does not put on enough roles to bring any variation in the tetragonality of the barium titanate lattice structure. This effect has been proven by the dielectric constant measurement as the 1% zirconia doped samples shown higher dielectric constant than the 2% zirconia doped samples on many occasions. The effect of sintering temperatures (whether above or below 1300°C) needs to be considered as well. The twin peaks are not precise on most of the XRD plots for 2% zirconia doped samples (figure 4.24) which indicates the suppression of tetragonal phase in the structure during cooling. XRD data for 2% zirconia doped barium titanate samples (figure 4.24) do not show much variation from the XRD plot of pure barium titanate. However, the change in tetragonality with different sintering temperatures is notable. In figure 4.24 the top XRD plot is for pure barium titanate which shows two twin peaks from (200) and (201) family of planes typical of pure barium titanate. Armstrong et. al. [3] showed that zirconia diffusion into structure of barium titanate occurs above 1310°C and below that temperature zirconia stays at grain boundaries and act as grain growth inhibitors. This thesis has been able to yield results to show this theory correct by means of grains structure above and below 1300°C. The plot for 1320°C – 5 hrs sample shows that the twin peaks from (200) and (201) planes have reduced significantly.This indicates the induced distortion in lattice arrangement, because of zirconium ion diffusion that took place inside barium titanate to a great extent since Zirconium ion is much bigger in size than titanium ion and thus have less chance to move toward oxygen like titanium ion has and since the soaking time provided was quite high which therefore reduced the amount of tetragonality. The next plot for 1340°C – 30 minutes shows the similar results as no twin peaks appear.

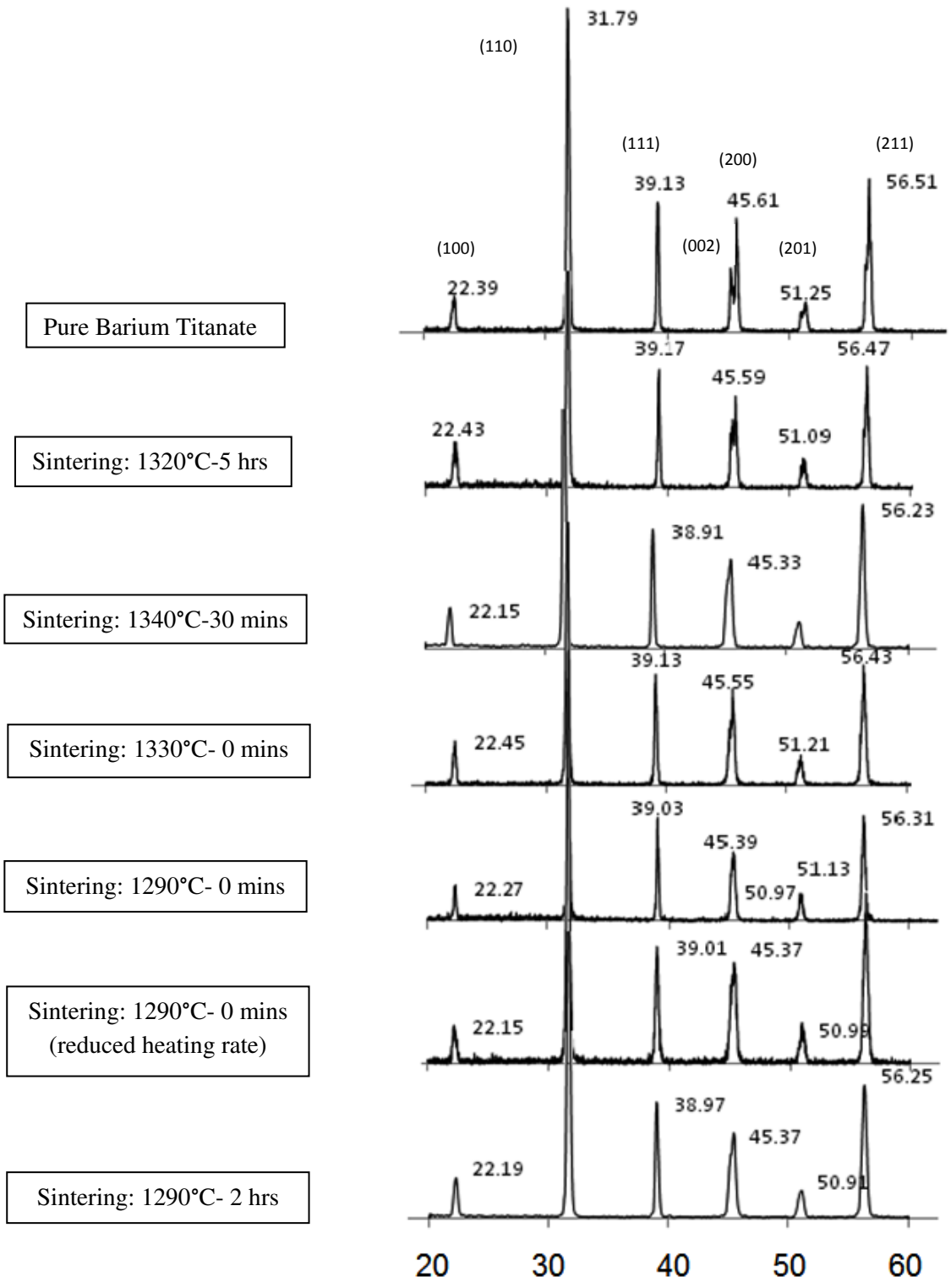

Figure 4.23: XRD plots for 1% zirconia added barium titanate

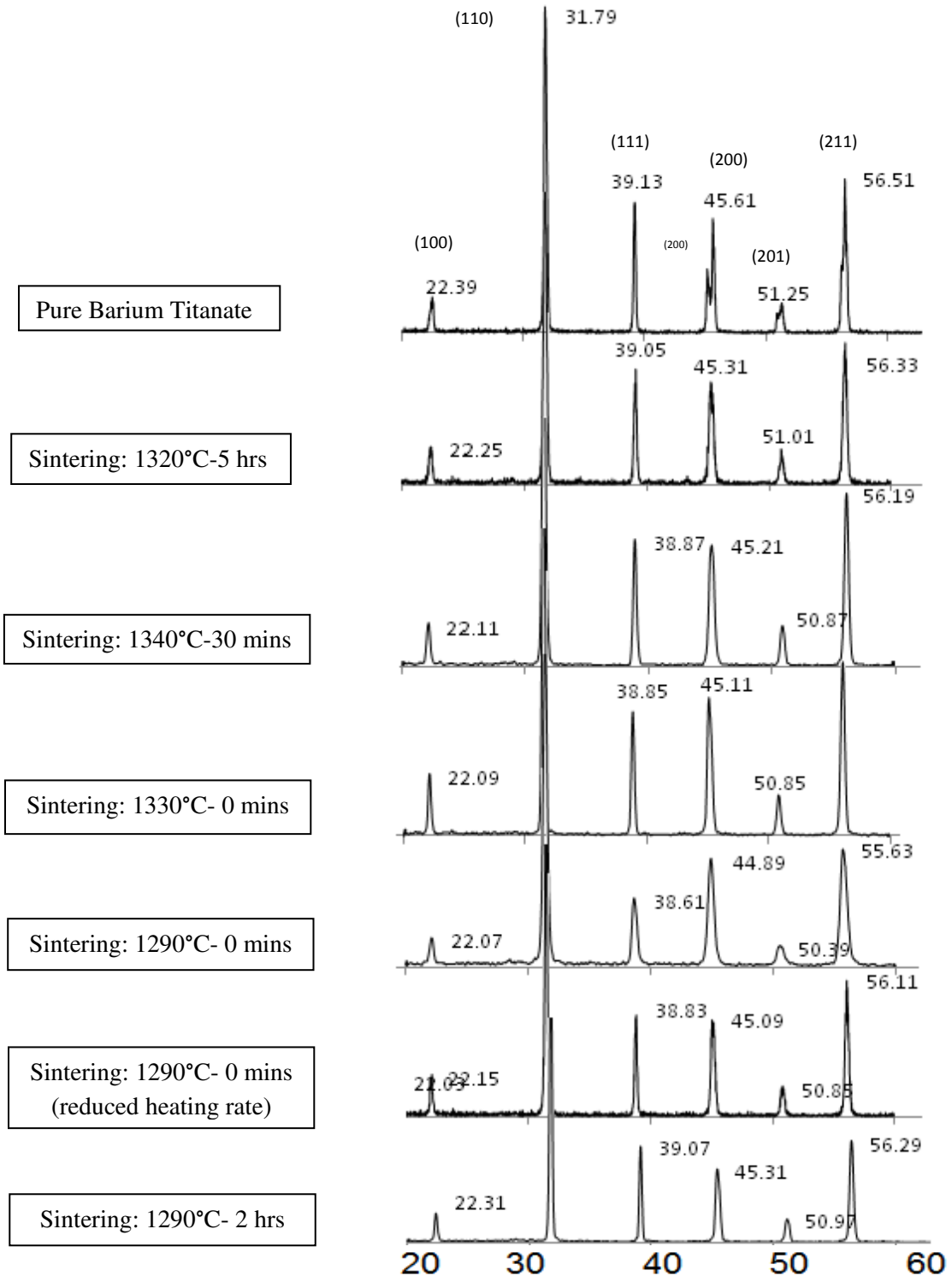

Figure 4.24: XRD plots for 2% zirconia added barium titanate

The fourth and fifth graphs present a little different situation where the samples were sintered for zero minute at 1330 and 1290°C. Although it was mentioned that zirconia diffusion occurs above

1300°C, in this cases the time at that temperatures for any kind of movement was not given (zero minute sintering).Therefore even after sintering above 1300°C there is a good chance that the zirconia particles wouldrather stay at grain boundaries than diffusing into the lattice of barium titanate.

Armstrong et al[3, 9]showed that the zirconia staying at grain boundaries may induce core-shell grain structure which eventually can resist the transformation from cubic to tetragonal state by inducing lattice strain. This would cause the twin peaks to disappear from the XRD data as shown in the figure 4.24. They also showed that high angle XRD reveals reactions from more complex planes like (400), (004) etc which strongly suggests the decrease in *c* lattice parameter and therefore causing significant change in the dielectric properties of the material [3]. The later plots in figure 4.24 show similar type of behavior with no twin peaks. The plots do not present any precise evidence regarding the existence of zirconia since the amount or zirconia is very low in the samples.

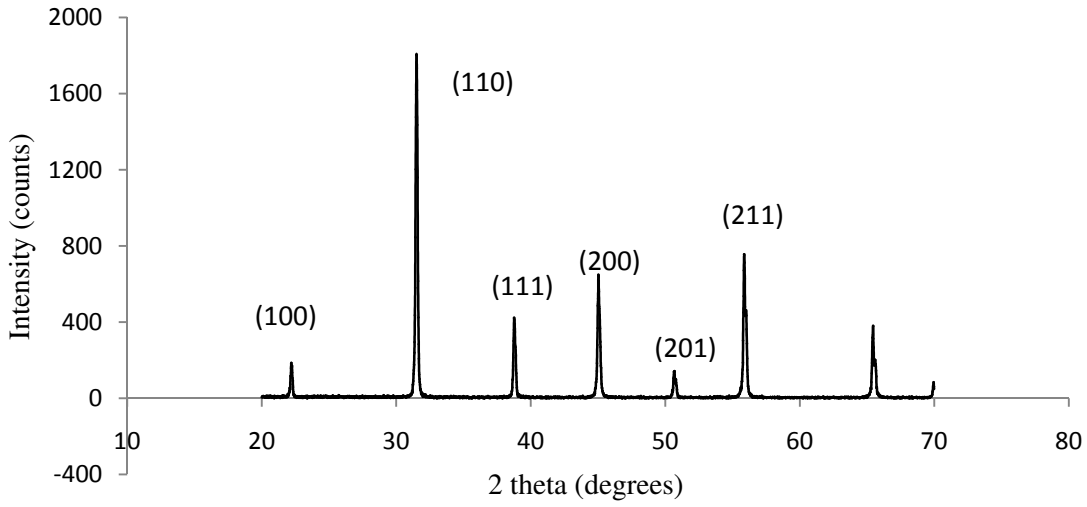

Figure 4.25: XRD plot for $BaTi_{0.8}Zr_{0.2}O_3$ sintered at 1290°C for 0 minute

Figure 4.25 shows the XRD plot for the stoichiometric composition of 20% zirconia doped barium titanate. The plot does not reveal any clearly defined twin peaks which means that the samples have had changes in *c* and *a*latticeparameters. XRD data show that the c/a ratio is only 1.003 which indicates a significant reduction in tetragonality from that of pure barium titanate. The microstructure of this zirconia doped sample as discussed in the earlier section, showed the grains to be much greater in size than the zirconia added samples sintered at same parameters, which means that the powder has zirconium ion well diffused into the crystal structure of barium titanate and thus almost no zirconia was left at grain boundaries to resist grain growth. This phenomenon at

the same time had reduced the tetragonality of barium titanate crystal since zirconium ion is much larger than titanium ion. Hence when zirconium ion sits in the octahedral void, it forms a more stable structure with more uniform distance from all its Ba^{2+} and O^{2-} neighbors. This does not allow the structure to change its shape as in pure barium titanate at curie point. Therefore the material shows no peak at its transition. This fits the dielectric measurement results, where it showed no peak during transition at curie point.

Table 4.1: Effect of zirconia addition on lattice parameter in $BaTiO_3$

Sample	a (Å)	c (Å)	c/a
$BaTiO_3$			
Powder	10.254	10.454	1.0195
1100°C/ 10h	10.315	10.384	1.0066
1330°C/ 0 min			
1% ZrO_2	10.29	10.41	1.011
2% ZrO_2	10.47	-- No splitting --	
1290°C/ 0 min			
1% ZrO_2	10.358	10.444	1.008
2% ZrO_2	10.578	10.604	1.002
$BaTi_{0.8}Zr_{0.2}O_3$	10.50	10.54	1.003
1290°C/0 min (Slower heating rate)			
1% ZrO_2	10.366	10.41	1.004
2% ZrO_2	10.507	10.489	1.0016
1320°C/ 5 h			
1% ZrO_2	10.27	10.375	1.013
2% ZrO_2	10.40	-- No splitting --	

4.5 Dielectric Properties Measurement

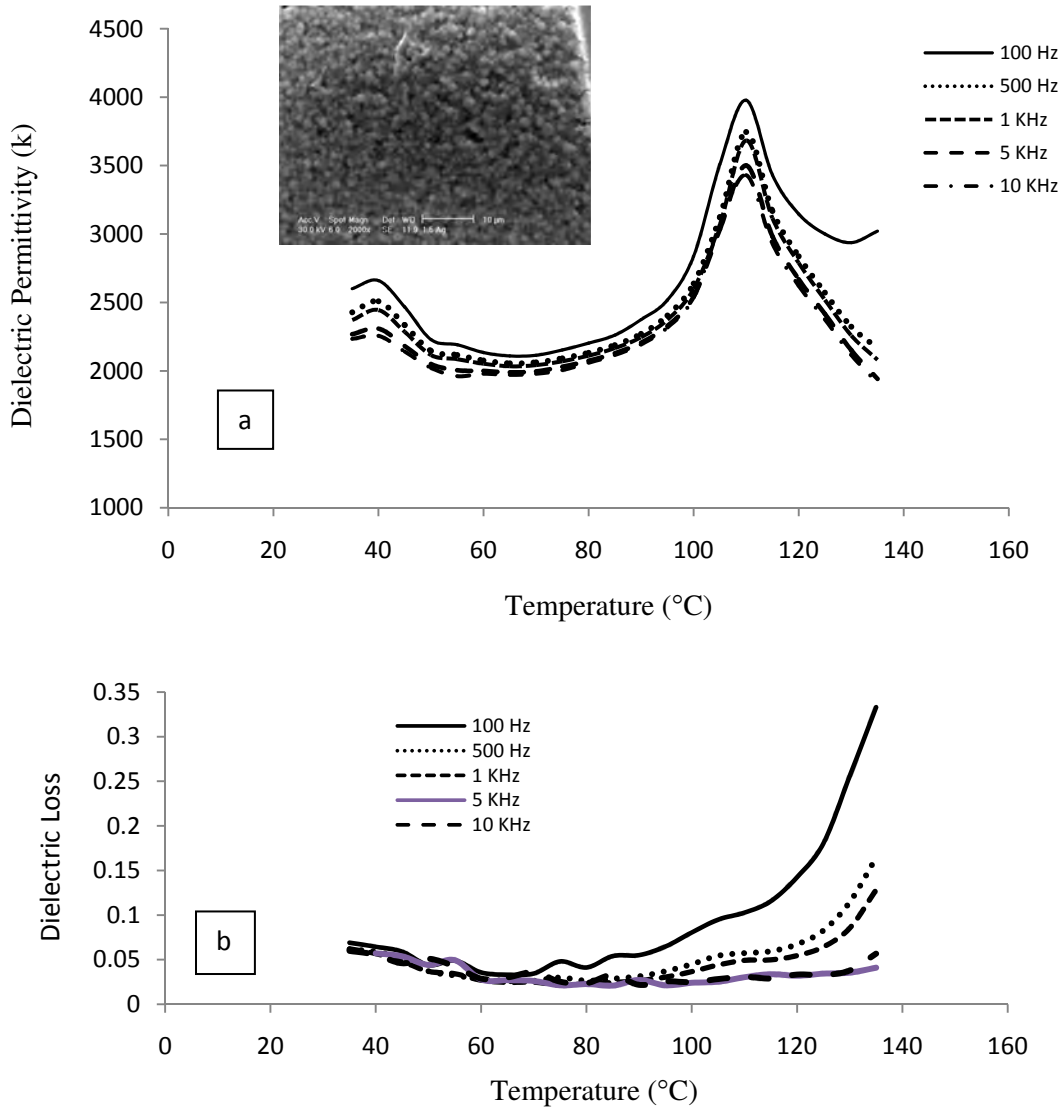

Figure 4.26: Barium Titanate sintered at 1100°C for 600 minute: k vs temperature (a) and loss vs temperature (b)

Figure 4.26 shows the temperature dependent permittivity response of pure barium titanate sample sintered at 1100°C for 10 hours in five different frequencies ranging from 100 Hz to 10 KHz, which is the typical requirement for capacitors in circuits. Pure barium titanate was sintered in a range of temperatures with both single and double stage heating. It was found that at the temperature range of 1210°C to 1230°C, maximum density occurred for 120 minutes of heating with grains in the range of 5 to 10 micron size. The associated dielectric constant (k) in those pure barium titanate samples was in the range of 800 to 1400 within the temperature range of 25 to 65°C. In attempts to achieve smaller grains, pure barium titanate was sintered at 1100°C for 600 minutes. As a result,

grain size dropped to around 1 micron with percent theoretical density being 96%. The fine grain size of the material showed improvement in permittivity than those with larger grains. The microstructure of the material is shown in the inset of figure 4.26 (top). The loss associated is also shown in figure 4.26 (bottom). The notable point is the transition temperature being at 110°C which in general is 120-130°C for the pure material. This proves that the cycle allows the cubic phase to be stable more than typical barium titanate does. This behavior is in conjunction with the XRD data for this sample where the twin peaks along (200) or (201) planes are less recognizable than the pure barium titanate powders and the c/a ratio had reduced significantly from 1.019 to 1.006 as discussed in XRD analysis part.

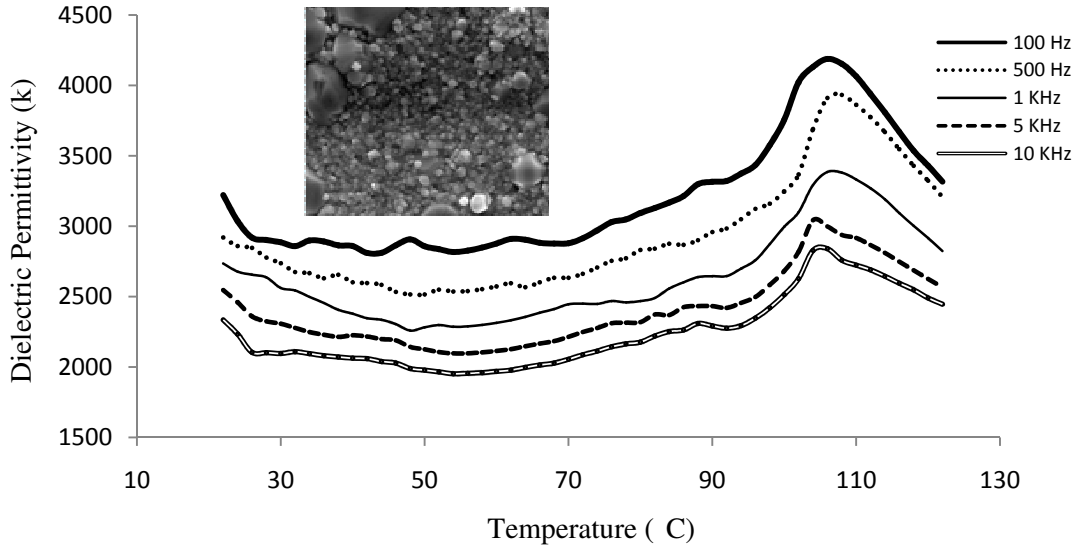

Figure 4.27: 1% Zirconia added Barium Titanate sintered at 1290°C for 0 minute

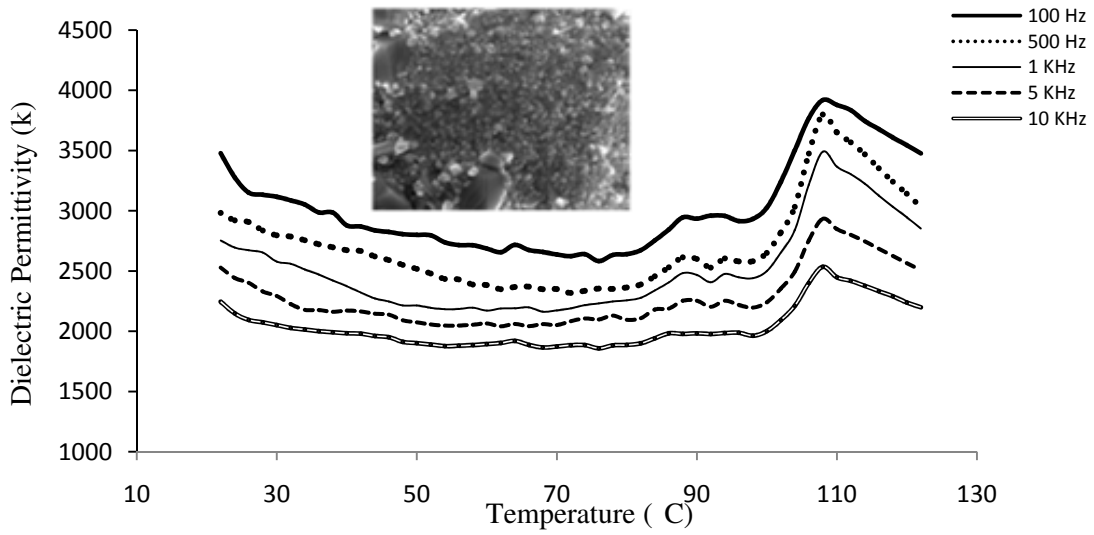

Figure 4.28: 2% Zirconia added Barium Titanate sintered at 1290°C for 0 minute

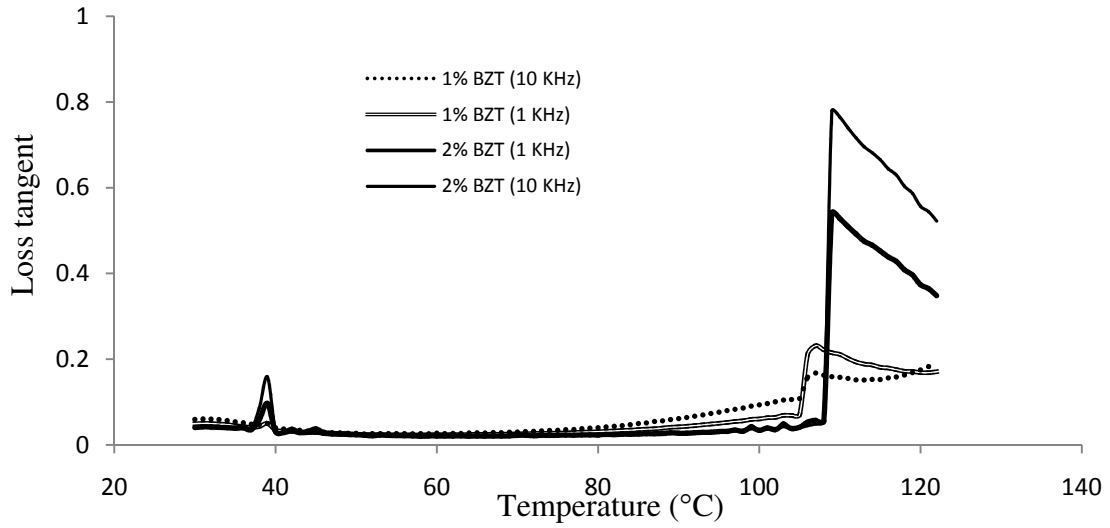

Figure 4.29: Dielectric loss for of Zirconia added Barium Titanate samples sintered at 1290°C for 0 minute

In figure 4.27 the permittivity response for 1% zirconia added barium titanate is shown for different frequencies. As the microstructure in the inset suggests, the grain size is 500 to 550 nm with bimodal distribution of grains in accordance with the work of Armstrong et.al [3]. The achievedpercent theoretical density was 95%. The dielectric constant is in the range of 2000 to 3000 showing improvement from that of pure barium titanate samples shown in figure 4.26 (a). The 2% zirconia added barium titanate showed (Figure 4.28) similar yet slightly lower dielectric constants than 1% samples. The structure is 96% dense and the grain size, although smaller than that for 1% samples, still has a bimodal distribution. The paraelectric to ferroelectric transition temperature was dropped to 106-108°C for 1 and 2% samples and the permittivity shows a flat response with temperature with the peak being depressed significantly. Figure 4.29 shows the loss for 1 and 2% samples and it indicates that the losses are not much of temperature dependent until the curie point is reached. The dielectric properties from these experimental variables could be attributed strongly to the fine grain size of the material.

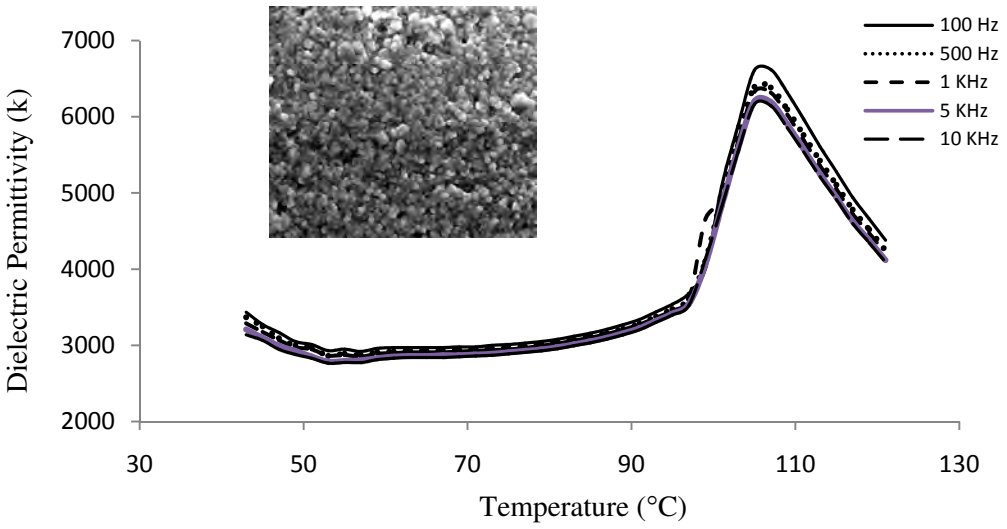

Figure 4.30: 1% Zirconia added Barium Titanate sintered at 1290°C - 0 minute- 1150°C – 2 hrs

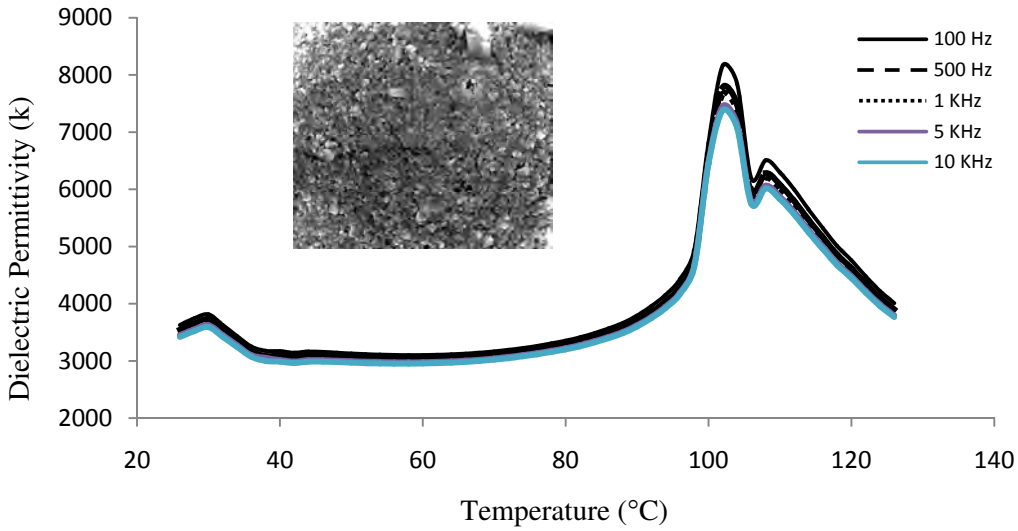

Figure 4.31: 2% Zirconia added Barium Titanate sintered at 1290°C - 0 minute- 1150°C – 2 hrs

Figure 4.30 shows the dielectric permittivity with temperature for 1% zirconia doped barium titante for two stage sintering. Here the permittivity was found to be in the range of 2800 and the Curie point was found to drop to 105°C. The grain size of this sample was in the range of 500 to 700 nm. The presence of zirconia at the grain boundaries posed considerable lattice strain to delay the cubic to tetragonal phase transformation. Figure 4.31 shows the plot for 2% samples subjected to the same parameters. The permittivity here is in the range of 2900 and the Curie point was found to be at 102°C, lower than that found in the 1% sample. The reason behind these two findings may due to

the greater stress imposed by zirconia particles at grain boundaries by means of higher zirconia

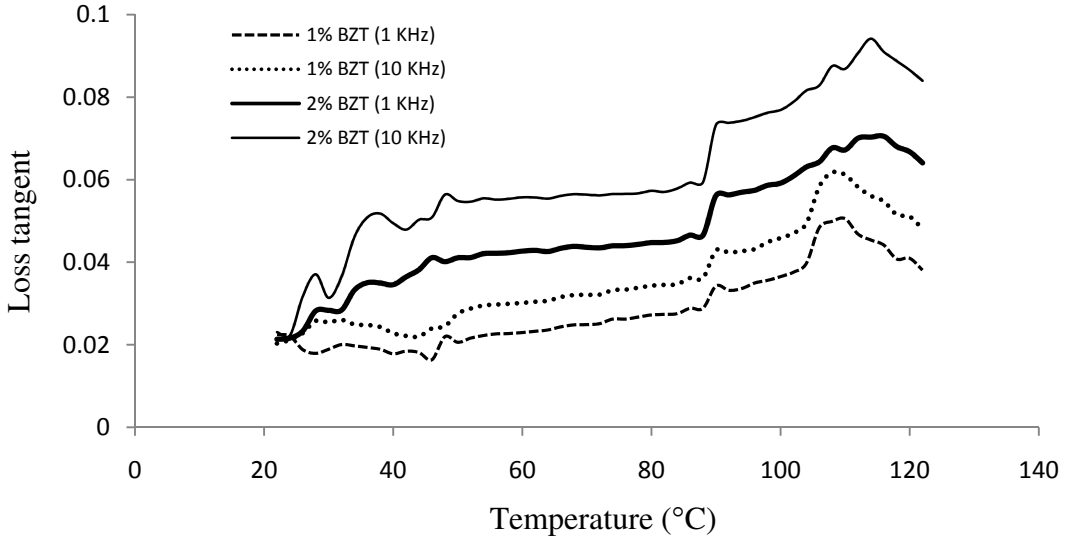

Figure 4.32: Dielectric loss for of Zirconia added Barium Titanate samples sintered at 1290°C - 0 minute - 1150°C – 2 hrs

content [3], which eventually dropped the cubic to tetragonal phase transformation temperature and therefore reduced the degree of tetragonality of the crystal structure. The responses are quite flat until the Curie point which is also a desired property for capacitor to keep stability in the device during its operation. The loss data (Figure 4.32) shows that 2% samples were subject to greater loss than the 1% samples. The losses are lower below the curie point which indicates the loss of domain structure in the material upon reaching the curie point.

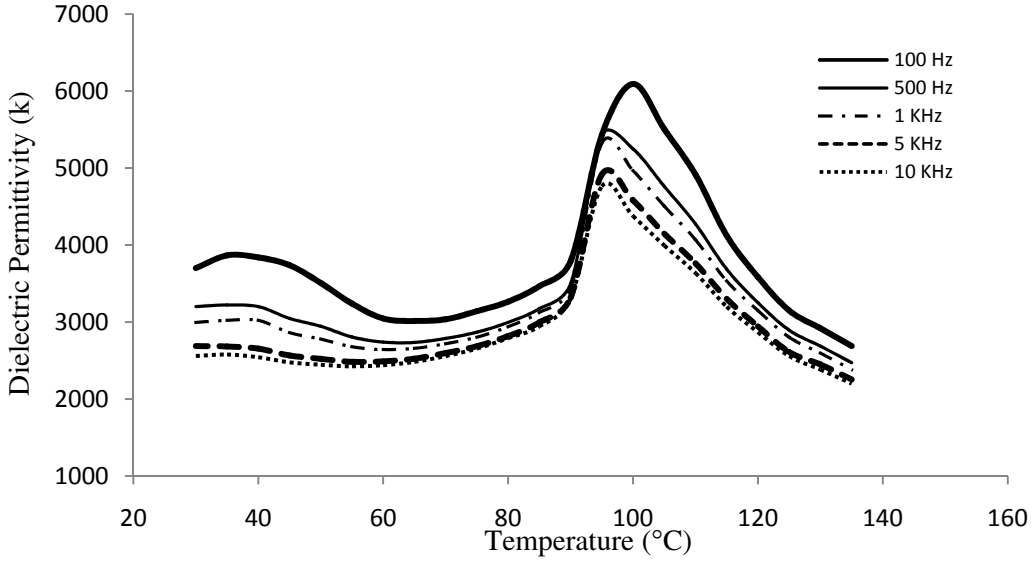

Figure 4.33: 1 % zirconia added barium titanate Sintered at 1290°C for 0 min - 1150°C for 15 hrs

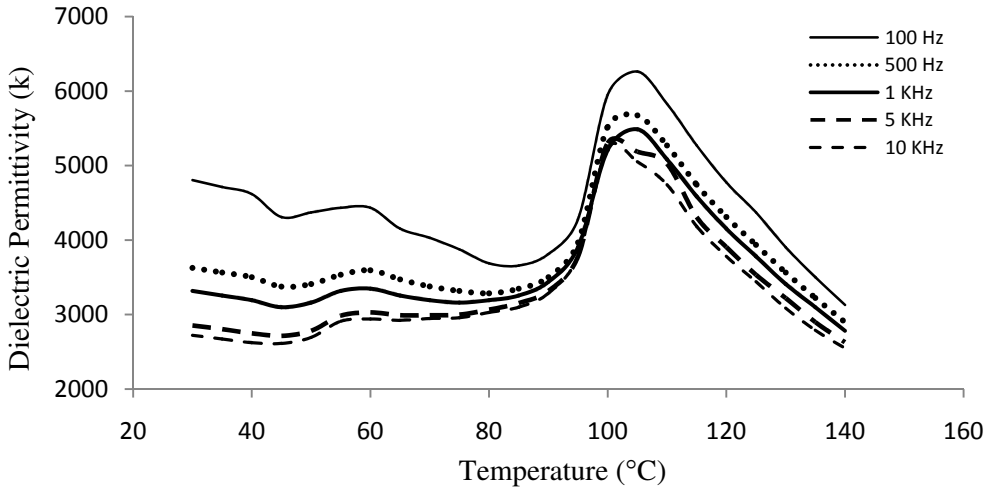

Figure 4.34: 2 % zirconia added barium titanate sintered at 1290°C for 0 min - 1150°C for 15 hrs

Figure 4.33 and 4.34 show the permittivity response of 1 and 2% samples sintered in two stages. However, the difference from the earlier experiments is in the order of sintering temperatures. Here the samples were first taken to higher temperature at 1290°C and then cooled to 1150°C where they were held for 15 hours. The condition certainly presents different environment for zirconia to interact with barium titanate since the particles were assumed in the first stage of sintering to come as closer as they can. This has been proven in this thesis by means of percent theoretical density achievement in the microstructure analysis part of this thesis. Therefore zirconia was subjected to different environment and this second stage has been tested for different holding period. None of the experiments yielded permittivity values more than 1500. However the 15 hours sintered samples yielded permittivity values in the range of 1500 to 3500 in the range of frequencies. The results also showed that the response with temperatures does not show variations as significant as those shown in (1180°C-6 hrs samples). This means there is a good possibility that the peak regarding tetragonal-orthorhombic phase transformation has been suppressed to some extent.

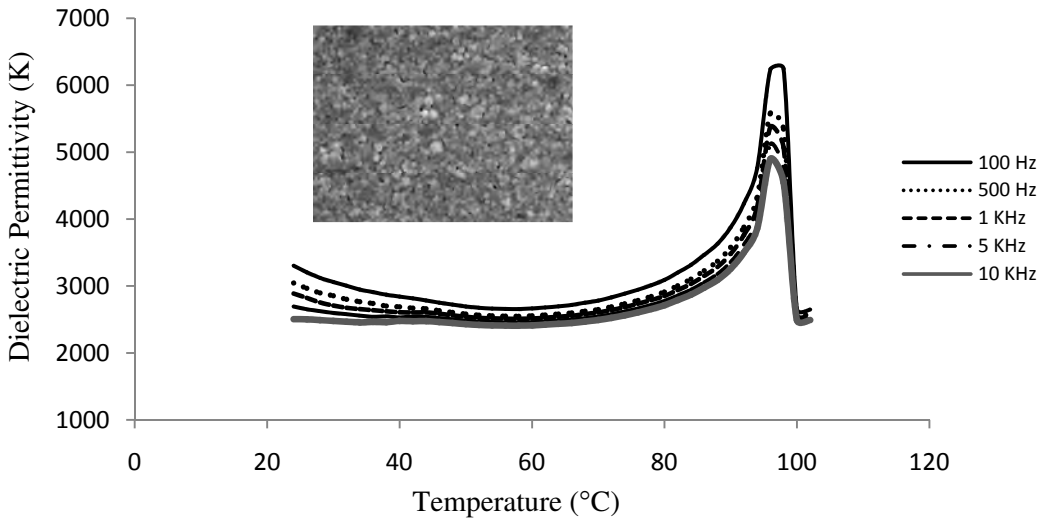

Figure 4.35: 1% Zirconia added Barium Titanate sintered at 1180°C – 4hrs - 1290°C – 0 minute

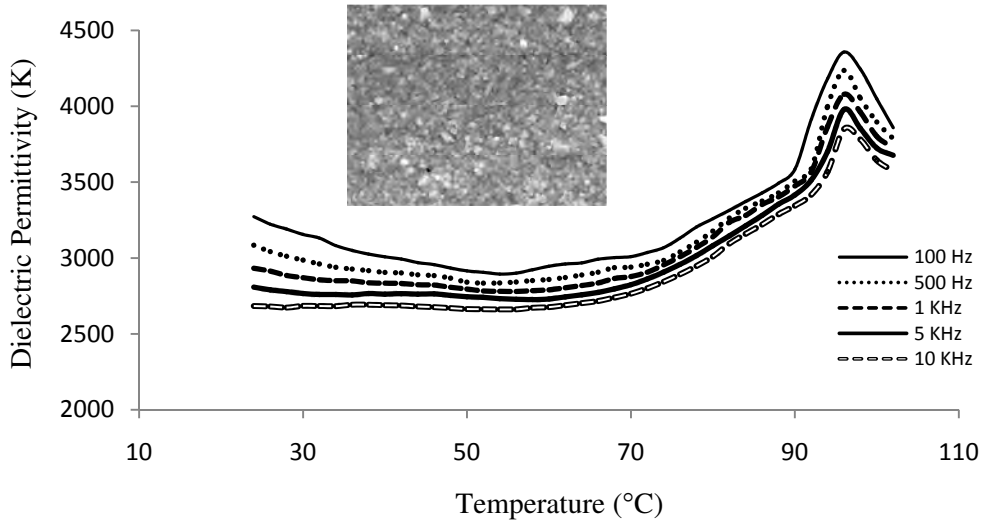

Figure 4.36: 2% Zirconia added Barium Titanate sintered at 1180°C – 4hrs - 1290°C – 0 minute

In figure 4.35 and 4.36, the permittivity response for 1 and 2% zirconia added samples sintered at two stages is shown. Here the samples were sintered first at 1180°C for 4 hours and then taken to 1290°C for 0 minute heating. The permittivity was found to be within 2200 to 2700 for 1% sample, 2600 to 3200 for 2% sample and the response is flat across the range of temperatures up to 80°C. The percent theoretical density of the structure was 97% and 96% for 1 and 2% samples respectively and grain size was in the range of 500 to 600 nm. The Curie point was found to be at 96-98°C. The possible reason behind is the uniform distribution of zirconia particles around the grains of barium titanate during the first stage of heating which by turn might have evenly distributed the stress across the structure, thus further delaying the cubic to tetragonal transformation.

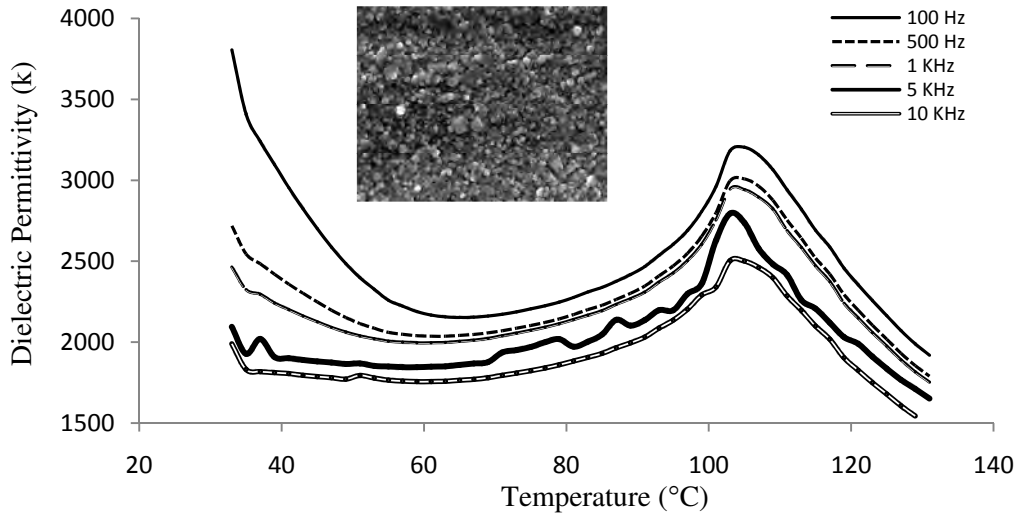

Figure 4.37: 1% Zirconia added Barium Titanate sintered at 1180°C – 6 hrs - 1290°C – 0 minute

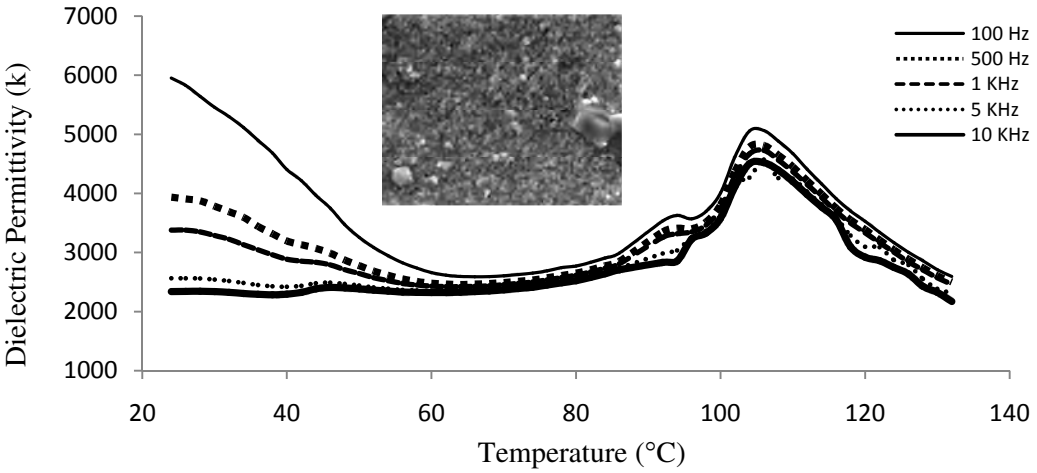

Figure 4.38: 2% Zirconia added Barium Titanate sintered at 1180°C – 6 hrs - 1290°C – 0 minute

Figure 4.37 and 4.38 suggest the permittivity of 1 and 2% samples sintered in two stages. Samples were held for 6 hours at 1180℃ before being taken to 1290℃. Compared to 4 hours sintered sample, the dielectric response produced for 6 hours sintered sample is irregular. The highest permittivity in these 1180℃ sintering groups was found to be for 4 hours sintered samples. Permittivity decreased for 6 hours sintered samples. This result along with large variation in permittivity indicate more uniform distribution of zirconia particles with time along the grain boundaries at 1180℃ before the actual 1290℃ sintering, which eventually reduces the tetragonality more and more. Permittivity for 4 hours sintered samples varied from 2500 to 3000 and that for 6 hours samples showed irregular permittivity response. More importantly, the 4 hours samples (both 1 and 2%) showed flat response whereas 6 hours samples did not. The tetragonal to orthorhombic transformation in pure barium titanate occurs ideally at around 0℃ and addition of

zirconia into barium titanate has been known to shift this point to higher temperatures [14]. This higher value of permittivity at lower temperatures is probably the continuation from the orthorhombic-tetragonal phase transition temperature and such variation at these temperatures indicates uniform distribution of particles. Unfortunately, that could not be proved experimentally on this occasion under current departmental facilities. Nevertheless the 6 hours samples indicated that a more uniform distribution is possible at lower first stage sintering temperatures with enough soaking. Figure 4.39 shows irregular loss data along with temperature. Here also 2% sample showed higher dielectric loss.

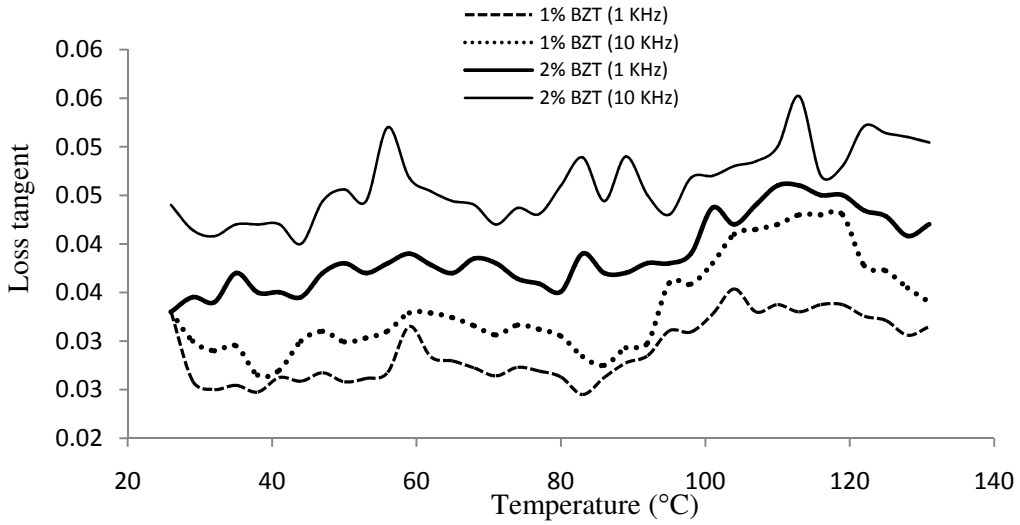

Figure 4.39: Dielectric loss for of Zirconia added Barium Titanate samples sintered at 1180°C – 6 hrs - 1290°C – 0 minute

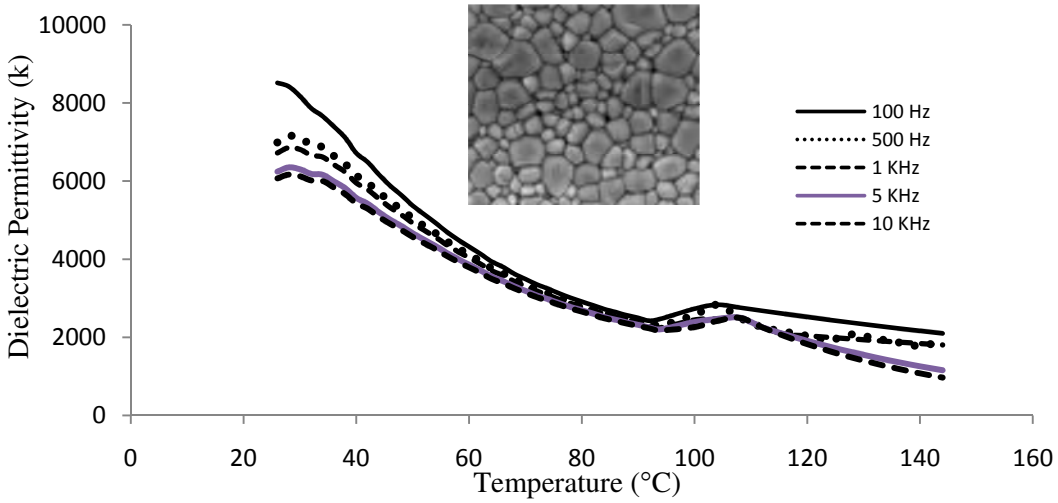

Figure 4.40: $BaTi_{0.8}Zr_{0.2}O_3$ sintered at 1290°C for 0 minute

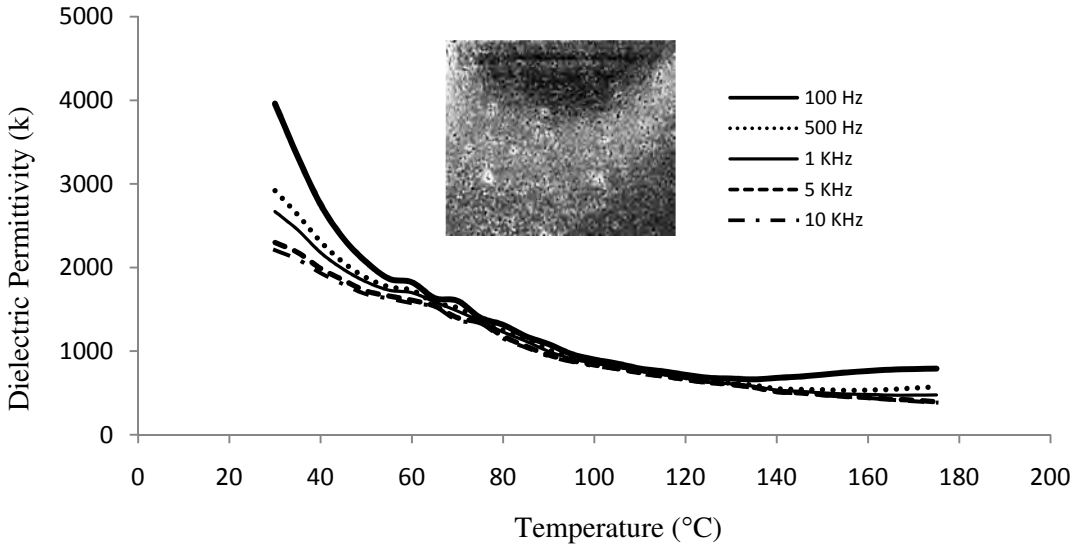

Figure 4.41: $BaTi_{0.8}Zr_{0.2}O_3$ sintered at 1250°C for 0 minute

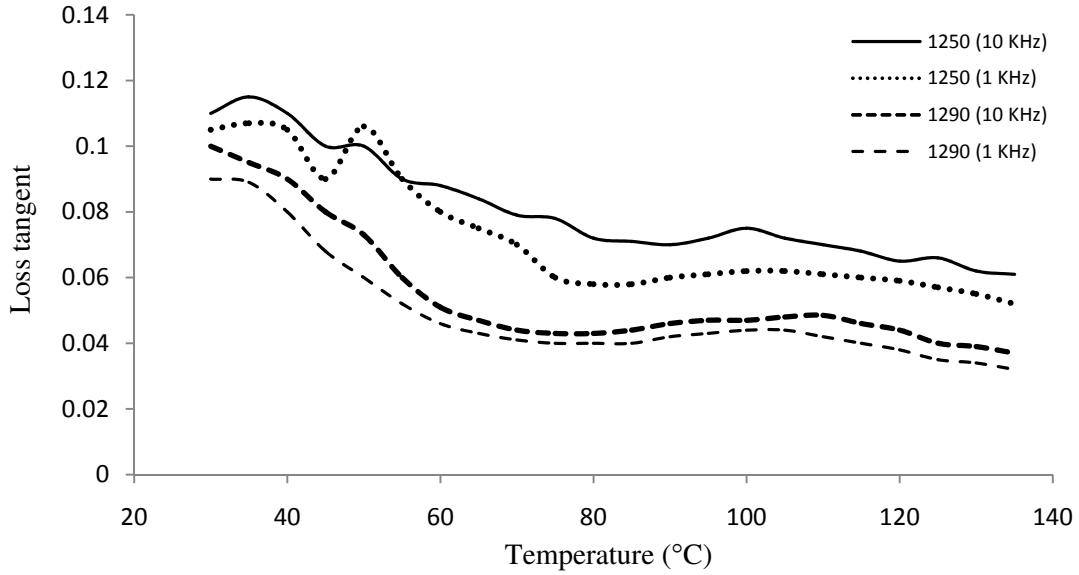

Figure 4.42: Dielectric loss for $BaTi_{0.8}Zr_{0.2}O_3$samples

Figure 4.40 and 4.41 show the temperature dependent dielectric constant values of 20% zirconia doped barium titanate. Samples were sintered at 1290°C and at 1250°C. For the sample sintered at 1250°C, the dielectric constant at lower temperatures showed range of values for different frequencies. However with increase in temperature the variation diminished slowly. For the sample sintered at 1290°C, although the variation of permittivity for different frequencies with temperature is quite as same as that for 1250°C, but the dielectric constant is much higher for sample sintered at 1290°C. The possible reason is the amount of porosity in 1250°C sample. The achievement in density is only 84% whereas the sample sintered at 1290°C achieved around 93% of theoretical

density. According to Goodman [10] $BaZrO_3$ is one of those materials that are capable of shifting the cubic to tetragonal phase transition temperature of barium titanate even down to room temperatures and the peak is broadened over a wide range of temperatures so high dielectric constant results. The 20% zirconia doped barium titanate samples discussed under current circumstance is a stoichiometric composition from crystallographic point of view. Therefore the material is a mixture of barium titanate and barium zirconate crystals. From figure 4.39 it can be seen that the permittivity is above 4000 below 60°C. Unfortunately, due to lack of data at lower than room temperatures any strong experimental support for this theory could not be presented from this thesis. According to Henning [14] the materials which shifts the curie point in each other's direction, can create a very wide region of broadened peaks which eventually can give very high dielectric constants. Since zirconia is such a material, therefore it can be concluded that the permittivity response shown in figures may well be in good agreement with the observations of Henning. Figure 4.42 shows steady loss value for these samples. The sample sintered at 1250°C has much higher amount of porosity and therefore has higher loss than the sample sintered at 1290°C.

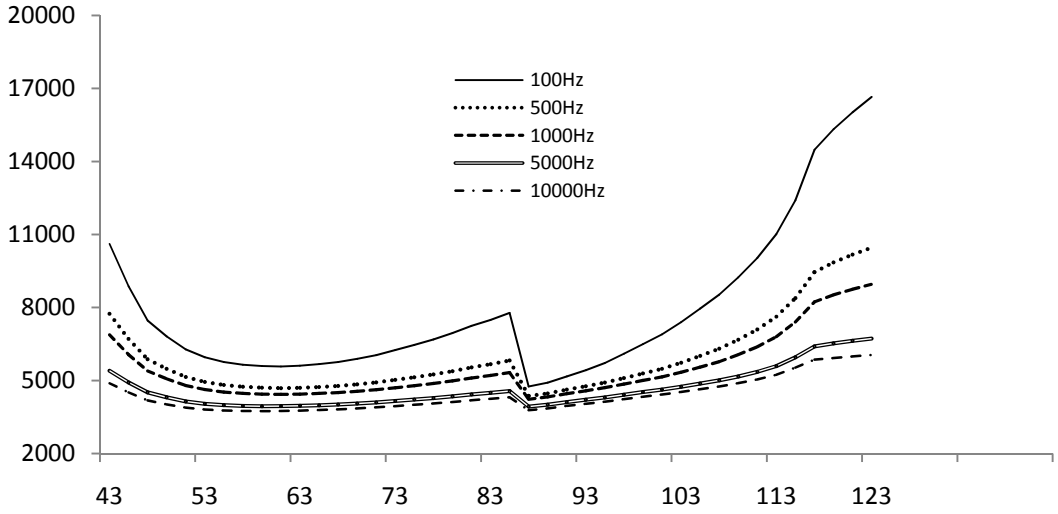

Figure 4.43: 0.2 wt% Nb_2O_5 doped $BaTiO_3$ sintered at 1275°C for 1 hour

Figure 4.43 shows the permittivity values for 0.2 wt% Nb_2O_5 doped $BaTiO_3$ with temperature. The notable features are shifting of curie point down to 85°C; at the same time the tetragonal to orthorhombic transition point also seem to have increased from 0°C. The dielectric constants are in the range of 4500 to 7000 and the response are almost constant across the range of temperatures. The next figure (4.43) shows the values for 0.3 wt% Nb_2O_5 doped samples. Permittivity resulted in the range of 2500 to 5000 for various magnitudes of frequencies. The decrease in k values may due

to increase in the amount of Nb_2O_5 along the grain boundaries that may as well work to suppress the cubic to tetragonal phase transformation. The reduction in curie point is a possible explanation to this theory.

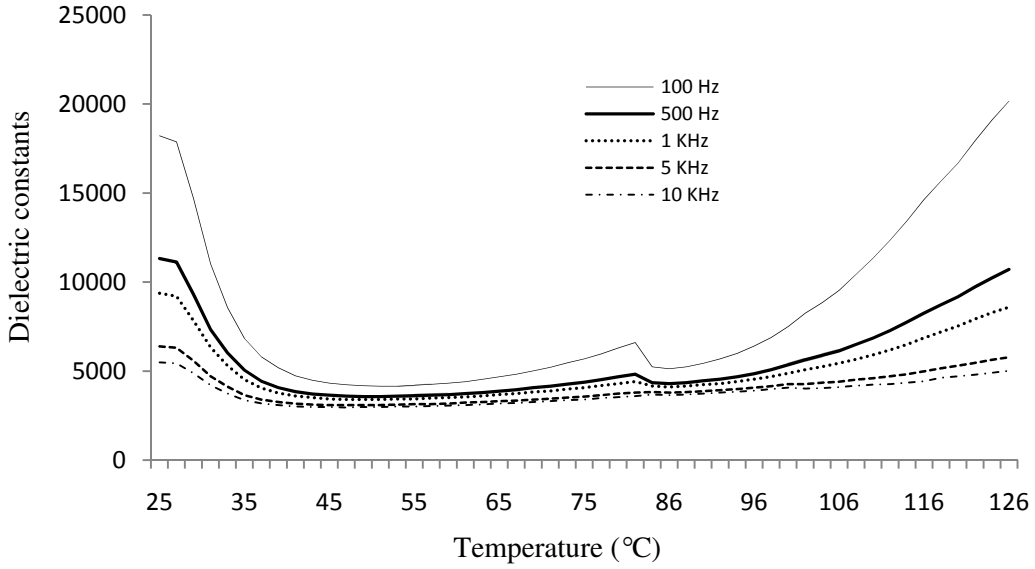

Figure 4.44: 0.3 wt% Nb_2O_5 doped $BaTiO_3$ at 1275°C for 1 hour

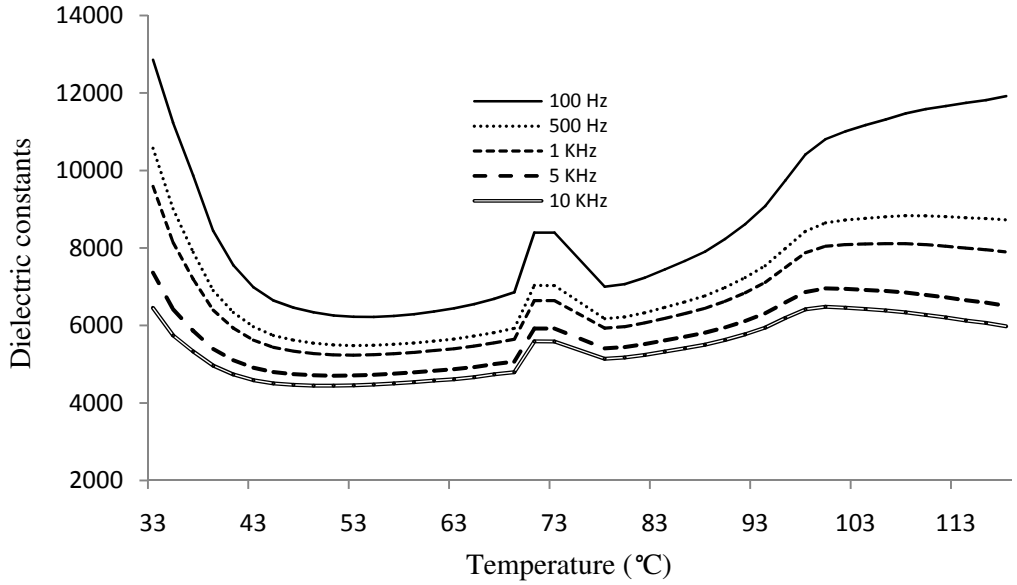

Figure 4.45: 0.4 wt% Nb_2O_5 doped $BaTiO_3$ at 1275°C for 1 hour

The curie point has been significantly suppressed by all three wt% addition. From the microstructures of figure 4.21, it can be seen that the sample contains more porosity than the other two samples. This may be a possible reason behind the drop in permittivity. Comparing the

permittivity from figure 4.44 and 4.45 it can be seen that although peak has been shifted more in 0.4 wt% sample, however at each and every frequency they are showing peaks. But the 0.3 wt% sample showed no peaks at all at frequencies higher than 5 KHz with permittivity values of more than 3000. Such behavior is expected for steady device application. Calculation would show that at curie point, 0.4 wt% samples had about 30-35% increase in permittivity.This strongly suggests that cubic phase has been stabilized to greater extent in 0.3 wt% sample than that in 0.4 wt% samples. 0.2 wt% samples have also shown behaviors like 0.3 wt% sample to some extent. Similar behavior was also observed for some ZrO_2 added samples.

5.Conclusion

The project was undertaken to explore the effects of sintering parameters and compositional variation on dielectric properties of pure and doped barium titanate. Majority of the thesis work was done on the properties of ZrO_2 modified $BaTiO_3$. Zr^{4+} ion replaces Ti^{4+} ion from the octahedral position because it forms $BaZrO_3$, which is thermodynamically a more stable compound. This stability is due to larger ion size of Zr^{4+} which is more stable than Ti^{4+} to the space availed by Ba-O framework. Due to this stability of crystal structure, ZrO_2 addition stabilizes the cubic phase beyond the regular curie temperature of 120℃. 1 and 2% ZrO_2 doped samples shifted the curie point down to 96℃ and Nb_2O_5 addition reduced the temperature to as low as 73℃ with considerable peak suppression in Nb_2O_5 added samples.

Table 5.1: Summary of properties achieved in the thesis

Parameters	ZrO_2 modified	Nb_2O_5 modified
Sintering temperature	1290°C	1275°C
Sintering time	0 minute/ double stage	0 minute/ 1 hour
Densification	>95%	>95%
Grain size	500 nm	700 nm
Grain growth	Above 1300°C	No grain growth upto 1320°C
Dielectric constant	~3000	~7000
Peak characteristics	Weak shifter/depressor	Strong shifter/depressor
k vs temperature	Flat below T_C	Flat across T_C
Quantity required	Up to 2 Wt%	Up to 0.4 Wt%

At the same time, the tetragonal to orthorhombic transition temperature was found to increase with ZrO_2 addition from 0℃ to in the range of 20 to 30℃. The reduction in tetragonality from that in pure barium titanate was confirmed by XRD. On many occasions the permittivity responses with temperature were quite flat which is in congruence for consistent device performance. As for sintering parameters, 1290℃ was found to be the optimum temperature for zirconia doped samples with a 0 minute holding time and 1275℃ with soaking from 0 minute to an hour for Nb_2O_5doped samples. For sintering with very small holding period grain size as small as 500 nm was found. XRD data are helpful on such low percentage doping to observe the change in tetragonality with doping or sintering. Two stage sintering was appropriate for bringing properties like depressing the

peak, broadening and shifting the peak to lower temperatures. Dielectric constant in ZrO_2 added samples was found to be in the range of 1500 to 3200 for up to 10 KHz frequency. The same for Nb_2O_5 was 2500 to 6500. The size of Nb^{5+} ion and its higher charge than the other species might have played important role in high dielectric constants. The higher dielectric constant in Nb_2O_5 added samples may be due to its resistance to grain growth and higher polarization introduced into $BaTiO_3$ lattice. Although, achievement of successful sintering was a challenge, ZrO_2 doped samples ($BaTi_{0.8}Zr_{0.2}O_3$) were found to suppress the curie peak significantly and have shown high permittivity at room temperatures.Table 5.1 shows all the properties that were received from this entire work.

6. Suggestion for future work

The experiments present some unique opportunity to study the change brought about in the material by the dopants like zirconium and niobium oxides. However the exact character and intercation among the materials during sintering could not be proved due to lack of technical facilities. In this thesis the review of earlier works played a major role since experimental works were not complete on many respect. The properties could be further enhanced just by introducing the "poling effect" through the samples having subject to strong electric field during the cubic-tetragonal phase transformation. XRD measurement should be done comprehensively on all the samples to get a precise idea about the changes in lattice parameters and the strain induced into the material due to sintering. Measurements should have been done at high angles to observe complex reactions from various planes. TEM observation is necessary to view the condition of grain boundary; especially if low temperature is chosen for sintering in which case, dopants may linger at grain boundaries.Also calcination of raw powders may be tested to have a clear distinction between the processes with and without calcination. Dielectric properties should be measured at temperatures as low as -20℃ to see the shift of orthorhombic to tetragonal phase transition temperature. The pressure used in the process of making pellets was 150 MPa; however in any future experiments the effects of pressure up to 300 MPa may be tested.

Bibliography

[1] D.H. Yoon, "Domain and grain structure in $BaTiO_3$", Journal of Ceramic Processing Research. Vol. 7, No. 4, pp. 343-354 (2006)

[2]K. Uchino, E. Sadanaga, T. Hirose, "Effect of processing parameters on dielectric properties of $BaTiO_3$",J. Am. Ceram. Soc., 72[8] (1989) 1555-1558, (1989)

[3]T. R. Armstrong, L. E. Morgens, A. K. Maurice, R. C. Buchanan, "Effects of Zirconia on Microstructure and Dielectric Properties of Barium Titanate Ceramics" J. Am. Ceram. Soc., 72 [4] 605-11 (1989)

[4]B.W. Lee, K.H. Auh, "Effect of grain size and mechanical processing on the dielectric properties of $BaTiO_3$", J. Mater. Res., Vol. 10, No. 6, 1995

[5]X. Wang, R. Chen, Z. Gui, L. Li, "The grain size effect on dielectric properties of $BaTiO_3$ based ceramics", Materials Science and Engineering, B99, 199-202(2003)

[6]T. Hoshina, K. Takizawa, J. li, T. Kasama, H. Kafemoto, T. Tsurumi, "Domain size effect on dielectric properties of Barium titanate ceramics", Japanese Journal of Applied Physics, Vol. 47, No. 9, pp, 7607-7611, 2008

[7]T. Ohno, D. Suzuki, H Suzuki, T. Ida, "Size Effect for Barium Titanate Nano-particles", J. Soc. Powder Technology, Japan, 41(2), 86-91 (2004)

[8]Y. Su, G.J. Weng, "The shift of Curie temperature and evolution of ferroelectric domain in ferroelectric crystals", Journal of the Mechanics and Physics of Solids, 53, 2071–2099(2005)

[9]T. R. Armstrong, R. C. Buchanan, "Influence of Core-Shell Grains on the Internal Stress State and Permittivity Response of Zirconia-Modified Barium Titanate", J. Am. Ceram.Soc., 73 [5] 1268-73 (1990)

[10]G. Goodman, "Ceramic Capacitor Materials"; Ch. 2 in Ceramic Materials for Electronics.Edited by R.C. Buchanan. Marcel Dekker, New York, 1986

[11]E. J. Brajer, "Polycrystalline Ceramic Material," U.S. Pat. No. 2708 243, 1955

[12]F. Kulscar, "Fired Ceramics Barium Titanate Body," US. Pat. No. 2735024, 1956

[13]D. Hennings, A. Schnell, and G. Simon, "Diffuse Ferroelectric Phase Transitions in $Ba(Ti_{1-x}Zr_x)0$, Ceramics," J. Am. Cerum. Soc.,65 [11] 539-44 (1982)

[14]T. N. Verbitskdia, G. S. Zhdanov, Iu. N. Venevtsev, and S. P. Soloviev, "Electrical and X-ray Diffraction Studies of the BaTi0,-BaZrO, System," Sov. Phys. Cystallogr. (Engl. Transl.), 3 [2] 182-92 (1958)

[15]R. C. Kell and N. J. Hellicar, "Structural Trdnsltlons in Barium Titanate-Zirconate Transducer Materials," Acustica, 6 (12) 235-38 (1956)

[16]N. M. ,Molokhia and M. A. Issa, "Dielectric Properties of $BaTiO_3$, Modified with ZrO_2, Prumanu,11,131 289-93 (1978)

[17]A. K. Maurice, "Powder Synthesis, Stoichiometry, and Processing Effects on Propenies of High Purity Barium Titanate"; M.S. Thesis. University of Illinois, Urbana, IL, 1984

[18]K. Kinoshinta and A. Yamaji, "Grain-Size Effects on Dielectric Properties in Barium Titanate," J. Appl. Phys., 47 [1] 371-74 (1976)

[19]G. Ark, D. Hennings, and G. de With, "Dielectric Properties of Fine-Grained Barium Titanate Ceramics," J . Appl. Phys., 58,141, 1619-25 (1985)

[20]N. C. Sharma and E. R. McCartney, "The Dielectric Properties of Pure Barium Titanate as a Function of Grain Size," J. Am. Ceram.Soc.,10[I61 16-20 (1974)

[21]G. H. Jonkkr and W. Noorland&,' "Grain Size of Sintered Barium Titanate"; pp. 255-64 in Science of Ceramics 1 ,Edited by G. H. Stewart. Academic Press, London, 1962

[22]H. T. Martirena and J. C. Burfoot, "Grain-Size Effects on Properties of Some Ferroelectrics Ceramics," J. Phys. Soc. C, 7, 3182-92 (1974)

[23]H. Kumazawa, K. Masuda, "Fabrication of barium titanate thin films with a high dielectric constantby a sol-gel technique", Thin Solid Films 353, 144-148, (1999)

[24]Electronic Industries Association RS-198, American Standard Requirements for Ceramic Dielectric Capacitors, Classes 1 and 2, American Standard Association, New York, 1958

[25]Y.I. Jung, S.Y.Choi"Grain growth behavior during stepwise sintering of barium titanate in hydrogen gas and air", J. of Am. Ceram. Soc., 86 (12) 2228 – 30 (2003)

[26]Merz, W.J., 1949. "The electric and optical behavior of BaTiO3 single-domain crystals", Phys. Rev. 76,1221–1225

[27]Merz, W.J., 1950. "The effect of hydrostatic pressure on the Curie point of bariumtitanate single crystals" Phys. Rev., 77, 52–54

[28]Merz, W.J., 1952. "Domain properties in $BaTiO_3$", Phys. Rev., 88, 421–422

[29]Merz, W.J., 1953. “Double hyeteresis loop of $BaTiO_3$ at the Curie point”. Phys. Rev., 91, 513-517

[30]Merz, W.J., 1954. Domain formation and domain wall motions in ferroelectric $BaTiO_3$ single crystals.Phys. Rev., 95, 690–698

[31]L. Wu, M. Chure, K. Wu, W. Chang, M. Yang, W. Liu, M. Wu, “Dielectric properties of barium titanate ceramics with differentmaterials powder size”, Ceramics International 35, 957–960, (2009)

[32]Y. Yuan, S. R. Zhang, X. H. Zhou, B. Tang, “Effects of Nb2O5 doping on the microstructure and dielectric properties of barium titanate ceramics”, J Mater Sci., 44, 3751-3757 (2009)

[33] Wang S.M., Kang S. J. L. “Effect of grain boundary structure on diffusion induced grain boundary migration in BaTiO3”, J. of Am. Ceram. Soc., 88[9] 3267-3269 (2005)

[34]Jaffe B, Cook W.R. and Jaffe H., “Piezoelectric Ceramics”, Academic Press Limited, India, 1971

[35]Kingery, Bowen, Uhlman,“Introduction to Ceramics”, John Willey & Sons, second edition, Singapore, 1976

[36]Richerson, “Modern Ceramic Engineering”, Marcel Dekker, 1992

[37]“Ceramic Materials for Electronics”, Edited by Relva C. Buchanan, Marcel Dekker, Second edition, 1994

[38]C. C. Barry, N. M. Grant, “Ceramic Materials, Science and Engineering”, Springer, 2007

[39]BarsoumM.M. “Fundamentals of ceramics”, The McGraw-Hill Companies, Inc., Taiwan, 1997

[40] YoonS.H., Lee.J.H, KimD.Y.andHwang.N.M “Core-shell structure of acceptor rich, coarse barium titanate grains”, J. of Am. Ceram.Soc.,85 (2) 3111-13 (2002).

[41] JungY.I., Choi .S.Y, and Kang S.J.L., “Grain growth behavior during stepwise sintering of barium titanate in hydrogen gas and air.”,J. of Am. Ceram.Soc.,86 (12) 2228-30(2003).

[42] Liang X., MengZ.and Wu W.“ Effect of acceptor and donor dopants on the dielectric and tunable properties of barium strontium titanate.” ,J. of Am. Ceram. Soc., 86(12) 2218-2222(2004).

[43] Valant M., and SuvorovD.“ Low temperature sintering of $Ba_{0.6}Sr_{0.4}TiO_3$.”, J. of Am. Ceram.Soc., 86(7)1222-1226(2004).

[44]ChoY.K., KangS.J.L., and Yoon D.Y. “ Dependence of grain growth and grain boundary structure on the Ba/ Ti ratio in $BaTiO_3$.” J. of Am. Ceram. Soc., 87(1) 119-24(2004)

[45] JinH.R., YoonS.H., LeeJ.H., LeeJ.H., Hwang N.M., KimD.Y.and HanJ.H., "Effect of external electric field on the grain-growth behavior of acceptor Mg doped , undoped and donor Nb doped barium titanate." J. of Am. Ceram. Soc., 87(9) 1747-1752(2004)

[46] BabiloP. and HaileS.M., "Enhanced sintering of Yuttrium-doped barium zirconate by addition of ZnO ." J. of Am. Ceram.Soc., 88(9)2362-2368 (2005).

[47]Chun.J.S. , Hwang N.M. and KimD.Y., " Abnormal grain growth occurring at the surface of a sintered BaTiO3 specimen .",J. of Am. Ceram.Soc.,87(9)1779-1781(2004).

[48] Wang.S.M., and KangS.J.L., "Effect of grain boundary structure on diffusion – induced grain boundary migration in $BaTiO_3$",J. of Am. Ceram.Soc.,88(9)3267-3269(2005).

[49] Siddique N. A., "Effect of zirconia doping and sintering temperature on the dielectric properties of Barium Titanate", Undergraduate thesis, Bangladesh University of Engineering and Technology, 2008

Appendix

Ionic crystal radii (in pm)

Coordination Number = 6

Ag^{+}	Al^{3-}	As^{5-}	Au^{+}	B^{3+}	Ba^{2+}	Be^{2+}	Bi^{3+}	Bi^{5+}	Br^{-}	C^{4+}	Ca^{2+}	Cd^{2+}
115	54	46	137	27	135	45	103	76	196	16	100	95
Ce^{4+}	Cl^{-}	Co^{2+}	Co^{3+}	Cr^{2+}	Cr^{3+}	Cr^{4+}	Cs^{+}	Cu^{+}	Cu^{2+}	Cu^{3+}	Dy^{3+}	Er^{3+}
87	181	75	55	80	62	55	167	77	73	54	91	89
Eu^{3+}	F^{-}	Fe^{2+}	Fe^{3+}	Ga^{3+}	Gd^{3+}	Ge^{4+}	Hf^{4+}	Hg^{2+}	Ho^{3+}	I^{-}	In^{3+}	K^{+}
95	133	78	65	62	94	53	71	102	90	220	80	138
La^{3+}	Li^{+}	Mg^{2+}	Mn^{2+}	Mn^{4+}	Mo^{3+}	Mo^{4+}	Mo^{6+}	N^{5+}	Na^{+}	Nb^{5+}	Nd^{3+}	Ni^{2+}
103	76	72	83	53	69	65	59	13	102	64	98	69
Ni^{3+}	O^{2-}	OH^{-}	P^{5+}	Pb^{2+}	Pb^{4+}	Rb^{+}	Ru^{4+}	S^{2-}	S^{6+}	Sb^{3+}	Sb^{5+}	Sc^{3+}
56	140	137	38	119	78	152	62	184	29	76	60	75
Se^{2-}	Se^{6+}	Si^{4+}	Sm^{3+}	Sn^{4+}	Sr^{2+}	Ta^{5+}	Te^{2-}	Te^{6+}	Th^{4+}	Ti^{2+}	Ti^{3+}	Ti^{4+}
198	42	40	96	69	118	64	221	56	94	86	67	61
Tl^{+}	Tl^{3+}	U^{4+}	U^{5+}	U^{6+}	V^{2+}	V^{5+}	W^{4+}	W^{6+}	Y^{3+}	Yb^{3+}	Zn^{2+}	Zr^{4+}
150	89	89	76	73	79	54	66	60	90	87	74	72

Coordination Number = 4

Ag^{+}	Al^{3-}	As^{5-}	B^{3-}	Be^{2+}	C^{4-}	Cd^{2-}	Co^{2-}	Cr^{4+}	Cu^{+}	Cu^{2+}	F^{-}	Fe^{2-}
100	39	34	11	27	15	78	58	41	60	57	131	63
Fe^{3-}	Ga^{3-}	Ge^{4+}	Hg^{2+}	In^{3+}	Li^{+}	Mg^{2-}	Mn^{2+}	Mn^{4+}	Na^{+}	Nb^{5+}	Ni^{2-}	O^{2-}
49	47	39	96	62	59	57	66	39	99	48	55	138
OH^{-}	P^{5+}	Pb^{2+}	S^{6-}	Se^{6+}	Sn^{4+}	Si^{4+}	Ti^{4+}	V^{5+}	W^{6+}	Zn^{2+}		
135	17	98	12	28	55	26	42	36	42	60		

Coordination Number = 8

Bi^{3-}	Ce^{4-}	Ca^{2-}	Ba^{2-}	Dy^{3-}	Gd^{3-}	Hf^{4+}	Ho^{3-}	In^{3+}	Na^{+}	Nd^{3-}	O^{2-}	Pb^{2-}
117	97	112	142	103	105	83	102	92	118	111	142	129
Rb^{+}	Sr^{2-}	Th^{4-}	U^{4+}	Y^{3-}	Zr^{4+}							
161	126	105	100	102	84							

Coordination Number = 12

Ba^{2+}	Ca^{2+}	La^{3+}	Pb^{2+}	Sr^{2+}
161	134	136	149	144

Terms used to describe dielectric behavior

Parameter	*Definition*	*Units/value*	*Conversion factor*
C	Capacitance	F, farads	$1\,F = 1\,C/V = 1\,A^2s^4kg^{-1}m^{-2}$
ε_0	Permittivity of a vacuum	8.85×10^{-12} F/m	
ε	Permittivity	F/m	
ε_r	Relative permittivity ($\varepsilon/\varepsilon_0$)	Dimensionless	
κ (same as ε_r)	Dielectric constant	Dimensionless	
P	Polarization	C/m^2	
Q	Charge	C, coulombs	1 C = 1 As
μ	Dipole moment	C·m	
V	Voltage	V	
q or e	Electron charge	0.16 aC	
D	Dielectric displacement	C/m^2	$D = Q/A$
θ_c	Curie temperature	K	0 K = −273°C
T_{cw}	Curie–Weiss temperature	K	
E_c	Coercive field	V/m	
χ	Dielectric susceptibility	Dimensionless	
ξ	Electric field strength	V/m	
C	Curie constant	K	

Noncentrosymmetric crystal:

Crystal system	*Noncentrosymmetric point groups*	*Piezoelectric*	*Pyroelectric*
Triclinic	1	Yes	Yes
Monoclinic	2	Yes	Yes
	m	Yes	Yes
Orthorhombic	mm2	Yes	Yes
	222	Yes	No
Tetragonal	4	Yes	Yes
	$\bar{4}$	Yes	No
	422	Yes	No
	4mm	Yes	Yes
	$\bar{4}$2m	Yes	No
Trigonal	3	Yes	Yes
	32	Yes	No
	3m	Yes	Yes
Hexagonal	6	Yes	Yes
	$\bar{6}$	Yes	No
	622	Yes	No
	6mm	Yes	Yes
	$\bar{6}$m2	Yes	No
Cubic	23	Yes	No
	432	No	No
	$\bar{4}$3m	Yes	No

Curie temperature and curie constant for several dielectrics:

Ceramic	*Structure*	θ_c *(K)*	*C (K)*	*Oxide*	*Structure*	θ_c *(K)*	*C (K)*
$SrTiO_3$	Perovskite	~0	7.0×10^4	$LiNbO_3$	Ilmenite	1470	
$BaTiO_3$	Perovskite	393	12.0×10^4	$LiTaO_3$	Ilmenite	890	
$PbTiO_3$	Perovskite	763	15.4×10^4	$Cd_2Nb_2O_7$	Pyrochlore	185	7.0×10^4
$CdTiO_3$	Perovskite	1223	4.5×10^4	$PbNb_2O_6$	Tungsten bronze	843	30.0×10^4
$KNbO_3$	Perovskite	712	27.0×10^4				

Summary of signals used in SEM:

Signal	*Energy*	*Source*	*Use*
Secondary electrons	~5 eV	Loosely bound electrons scattered from surface	Main signal for image formation
Backscattered electrons	Energies up to incident beam energy	Beam electrons scattered back after collision	Atomic number contrast, channeling patterns, magnetic contrast
Characteristic X-rays	Discrete values for each element	Interband transitions usually involving K and L	Chemical analysis
Light (cathodoluminescence)	UV, visible, IR	Interband transitions between higher energy levels	Imaging dislocations in semiconductors

X ray diffraction analysis:

Type of analysis	*Method*	*Sample*
Crystal geometry	Moving crystal-spot pattern	Single crystal
	Computer positioned diffractometer	Single crystal
	Solution of *d*-spacing equations	Powder
Arrangement of atoms	Analysis of diffracted intensities	Single crystal
	Refinement of whole pattern	Powder
Symmetry	Moving crystal-spot pattern	Single crystal
	Stationary crystal-spot pattern	Single crystal
Identification of compound	Identification of cell parameters	Single crystal
	Matching of *d*-*I* set	Powder
Crystal orientation	Single-crystal back reflection	Large single crystal
	Texture analysis	Powder compact
Size of crystal	Line broadening	Powder
Magnitude of strain	Line shifts	Powder compact
Amount of phase	Quantitative analysis	Powder
Change of state	Special atmosphere chambers	Single crystal or powder
Crystal perfection	Direct imaging	Single crystal
	Line shape analysis	Powder

Properties of X-rays and Neutrons:

Property	*X-ray*	*Neutron*
Wavelength	0.05–0.25 nm	0.01–2 nm
Energy	12.4 keV	80 MeV
Velocity	3×10^8 m/s	4×10^3 m/s
Production	X-ray tube	Nuclear reactor
	Synchrotron	Electron linear accelerator pulsed source
		Proton spallation pulsed source
Detection	Photographic film	$^{10}BF_3$ or ^3He proportional counter
	Proportional counter	^6Li scintillation counter
	Scintillation counter	